

**Effect of simulated ocean acidification on the
composition of microbial assemblages in New Zealand's
coastal sediment and their potential for ammonia
oxidation**

Cintya Elizabeth Del Río Hernández

**A thesis submitted to
Auckland University of Technology
in partial fulfilment of the requirements for the degree of
Master of Science (MSc)**

2016

School of Applied Sciences

Table of contents

List of figures	3
List of tables.....	5
List of equations	7
Attestation of authorship	8
Acknowledgements	9
Abstract	10
Literature review	12
Section I.....	12
Role of benthic–pelagic coupling in coastal ecosystem functioning.....	12
Metabolic pathways of organic matter remineralisation	15
Response of microbial assemblages to environmental changes.....	23
Effect of anthropogenic CO ₂ on the ocean’s pH and nutrient cycling.....	25
Perturbation experiments for ocean acidification research	31
Section II.....	33
Molecular techniques to assess metabolic activity and assemblage composition	33
Polymerase chain reaction (PCR)	33
DNA sequencing.....	34
Quantitative polymerase chain reaction (qPCR)	35
Reverse transcription quantitative polymerase chain reaction (RT-qPCR)	36
Research questions and hypotheses	37
Material and methods	39
Experimental design	39
Study sites	39
Sediment sampling.....	41
Sediment incubation	44
Experimental units	44
Environmental control	45
Seawater analyses	49
Sediment analyses.....	50
Porewater pH	50
Granulometry, large fauna and microbial mats.....	50
Molecular analyses.....	51

DNA and RNA extraction.....	51
DNA sequencing.....	53
Quantitative polymerase chain reaction	54
Reverse transcription quantitative polymerase chain reaction.....	56
Data analysis.....	57
Statistical analysis	59
Results	61
Performance of experimental units	61
Temperature and salinity.....	61
Seawater carbonate chemistry	64
Physicochemical sediment characteristics	71
Modulation of pore water pH	75
Composition of microbial assemblages.....	77
Abundance of <i>amoA</i> genes and transcripts.....	85
Protocol development and troubleshooting.....	85
Abundance of <i>amoA</i> genes and transcripts after incubation	88
Discussion	93
Effect of acidified seawater on the structure of benthic microbial assemblages	93
Effect of acidified seawater on coastal sediment pore water pH	93
<i>Temporal variations of pH in the upper oxic zone</i>	93
<i>Spatial distribution of pH in the suboxic zone</i>	95
Similar structure of the microbial assemblage in the Control and Treatment estuarine sediment.....	96
Effect of acidified seawater on the potential for ammonia oxidation	98
Strategies to improve the recovery of ammonia-oxidising microorganisms for future research	98
<i>Investigating the oxic–anoxic boundary</i>	98
<i>Increasing nucleic acids extraction yields</i>	99
<i>Trying other methods to overcome inhibitors</i>	99
Benthic mesocosms for ocean acidification research	101
Conclusion	104
References	105

List of figures

Figure 1. The nitrogen cycle. The dashed line represents the boundary between the oxic and the suboxic/anoxic zone.	19
Figure 2. Map showing the location of the estuarine sediment sampling site, Tauranga Harbour (S 37° 29' 29", E 175° 56' 51").	42
Figure 3. Map showing the location of the coastal sediment sampling site, Man O'War Bay (S 36° 47' 38", E 175° 10' 14").	43
Figure 4. Diagram showing the flow of seawater in one experimental unit.	45
Figure 5. Functioning of the pH regulation system.	47
Figure 6. Temperature of seawater in the incubation tanks.	62
Figure 7. Salinity of the seawater in incubation tanks.	63
Figure 8. 24-hour monitoring of seawater pH in one experimental unit using a 5% CO ₂ in oxygen gas mixture.	65
Figure 9. Time-series of seawater pH in the mixing barrel (black lines) and incubation tank (blue lines) in two experimental units.	66
Figure 10. Time-series of seawater total alkalinity (A _T) and concentration of dissolved inorganic carbon (DIC) in the Control and Treatment incubation tanks.	68
Figure 11. Time-series of estimated versus measured pH of the seawater in the Control and Treatment incubation tanks.	70
Figure 12. Photographs of Treatment and Control sediment cores' surface.	72
Figure 13. Sediment particle size distribution.	74
Figure 14. Average pore water pH profiles in coastal sediment in Control sediment C15 time-zero, Treatment sediment C2 time-zero, Control sediment C15 final time-point, Treatment sediment C2 final time-point.	76
Figure 15. Hierarchical cluster analysis of normalised OTU frequencies at time-zero (T0, pH 8.1) and final analyses (Final C, pH 8.1 and Final T, pH 7.8) showing no defined clustering patterns between treatments in any of the two types of sediment.	79
Figure 16. Similarity profile analysis of normalised OTU frequencies at time-zero (T0, pH 8.1) and final analyses (Final C, pH 8.1 and Final T, pH 7.8) showing no defined clustering differences between treatments in any of the two types of sediment	80

Figure 17. Relative abundance of phyla and Proteobacteria classes found in coastal and estuarine sediment in time-zero (T0, pH 8.1) and final analyses (Final C, pH 8.1 and Final T, pH 7.8).	83
Figure 18. Sequence of steps followed during the protocol development and troubleshooting.	86
Figure 19. Gradient PCR analysis for amoA bacterial and archaeal primers in sediment and soil DNA showing the most suitable annealing temperature is ~49 °C for both primers (most intense, discrete and well-defined bands).	86
Figure 20. Effect of sediment-overlying seawater pH on the abundance of bacterial amoA genes in estuarine sediment.	89
Figure 21. Effect of sediment-overlying seawater pH on the abundance of archaeal and bacterial amoA transcripts in coastal sediment.	90

List of tables

Table 1. Experiment timeline.....	40
Table 2. Red Sea Coral Pro Salt product specification	44
Table 3. Initial settings for the CapCTRL pH regulation system	48
Table 4. Standard buffers used for the calibration of pH meters and probes	49
Table 5. Calibration parameters of the pH sensors	49
Table 6. Temperature, time and cycle conditions for the PCR to generate the library of DNA fragments for sequencing	53
Table 7. PCR reactions setup to generate the library of DNA fragments for sequencing.....	54
Table 8. Primers used to target bacterial and archaeal <i>amoA</i> genes, melting temperature (T_m), sequences and fragment size.....	54
Table 9. Concentration of archaeal and bacterial standards	55
Table 10. Composition of the qPCR master mix	55
Table 11. Temperature, time and cycle conditions for the archaeal and bacterial qPCR assays	56
Table 12. Temperature, time and cycle conditions for the archaeal and bacterial RT-qPCR assays	57
Table 13. Temperature and salinity of incubation tanks during the experiment	61
Table 14. Seawater pH of experimental units during the experiment.....	67
Table 15. Carbonate chemistry of incubation tanks during the experiment.	69
Table 16. Large fauna and microbial mats found in sediment cores	71
Table 17. Granulometric indices, water content and organic matter content for coastal and estuarine sediments.....	73
Table 18. Median, maximum and minimum pore water pH readings at the oxic zone (upper 2 mm) during time-zero and final time-point analyses for the Control and Treatment sediment in darkness and light conditions.....	75
Table 19. Percentage of reads of ammonia-oxidising archaea and bacteria identified in coastal and estuarine sediment.	78
Table 20. Statistical analyses of microbial assemblages in coastal and estuarine sediment.....	81
Table 21. Diversity indices of microbial assemblages in coastal and estuarine sediment.....	82
Table 22. Twenty most abundant operational taxonomic units in coastal and estuarine sediment identified with a nucleotide BLASTn search.....	84
Table 23. Average C_T of diluted DNA templates targeting bacterial and archaeal <i>amoA</i> genes.	87
Table 24. Summary of results where the determination of <i>amoA</i> genes or transcripts abundance was possible	89

Table 25. Relative abundance of bacterial <i>amoA</i> genes in estuarine sediment	89
Table 26. Relative abundance of archaeal <i>amoA</i> transcripts in coastal sediment	91
Table 27. Standard curve parameters for the final RT-qPCR analyses in coastal sediment.....	92
Table 28. Concentration of DNA and RNA extracted from coastal and estuarine sediment for final analyses.....	92
Table 29. Ranges of seawater pH in three published experimental units for ocean acidification research and in the present study	101

List of equations

Equation (1)17
Equation (2)25
Equation (3)25
Equation (4)25
Equation (5)25
Equation (6)27

Attestation of authorship

I hereby declare that this submission is my own work and that, to the best of my knowledge and belief, it contains no material previously published or written by another person (except where explicitly defined in the acknowledgements), nor material which to a substantial extent has been submitted for the award of any other degree or diploma of a university or other institution of higher learning.



Cintya Del Río

Acknowledgements

I encountered many challenges throughout the course of this project. The implementation of a new facility at Auckland University of Technology and a new analytical method at University of Waikato were not easy tasks. I learned to better trust myself and that research is not about finding the result one wants to find. I discovered that lessons go deeper when things happen differently from what one has expected. After all, numerous life-changing discoveries have been made by accident.

I would like to express my deepest gratitude to my primary supervisor, Kay Vopel, for your infinite patience, for listening, for your continuous support and caring, and for believing in me. Your guidance at every step of this process was fundamental for the completion of this thesis. More than a supervisor, you have been a leader and friend to me.

I also wish to express my sincerest gratitude to my second supervisor, Charles Lee, who has supported me with his expertise and practical thinking. Thank you for cheering me up when things did not go as I expected and thanks for your empathy which made my stays at Hamilton smoother. I would also like to thank you and Craig Cary for the financial support and for your hospitality at the Thermophile Research Unit.

A very special thanks to Roanna Richards-Babbage and Georgia Wakerley for making my life nice and easy while working in Hamilton. Thank you for your patience and willingness to help. It was an absolute pleasure working with you.

My sincere thanks also goes to all the people who helped me with the facility setup and maintenance: Chris Pook, Owen Fox, Levin Dumm, Camila Cotrim, Indiana Mallinder and Hanne (Pancake) Gommerud. Pancake, also thank you for all your help with the sediment analyses and the diving with Nathan Fehr to collect my coastal sediment, my eternal gratitude to you two. Further, I thank Jo Adams for proofreading this thesis.

Finally, I would like to thank my biological and adoptive family for the good vibe, financial, emotional and spiritual long-distance support. Without all of you, this journey would have been much harder: Mom, Javier, Garbanzo, Dad, Suegris, Ilse, Nohe, Guadarrama family and my Mijas. And my greatest thanks go to my beloved husband for always being there. Malilo, this is our Masters, our thesis and our proof that wishes do come true. Te amo.

Abstract

The ocean's pH has decreased by 0.1 units in the last two centuries due to anthropogenic CO₂ emissions and it is predicted will continue to decrease by 0.3 units during the next century. One key ecosystem process that may be altered by such a decrease is the microbial oxidation of ammonia, the first step of nitrification. At low pH, the equilibrium concentration shifts towards ammonium rather than ammonia and therefore ammonia oxidation by microorganisms can be inhibited. Previous studies have demonstrated an inhibitory effect of a low seawater pH on ammonia oxidation in the seawater column. Such effect on ammonia oxidation in coastal sediment, however, is not well understood.

The relevance of studying the potential effect of acidified seawater on the oxidation of ammonia in coastal sediment is that nitrate, the end product of nitrification, is the second most preferred electron acceptor used by microorganisms to decompose organic matter. Nitrate is also an essential source of nitrogen for primary producers.

I established a facility of recirculating seawater to study the effect of an experimental pH decrease of 0.3 units on the oxidation of ammonia in two contrasting types of coastal sediment, sandy and muddy sediment. My objectives were to investigate (1) the assemblage structure of ammonia-oxidising archaea and bacteria; and (2) the gene expression of *amoA*, the gene for the enzyme that catalyses ammonia oxidation. I also investigated the effect of the seawater pH decrease on the pH of the muddy sediment pore water.

Overall, my study was inconclusive. I was able, however, to demonstrate that the seawater pH decrease altered the pore water pH in muddy sediment. I found enhanced pore water pH diel variations at the upper oxic zone, which were attributed to intensified respiration and photosynthesis of diatoms stimulated by the supply of CO₂. This suggested that the diatom's CO₂-growth stimulation might play an important role in the effect of the future acidified ocean on the sediment's biogeochemistry. I also demonstrated a shift in the pore water pH at the suboxic zone towards lower pH, suggesting that the seawater pH decrease exceeded the buffering capacity of the sediment. In terms of sandy coastal sediment, I was able to determine that the experimentally lowered seawater pH did not have a significant effect on the structure of the overall microbial assemblage (not only ammonia-oxidising microorganisms, which were scarce).

The reason for this study to be inconclusive was low statistical power. Such low statistical power resulted mainly from the excessive depth of sediment sampled for analyses, the low amounts of nucleic acids extracted from the sediments and the presence of inhibitors

in these extractions, which prevented the nucleic acids from being amplified or detected by the technique used. Informing the sampling with a preliminary pore water pH profile, improving the nucleic acids extraction technique and trying alternative methods to overcome inhibition would improve the outcome of future studies.

Literature review

This literature review is divided into two sections. The first section encompasses the information I reviewed to develop two research questions. The second section discusses the molecular techniques I used to answer these questions.

Section I

Role of benthic–pelagic coupling in coastal ecosystem functioning

The coast, where masses of seawater interact with air and land, is a complex and fascinating ecosystem whose functioning raises a vast number of so far unanswered questions. Countless macro- and microscopic organisms interact with each other to feed, grow and survive by means of energy, organic matter and nutrient exchange. Such exchanges take place not only in the sediment and seawater independently, but rather interactions occur between these two oceanic realms. These interactions are known as benthic–pelagic coupling.

Raffaelli et al. (2003) defined benthic–pelagic coupling as exchange of solutes and particles between the seabed and the overlying column of seawater. Marcus and Boero (1998) described this coupling as the sequence of events outlined below. First, disturbance of the seafloor suspends sediment, which increases the concentration of particulate organic matter and dissolved nutrients in the seawater column. For instance, Couceiro et al. (2012) found that resuspension of cohesive sediments in the North Sea increased the concentration of dissolved silicon, nitrate and phosphate in the seawater column by as much as 125%. Usually, winds (Arfi & Bouvy, 1995) and storms (Nielsen & Kiørboe, 1991) induce such resuspension. Suspended organic matter and dissolved nutrients stimulate the primary production that feeds higher trophic levels in the pelagic food web (Arfi & Bouvy, 1995; Fanning, Carder, & Betzer, 1982). The microbial decomposition of dead organisms makes available more organic matter. Organic particles settle, carrying essential compounds for benthic organisms. Finally, benthic organisms release nutrients to the overlying seawater, which further contribute to primary production (Mortazavi, Riggs, Caffrey, Genet, & Phipps, 2012).

Nixon (1981) carried out preliminary work in this field. This author suggested a link between the production of organic matter in seawater and the consumption of organic matter in coastal sediment. He also suggested an association between benthic consumption of organic matter and the release of nutrients from the sediment to the seawater. Later, Kelly and Nixon (1984) demonstrated this coupling with a laboratory microcosm experiment. They observed an increased release of nutrients and uptake of dissolved oxygen in sediments underlying

seawater supplied with organic matter. The amount of oxygen consumed and of nutrients released was a function of the quantity of organic matter supplied.

Jensen, Lomstein and Sørensen (1990) also found high rates of ammonium release and nitrate uptake after seasonal sedimentation of the phytoplankton bloom in a Danish bight. Their *in situ* experiment further demonstrated the link between the supply of organic matter to sediments and the sediment–seawater column nutrient exchange. More recently, Zapperi, Pratolongo, Piovan, and Marcovecchio (2015) published evidence for a consistent response after seasonal diatom blooms in an intertidal mudflat of the Bahía Blanca Estuary, in the southwest Atlantic Ocean. Nixon (1981) also suggested that benthic–pelagic coupling is stronger in shallow than in deep waters, because pelagic remineralisation reduces the amount of organic matter that reaches the seafloor. Hargrave (1973), for instance, found that sediments’ oxygen uptake was lower in the deep sea than in shallow waters. The low oxygen uptake reflected the low quantities of organic matter that reached the sediment because pelagic communities oxidised such organic matter. In fact, numerous studies have demonstrated that the oxygen penetration depth in sediments is a function of the water column depth (Glud, 2008 and literature cited therein). For instance, in the Southeast Atlantic deep-sea, pore water oxygen penetration varies from ~5 mm at a water depth of 600 m to >40 mm at a water depth of >4900 m (Glud, Gundersen, Jørgensen, Revsbech, & Schulz, 1994).

Primarily, two physical mechanisms mediate the sediment–seawater exchange of organic matter and nutrients. The most dominant of these mechanisms is advection—the transport of dissolved or particulate matter in seawater due to winds and tides (e.g., Ahmed, Elhassan, and Bashir 2012). Winds and tides stimulate the resuspension of particles from the sediment but the primary production may not be stimulated until the disturbance has ceased. Lawrence et al. (2004), for example, found that the planktonic community in shallow waters decreased after resuspension of sediment due to strong winds. When the winds ceased, the concentration of nutrients in seawater declined and the planktonic biomass increased. They proposed that, although advection increased the concentration of nutrients in the seawater column, other accompanying processes may have limited primary production. Reduction of light availability, for instance, may have delayed the growth stimulation until the particles settled.

Diffusion is another important transport process that influences the exchange of matter between the seafloor and seawater column (Hannides, Dunn, & Aller, 2005 and literature cited therein). According to Mehrer and Stolwijk (2009) diffusion refers to the mixing caused by movement of molecules due to gradients in the concentration of solutes. Solutes

are transported within sediments and through the sediment–water interface over small scales due to such concentration gradients (Kristensen et al., 2012). However, fauna inhabiting sediments can increase or decrease substantially such diffusive transport. For instance, Hannides et al. (2005) found that faunal secretions that increase the pore water viscosity (e.g., mucus) inhibited the diffusive transport of solutes. In contrast, other faunal activities within sediments can significantly increase not only the transport of solutes but also the transport of particles. Such transport processes stimulated by fauna are known as bioturbation.

Kristensen et al. (2012) defined bioturbation as “all transport processes carried out by animals that directly or indirectly affect sediment matrices. These processes include both particle reworking and burrow ventilation” (p. 288). In this context, reworking refers to the displacement of particles due to animal burrowing, gallery formation, and particle ingestion and excretion. Ventilation refers to the animal’s flushing of burrow openings with overlying seawater to respire and feed. This flushing transports solutes around burrows, or from the burrow to the overlying seawater.

Howe, Rees, and Widdicombe (2004) showed that the effect of bioturbation on nutrient fluxes depends on the specific faunal transport process. They found that the presence of the mud lobster *Upogebia deltaura* (Leach, 1815) increased the rate of benthic denitrification. In contrast, the presence of the burrowing ghost shrimp *Callinassa subterranea* (Montagu, 1808) did not cause any significant changes. Howe and co-workers explained these findings with differences in the rate at which these two species ventilate their burrows, which is three times higher for *U. deltaura* than it is for *C. subterranea*.

Human activity can also have an effect on benthic–pelagic coupling at regional or global scales (Smith et al., 2000). For instance, farming of marine organisms has resulted in organic enrichment of the seabed, causing important changes in the macrobenthic community such as decreased species richness and size of individuals and an increase in opportunistic species (Weston, 1990). Another example is bottom trawling, which according to Hughes et al. (2014), is the most widespread anthropogenic activity that directly alters benthic ecosystems. The fishing gear disrupts benthic habitats, altering many characteristics of the sediment including its biogeochemistry (Smith et al., 2000).

Eutrophication is another effect of anthropogenic activity that alters benthic–pelagic coupling (Smith et al., 2000). Nixon (1995) defined eutrophication as “an increase in the rate of supply of organic matter to an ecosystem” (p. 199). According to this author, nutrient enrichment is the most common factor that may increase such supply. Atmospheric input and

groundwater discharges are the principal reasons for this nutrient enrichment (Smith et al., 2000). The stimulation of primary production with nutrient enrichment results in an increased consumption of oxygen and water column turbidity (Meyer-Reil & Köster, 2000). Consequently, the sediment–seawater exchange of nutrients is also altered (Smith et al., 2000).

Climate change also has an effect on benthic–pelagic coupling at a global scale (Smith et al., 2000). For instance, a 50-year monitoring of the Narragansett Bay (in Rhode Island Sound in the United States) revealed that global warming had decreased the winter-spring phytoplankton blooms (Nixon et al., 2009). Such a decrease reduced the quantity of organic matter that reached the seafloor, resulting in a decreased oxygen uptake and nutrient regeneration in the sediment.

Another anthropogenic process that has been suggested to alter sediment–seawater fluxes at a global scale is ocean acidification (e.g., Gazeau, Rijswijk, Lara, & Middelburg, 2014; Widdicombe & Needham, 2007; Widdicombe et al., 2013). Ocean acidification refers to the absorption of the increasing atmospheric CO₂ by the ocean, which decreases the seawater pH (Feely et al., 2004; IPCC, 2014). Widdicombe and Needham (2007) conducted the first study to investigate the effects of acidified seawater on sediment nutrient fluxes. They found higher rates of nitrate uptake and ammonium release in sediments inhabited by the polychaete *Nereis virens* Sars, 1835 exposed to acidified seawater compared to a control of natural seawater at pH ~7.9. They also found lower nitrite release and phosphate uptake rates at low pH, compared to the control sample in sandy mud from Plymouth Breakwater. A similar study by Widdicombe et al. (2009) revealed consistent changes in these nutrient fluxes in Norwegian sandy and muddy sediments inhabited by nematode and other macrofauna. These findings suggested that ocean acidification could have an effect on the coastal sediment–seawater nutrient exchange; that is, on benthic–pelagic coupling. More recently, Widdicombe et al. (2013) suggested that the effect of ocean acidification on benthic–pelagic coupling can be influenced by the presence of bioturbating organisms. These researchers found that the presence of two burrowing urchins, *Brissopsis lyrifera* (Forbes, 1841), and *Echinocardium cordatum* (Pennant, 1777), significantly altered nutrient fluxes in acidified treatments; the two urchins reduced the uptake and enhanced the release of nutrients.

Metabolic pathways of organic matter remineralisation

Microorganisms transform organic matter into inorganic matter with numerous oxidation–reduction (redox) reactions (Froelich et al., 1979). The electron acceptor that

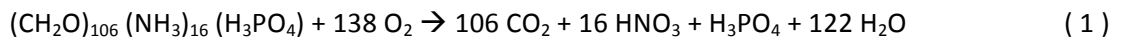
produces the greatest energy oxidises organic matter. Once depleted, the next most efficient electron acceptor continues oxidising organic matter. These redox reactions continue until all electron acceptors or organic matter are consumed. Froelich and co-workers (1979) determined that the order in which electron acceptors are consumed is as follows: oxygen, nitrates and manganese oxide, iron oxides, and sulfates.

Microorganisms use carbon and energy sources to drive these redox reactions. Autotrophic organisms, as named by Baas-Becking and Parks (1927), synthesise their own organic carbon from CO₂. This process is known as carbon fixation. In contrast, heterotrophs need an external organic carbon source because they are unable to synthesise their own (Payne, 1970). Through carbon fixation, autotrophs provide organic carbon to heterotrophs, which in turn oxidise such organic carbon back to inorganic carbon, keeping this nutrient cycling (Hügler & Sievert, 2010). Phototrophs are able to transform the energy of light into chemical energy, while chemotrophs need the energy produced from chemical reactions as Niel (1954) described. These differences in metabolic requirements, and the fact that different microorganisms use different electron acceptors, underline the importance of reaction coupling among microorganisms.

Froelich et al. (1979) also demonstrated that the supply of dissolved oxygen to sediments, and the pore water concentrations of substrates and products of aerobic and anaerobic remineralisation, influence the redox potential of sediments as a function of depth. Oxygen penetrates sediment by only a few millimetres, because microorganisms in the surface sediment consume this oxygen (Froelich et al., 1979; Glud, 2008). Moreover, permeable sediments have a more vigorous supply of oxygen compared to cohesive sediments because of pore water advection (Glud, 2008). Such advection results in a deeper oxic zone. Oxygen penetration also depends on seasonal environmental variations, such as nutrient and light availability. For instance, the sediment uptake of dissolved oxygen increases after a plankton bloom, followed by a gradual decrease after weeks (Hansen & Blackburn, 1992).

Based on vertical changes in the redox potential, sediments are divided into three zones; oxic, suboxic, and anoxic (Archer, Morford, & Emerson, 2002; Froelich et al., 1979; Revsbech, Sørensen, & Blackburn, 1980). Bioturbation alters this vertical zonation. For example, oxic, suboxic and anoxic zones may be radially distributed around burrows or fecal pellets (Aller, 1994; Aller & Aller, 1998; Jørgensen & Revsbech, 1985; Kristensen et al., 2012; Larsen, Borisov, Grunwald, Klimant, & Glud, 2011; Zhu, Aller, & Fan, 2006). Although bioturbation alters these patterns, the zonation model is a helpful tool to understand where and how remineralisation takes place.

Aerobic respiration is the most efficient pathway of all, based on the amounts of energy produced when oxygen serves as an electron acceptor (Froelich et al., 1979). The oxidation of one mole of glucose into CO₂ yields 32 ATP moles; whilst fermentation yields two ATP moles (Pfeiffer, Schuster, & Bonhoeffer, 2001). Aerobic remineralisation occurs in the oxic zone, where the concentrations of oxygen satisfy the requirements of aerobic microorganisms. The following stoichiometric reaction represents the aerobic oxidation of organic matter (Froelich et al., 1979):



Two relevant features might be highlighted from Equation (1). Firstly, Equation (1) represents a C:N:P ratio of 106:16:1, also known as the Redfield ratio (Redfield, 1934). This ratio represents the proportion of organic derivatives in plankton and seawater. Secondly, Equation (1) shows that ammonia (NH₃) oxidation is coupled to aerobic respiration. Ammonia oxidation is the first step of nitrification, the pathway investigated in the present research.

Microorganisms oxidise organic matter and reduce nitrate to nitrogen gas through denitrification, a pathway named by Gayon and Dupetit (1886). This pathway occurs in the suboxic zone where the sediment pore water contains only little oxygen but high concentrations of nitrate (Froelich et al., 1979). As reported by Devol (2015), numerous *Proteobacteria* and some species of archaea and foraminifera are capable of denitrification.

In manganese reduction, manganese oxide serves as the electron acceptor. Even though nitrate is preferred over manganese, both denitrification and manganese reduction happen simultaneously in the suboxic zone (Devol, 2015; Froelich et al., 1979). As stated in Nealson and Saffarini (1994), manganese oxide forms crystals that are difficult to assimilate. *Shewanella putrefaciens* (Lee et al. 1981) MacDonell and Colwell 1986, *Bacillus infernus* Boone et al., 1995 and species from the genera *Geobacter*, *Desulfuromonas*, *Desulfuromusa* and *Pelobacter* are capable of reducing manganese oxides (Lovley, 2013; Nealson & Saffarini, 1994).

Iron III hydroxide is the oxidant molecule in iron reduction. Similar to manganese reduction, oxidised iron forms crystals; thus reducing its uptake availability (Nealson & Saffarini, 1994). A species of the genus *Pseudomonas* was the first bacterium isolated, which was capable of coupling iron reduction to its respiratory growth (Balashova & Zavarzin, 1979). In addition to the manganese reducers mentioned above, *Geothrix fermentans* Coates et al., 1999, *Geovibrio ferrireducens* Caccavo et al., 2000, *Deferribacter thermophilus* Greene et al.,

1997 and *Ferribacterium limneticum* Cummings et al., 2000 are also capable of reducing iron oxide.

In contrast to manganese oxide, iron oxide reduction cannot occur until nitrate is depleted because nitrate (Sørensen, 1982) and manganese oxide (Postma, 1985) reoxidise reduced iron. Therefore, iron oxide reduction occurs in a deeper layer of the suboxic zone. The iron reduction zone can be easily traced in the sediment. Lyle (1983) demonstrated that the brown–green colour boundary indicates the depth at which reduction of iron Fe(III) to Fe(II) occurs.

Finally, two pathways occur in the anoxic zone: sulfate reduction and methanogenesis. During sulfate reduction, the sulfide generated reacts with iron-forming iron monosulfides, which colour the sediment black (Berner, 1964). As Rabus, Hansen, and Widdel (2013) reported, the involved bacteria in sulfate reduction are anaerobes from the families *Desulfobacteraceae* and *Desulfovibrionaceae*. Sulfate reduction is known as the dominant anaerobic pathway of remineralisation in sediments (Jørgensen, 1982). However, Canfield et al. (1993), and Thamdrup and Dalsgaard (2000), demonstrated that which anaerobic pathway dominates depends on the composition of the sediment. For instance, in sediments with high concentrations of manganese oxides, manganese reduction may dominate anaerobic remineralisation.

During methanogenesis, acetate or CO₂ are reduced to methane (Nealson, 1997). The involved microorganisms in this metabolic pathway belong to the order *Methanobacteriales*, *Methanococcales*, *Methanomicrobiales*, *Methanosarcinales* and *Methanopyrales* (Hedderich & Whitman, 2013). Moreover, Boetius et al. (2000) found that methane is reoxidised to CO₂. The bacteria capable of oxidising methane are unknown. Hoehler, Alperin, Albert, and Martens (2012), however, have suggested that a consortium of methanogens and sulfate reduction bacteria are involved. McGlynn et al. (2015) and Wegener, Krukenberg, Riedel, Tegetmeyer, and Boetius (2015) recently hypothesised a “direct interspecies electron transfer” (p. 587) in these consortia because no metabolite exchanges were found between methanogens and sulfate reduction bacteria.

Nutrient cycles and organic matter remineralisation are closely related. By making use of the energy derived from redox reactions, microorganisms increase their biomass and recycle nutrients. One important cycle is the nitrogen cycle, which controls the productivity of many marine ecosystems (Zehr & Kudela 2011). The oceanic nitrogen cycle involves the following pathways (Fig. 1): biological N₂ fixation, nitrification, anaerobic ammonia oxidation

(anammox), dissimilatory nitrate reduction, denitrification, assimilatory nitrate and nitrite reduction, ammonification or nitrogen remineralisation, and ammonia assimilation (Zehr & Kudela 2011).

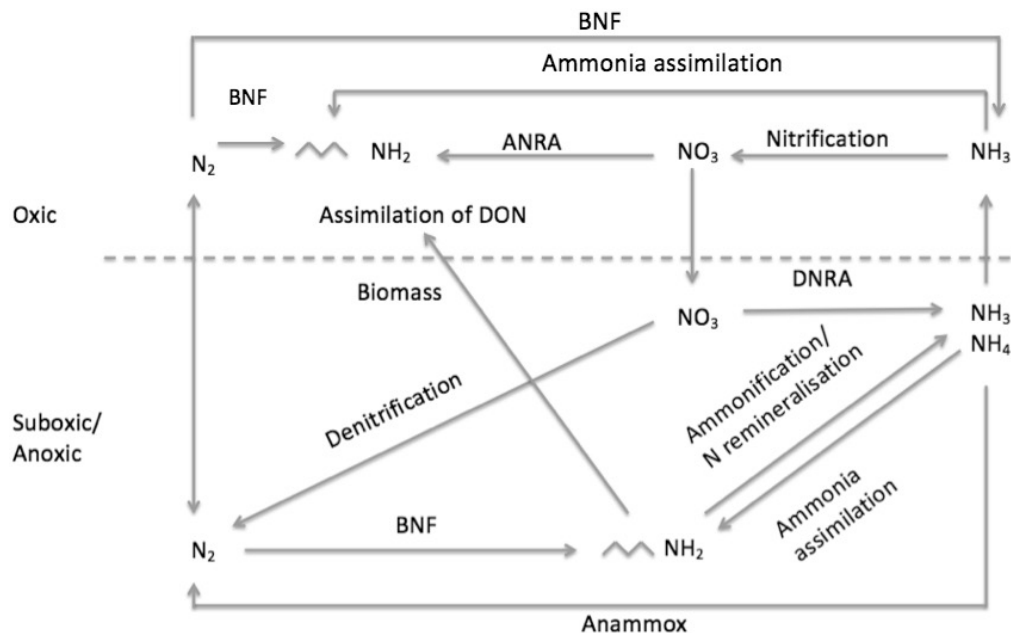


Figure 1. The nitrogen cycle. The dashed line represents the boundary between the oxic and the suboxic/anoxic zone. The symbol $\sim NH_2$ represents dissolved organic nitrogen. BNF, biological N_2 fixation; anammox, anaerobic ammonia oxidation; ANRA, assimilatory nitrate reduction to ammonium; DNRA, dissimilatory nitrate reduction to ammonium.

Microorganisms fix atmospheric N_2 in a step called biological N_2 fixation. Nitrogenase is the enzyme these microorganisms use to break the N_2 triple bond (Peters, Fisher, & Dean, 1995). Nitrogen-fixing microorganisms are called diazotrophs, which according to Corredor (1999) means “eater of nitrogen” (p. 6). Diazotrophs comprise heterotrophs (Zehr, Carpenter, & Villareal, 2000), some diatom endosymbionts (Carpenter et al., 1999), and phototrophic cyanobacteria such as *Trichodesmium* (Carpenter & Romans, 1991). The latter is believed to fix half of the total CO_2 in the marine environment (Mahaffey, Michaels, & Capone, 2005).

Organic nitrogen may undergo one of two pathways. In one of the pathways, heterotrophic or autotrophic organisms can assimilate dissolved organic nitrogen, such as urea (Baker, Gobler, & Collier, 2009) and amino acids (Rivkin & Putt, 2007; Zehr & Kudela, 2011). In a second pathway, heterotrophic bacteria can break organic nitrogen molecules to release

ammonium through deamination (Herbert, 1999). This step is known as ammonification or nitrogen remineralisation. The molecules that bacteria degrade include amino acids (Boon, Moriarty, & Saffigna, 1986), ribonucleic acids (Lomstein et al., 1998) and urea (Therkildsen, King, & Lomstein, 1996).

Ammonia and ammonium resulting from ammonification may undergo one of the three following pathways: firstly, ammonia or ammonium may be assimilated into organic nitrogen. This is the reverse step of ammonification and is known as ammonia assimilation. Blackburn and Henriksen (1983) suggested that this pathway explained the differences between the net production of ammonium and the net nitrogen flux from sediments. Dähnke, Moneta, Veuger, Soetaert, and Middelburg (2012) found that benthic microalgae play an important role in this step. The enzymes glutamine synthetase, glutamate synthase, and glutamate dehydrogenase catalyse this reaction (Brown and Herbert 1977).

Secondly, under anoxia, ammonia and ammonium may be oxidised to N_2 in a step discovered by Mulder, Graaf, Robertson, and Kuenen (1995), known as anammox. In anammox, anaerobic bacteria use nitrite (van de Graaf et al., 1995) or ferrous and manganese ions (Huang, Gao, Peng, & Tao, 2014) as electron acceptors. According to Devol (2015), anammox bacteria belong to the phylum Planctomycetes, mostly from the genus *Candidatus Scalindua* Schmid et al. 2003 (Lam & Kuypers, 2011).

Thirdly, ammonia may be oxidised to nitrite followed by the oxidation of nitrite to nitrate. Winogradsky (1981) demonstrated that different bacteria mediated each of the two steps of this reaction, known as nitrification. The first step, ammonia oxidation, is the focus of the present research. The enzyme ammonia monooxygenase catalyses the oxidation of ammonia (Alzerreca, Norton, & Klotz, 1999). The genes *amoA*, *amoB* and *amoC* encode the three subunits that comprise this enzyme. Such genes belong to the *amo* operon, which Alzerreca and co-workers (1999) sequenced contributing to a finer differentiation of ammonia-oxidising microorganisms. Some authors refer to this first step as 'ammonium oxidation' (e.g., Stark & Firestone, 1996; Ward, 2008; Wuchter et al., 2006). However, Suzuki et al. (1974), and Stein, Arp, and Hyman (1997) found that ammonia is the actual substrate of this enzyme rather than ammonium. When the seawater pH decreases, the balance between ammonia and ammonium changes, favouring the ionised ammonium form. Thus, changes in pH, for instance, due to ocean acidification, might have an effect on nitrification.

Purkhold et al. (2000) presented the phylogeny of all recognized species of ammonia-oxidising bacteria. This study demonstrated that they belong to two lineages within the

Proteobacteria: the Gammaproteobacteria *Nitrosococcus* and the Betaproteobacteria *Nitrosomonas*, *Nitrosospira*, *Nitrosolobus* and *Nitrosovibrio*. Moreover, Treusch et al. (2005) proved that archaea were also capable of oxidising ammonia. Könneke et al. (2005) later confirmed this with the isolation of marine ammonia-oxidising archaea. These ammonia-oxidising archaea belong to the Thaumarchaeota phylum. In fact, archaea dominate nitrification in oligotrophic environments, as Martens-Habbena, Berube, Urakawa, Torre, and Stahl (2009) demonstrated.

Nitrite-oxidising bacteria, such as *Nitrobacter*, *Nitrospina*, and *Nitrospira* mediate the second step of nitrification with the enzyme nitrite oxidoreductase (Lücker & Daims, 2013). Since the study conducted by Winogradsky (1981), nitrification had always been acknowledged as a two-step reaction; each step catalysed by different microorganisms. However, recent findings of Daims et al. (2015) suggested that a strain of the genus *Nitrospira* was capable of catalysing both steps. These authors discovered a strain of *Nitrospira* '*Candidatus Nitrospira inopinata*' that potentially contains the genes for ammonia oxidation and nitrite oxidation. They suggested the term 'comammox' to refer to this complete ammonia oxidation. Costa, Pérez and Kreft (2006) previously coined such term in a hypothetical scenario.

Nitrate resulting from nitrification may undergo two pathways apart from denitrification. Bacteria and cyanobacteria that possess nitrate and nitrite assimilation genes assimilate nitrate and reduce it to nitrite and ammonium (Flores, Frías, Rubio, & Herrero, 2005). This step is called assimilatory nitrate reduction to ammonium. Under anoxia, bacteria can reduce nitrate to ammonium. This step is known as dissimilatory nitrate reduction to ammonium. Sørensen (1978) suggested that this step is as important as denitrification in the benthic turnover of nitrate. Moreover, Gardner, McCarthy, An, and Sobolev (2006) suggested that this pathway together with nitrogen fixation are key steps to add and retain nitrogen in sediments. In this pathway, heterotrophic bacteria from the genus *Thioploca* use sulfur compounds as an electron donor. These bacteria oxidise sulfide to elemental sulfur and then sulfur to sulfate in a second step (Otte et al., 1999). Other bacteria that may undergo this pathway belong to the genera *Beggiatoa* and *Thiomargarita*. The former oxidise sulfide with internally stored nitrate (Preisler et al., 2007). The latter use nitrate and oxygen to oxidise sulfide (Schulz & Beer, 2002).

Various factors can inhibit or stimulate reaction steps in the nitrogen cycle (Herbert, 1999). In benthic nitrification, for instance, diatoms inhibit (Henriksen & Kemp, 1988; Risgaard-Petersen, Nicolaisen, Revsbech, & Lomstein, 2004) whereas bioturbation stimulates (Howe et al., 2004) the metabolism and growth of the nitrifying population. Henriksen and Kemp (1988)

conducted preliminary work in this field. These authors incubated sediment cores in continuously flowing seawater in a 12-hour dark and light cycle leaving a control in the dark. Differently from the sediment core incubated in the dark, a mat of diatoms developed in the sediment core that received light. Benthic nitrification rates were 90% lower in the diatom-colonised sediment than in the control, suggesting that photosynthesis of the diatom mat inhibited the benthic nitrifying population through the uptake of ammonia and CO₂. Photosynthesis increased the pore water pH and oxygen concentration. Although oxygen is necessary for nitrification, high concentrations can also inhibit nitrification, as Gundersen (1966) demonstrated in pure cultures of nitrifying bacteria supplied with oxygen. Because the ratio between oxygen consumption and nitrite formation remained nearly the same, Gundersen suggested that the assimilation of CO₂ rather than the oxidation of substrates, ammonia and nitrate, was inhibited. Such inhibition was due to electron donors reacting readily to oxidise substrates and being less available to assimilate CO₂.

Risgaard-Petersen et al. (2004) further investigated this inhibition by competition for nutrients, or “competitive exclusion” (p. 5535). They investigated the abundance of ammonia-oxidising bacteria and potential nitrification activity in microcosms with and without a mat of diatoms. As in the experiment above, a 12-hour dark and light cycle promoted the growth of diatoms. Ammonia-oxidising bacteria in the diatom-colonised sediments showed <20% of their potential activity, suggesting bacterial starvation. Such starvation resulted in a decreased abundance of ammonia-oxidising bacteria. This decrease in abundance was correlated with an increase in the abundance of diatoms. Similarly to Henriksen and Kemp (1988), Risgaard-Petersen et al. (2004) suggested that diatoms consumed most of the ammonia, limiting this nitrogen source for bacteria. Risgaard-Petersen et al. (2004), however, reported that diatom dark respiration (e.g., Burris, 1977) decreased the oxygenation of the sediment porewater during the hours of darkness. Only during the day, oxygen could penetrate beyond the subsurface of the sediment where ammonia-oxidising bacteria were present. Yet during the day, diatoms consumed ammonia and CO₂, thus starving ammonia-oxidising bacteria during light and dark.

Howe et al. (2004) demonstrated that, in contrast to diatom mats, bioturbation had a positive effect on benthic nitrification. The increased benthic denitrification rates stimulated by the mud lobster *U. deltaura* discussed above were due to increased nitrification. Ventilation of *U. deltaura* burrows increased the concentration of oxygen and ammonia in the pore water, which stimulated the growth and metabolism of benthic nitrifying bacteria. Since nitrate is the

final product of nitrification and substrate for denitrification, the increased production of nitrate stimulated the growth of denitrifying bacteria.

Response of microbial assemblages to environmental changes

Environmental changes have an effect on the structure and functioning of all aquatic (and terrestrial) ecosystems. A review on the literature of this topic by Allison and Martiny (2008) revealed that microbial assemblages have been altered in response to environmental stress in most global change experiments. Allison and Martiny (2008) suggested that the response of a microbial assemblage to an environmental change depends on its resistance, resilience and functional redundancy. If the ecosystem was disturbed, the composition of a resistant microbial assemblage is not altered. A resilient assemblage changes its structure after a disturbance but the original structure is later restored. A functionally redundant assemblage changes its original structure permanently; but its performance remains unaltered. If a microbial assemblage does not possess any of these characteristics, the environmental disturbance will alter the composition and functionality of the assemblage permanently.

For example, McKew, Taylor, McGenity, and Underwood (2011) investigated the response of microbial assemblages in sediments from saltmarsh creeks to desiccation. These authors desiccated sediments in the laboratory for 23 days followed by a 4-day rewetting. The assemblage structure did not change significantly during the first 14 days. Thus, the assemblage was resistant to desiccation for this period of time. By day 23, the abundance of halophilic bacteria increased because these bacteria were more adapted to the hypersaline environment caused by desiccation. The overall enzymatic activity decreased over time. After rewetting the sediments, the enzymatic activity recovered. However, the assemblage did not return to its original structure suggesting that the assemblage was functionally redundant.

Logue, Findlay and Comte (2015) suggested that adaptability and plasticity of microorganisms determine the response of the microbial assemblage to environmental changes. Moreover, Wallenstein and Hall (2012) proposed that the adaptation of assemblages to environmental changes depends on the relative contribution of the different species comprising the assemblage. These authors also proposed that such adaptation depends on the abundance and adaptability of specific traits within the assemblage. For instance, Mitchell et al. (2009) demonstrated that microorganisms possess adaptive traits for “environmental anticipation” (p. 220). That is to say, traits that, after a first environmental stimulus, enable microorganisms to adapt more rapidly to a second one. Traits might be passed from parents to

offspring or between species in the assemblage (horizontal gene transfer, Koonin, Makarova, & Aravind, 2001) accelerating adaptation (e.g., Rensing, Newby, & Pepper, 2002).

Furthermore, Wallenstein and Hall (2012) stated that the adaptability of assemblages is likely to be faster in environments that experience many climate fluctuations. For instance, Tait, Laverock, Shaw, Somerfield, and Widdicombe (2013) did not find significant changes in the structure of benthic microbial assemblages at low seawater pH treatments. These authors argued that the lack of changes could be a result of the already low and highly fluctuating pH within coastal sediments, thus supporting the statement above. Conversely, a low frequency of climate fluctuations would result in delayed assemblage adaptation. In this case, the assemblage would be obliged to perform in an unsuitable environment, possibly resulting in changes in the biogeochemical functioning of the assemblage (Wallenstein & Hall, 2012).

In addition to climate change, other anthropogenic environmental changes can alter the structure of microbial assemblages, such as eutrophication (Meyer-Reil & Köster, 2000). Because of the increased consumption of oxygen due to the stimulation of primary production by nutrient enrichment, benthic metabolic pathways of organic matter remineralisation become mostly anaerobic. Mahmoudi et al. (2015) for instance, found that sulfate-reducing bacteria dominated surface sediments in the Caspian Sea, which is a heavily polluted and eutrophic environment.

Faunal activity in sediments can also change the environment, resulting in changes in the structure of microbial assemblages. Laverock et al. (2010), for instance, found significant differences in the structure of benthic microbial assemblages related to the mud lobster *U. deltaura* and the burrowing shrimp *C. subterranea*. The structure of assemblages in the sediment surrounding burrows was different from that of sub-surface sediment, but similar to that of surface sediment. These findings suggested that particle mixing and burrow irrigation altered the distribution of bacteria.

Such findings were also consistent with the radial distribution of oxic, suboxic and anoxic zones around burrows mentioned before (Aller, 1994; Aller & Aller, 1998; Jørgensen & Revsbech, 1985; Kristensen et al., 2012; Larsen et al., 2011; Zhu et al., 2006). The redox potential distribution from surface to sub-surface sediment is similar to the distribution from the burrows' lumen to sub-surface sediment. This distribution around burrows suggests that organic matter remineralisation occurs radially around the burrow rather than with sediment depth (e.g., Aller, 1994). Therefore, the structure of the assemblages around burrows was expected to be similar to that of surface sediment. In sub-surface sediment, microbial

assemblages were expected to be different because the anoxic environment only allowed anaerobic remineralisation.

Effect of anthropogenic CO₂ on the ocean's pH and nutrient cycling

Seawater absorbs atmospheric CO₂ (Equation 2), which reacts with water to form carbonic acid (Equation 3). This carbonic acid is then dissociated into bicarbonate and hydronium (Equation 4), which can be further dissociated into carbonate and hydronium (Equation 5). Although these reactions occur simultaneously, the formation of bicarbonate (Equation 4) is the most thermodynamically favoured in the ocean. In fact, the ratio between carbonic acid and bicarbonate in Equation 4 is 1:170, whereas the ratio of bicarbonate and carbonate in Equation 5 is 9:1. This means that ~90% of the dissolved inorganic carbon in the ocean is bicarbonate, followed by ~10% of carbonate, and only <1% of carbonic acid and CO₂ (Mackie, McGraw, & Hunter, 2011; Riebesell, Fabry, Hansson, & Gattuso, 2010):



Since the industrial revolution 200 years ago, emissions from land use, industrial processes, fossil fuel and cement emissions, have increased the concentration of atmospheric CO₂ (Canadell et al., 2007; Raupach et al., 2007). The concentrations of gaseous and aqueous CO₂ need to be in equilibrium (Equation 2) and thus the ocean has absorbed ~30% of this CO₂ (IPCC, 2014). Such absorption of CO₂ has resulted in an increase of the concentration of hydronium by about 30% because the formation of the most abundant carbonate species, bicarbonate, is accompanied by the formation of hydronium (Equation 4). In addition, the formation of carbonate (Equation 5) is less favoured, decreasing the buffering capacity of the seawater. A decrease of 1 pH unit means that the concentration of hydronium has increased 10 times. Thus, the accumulation of hydronium and removal of carbonates in the seawater has resulted in a decrease of 0.1 units of the seawater pH in the last 200 years (IPCC, 2014, Mackie et al., 2011). Scientists project that, during the next century, the ocean's pH will continue to decrease by 0.30 to 0.32 units (scenario RCP6.0, IPCC, 2014).

Waldbusser and Salisbury (2014) draw a distinction between "carbonate weather" and "carbonate climate" (p. 224). They defined any local daily or seasonal fluctuations of the

seawater carbonate chemistry as carbonate weather and they used the term carbonate climate for regional fluctuations over years or centuries. The effect that ocean acidification, or the future carbonate climate, will have on coastal carbonate weather is difficult to predict because carbonate weather is site-dependent and thus carbonate chemistry responses are variable around the globe (Hofmann et al., 2011).

Numerous factors determine the variability of carbonate weather. For instance, Salisbury, et al. (2009) found that riverine discharge of freshwater to coastal waters decreased the concentration of dissolved inorganic carbon in the Gulf of Maine. River inputs also increase the concentration of nutrients that may result in eutrophication as studied by Lohrenz et al. (1997). These authors found an elevated concentration of nutrients and high primary productivity due to discharges of the Mississippi River into the northern Gulf of Mexico. This can result in variations in carbonate chemistry, as Sunda and Cai (2012) demonstrated. They found that the seawater's total alkalinity decreased and the concentration of dissolved inorganic carbon increased in bottom waters as a result of eutrophication. The reason was that the elevated amount of organic matter from primary producers was respired by heterotrophic bacteria, which released CO₂ through remineralisation. Such elevated concentration of CO₂ increased the concentrations of dissolved inorganic carbon but decreased the concentration of carbonates, thus decreasing alkalinity.

In addition, upwelling of nutrient-enriched deep seawater increases the partial pressure of CO₂ (Evans, Hales, & Strutton, 2011; Hauri et al., 2013). Hauri et al. (2013) also demonstrated increased concentration of dissolved inorganic carbon and fluctuations in calcium carbonate saturation state due to upwelling. Atmospheric inputs further alter the coastal seawater carbonate weather. For instance, rain increases the uptake of atmospheric CO₂ (Turk et al., 2010) and the deposition of atmospheric nitrate and ammonia due to agriculture or combustion of fuels increase and decrease total alkalinity, respectively (Doney et al., 2007).

Sediments possess a natural spatial distribution in carbonate chemistry, which results from biogeochemical reactions. Products resulting from such reactions either increase or decrease pore water pH (Jourabchi, Cappellen, & Regnier, 2005; Soetaert, Hofmann, Middelburg, Meysman, & Greenwood, 2007) and alkalinity (Wolf-Gladrow, Zeebe, Klaas, Körtzinger, & Dickson, 2007). For instance, aerobic consumption of organic matter, which takes place in the oxic zone, decreases the pore water pH. However, photosynthesis, which takes place in the upper oxic zone, increases the pH (Soetaert et al., 2007). Reactions occurring in the suboxic zone produce and consume similar quantities of protons, thus stabilising the pH.

For example, denitrification and iron oxidation produce protons, whereas dissolution of calcite and reduction of iron and manganese oxides, coupled to sulfide oxidation, consume protons (Jourabchi et al., 2005). In the anoxic zone, the pore water pH decreases again due to sulfate reduction until all organic matter is consumed (Jourabchi et al., 2005).

Spatial distribution of pore water total alkalinity is due to the total concentration of major ions and acid–base species; or in other words, due to the excess of proton acceptors over proton donors (Wolf-Gladrow et al., 2007). For instance, the assimilation of nitrate or nitrite by photoautotrophs, which inhabit the upper oxic zone, increases total alkalinity; whereas their assimilation of ammonia as a nitrogen source decreases such alkalinity. Nitrification, which occurs in the oxic–suboxic interface, decreases total alkalinity with the formation of nitrate. In the suboxic zone, however, total alkalinity increases due to the uptake of this nitrate for denitrification. In the anoxic zone, methane oxidation by sulfate reduction increases alkalinity. Apart from the alterations in the spatial distribution of potential redox, bioturbation contributes to fluctuations in benthic carbonate chemistry due to increased rates of remineralisation, which result in increased availability of CO₂ (Santos, Eyre, & Huettel, 2012).

The carbon cycle is coupled to other nutrient cycles and remineralisation pathways in the marine ecosystem (Hutchins, Mulholland, & Fu, 2009). The effect that ocean acidification could have on the organisms involved in such pathways may depend on their metabolic requirements. For instance, elevated concentration of CO₂ is beneficial for autotrophs, because of their dependence on inorganic carbon (e.g., Hutchins et al., 2007; Kranz et al., 2010; Shetye, Sudhakar, Jena, & Mohan, 2013). As a consequence, some heterotrophs indirectly benefit due to the increased autotrophic production of organic carbon. This is known as ‘CO₂ fertilisation’ (Hutchins et al., 2009).

In contrast, organisms that depend on calcium carbonate to build their shells could be negatively affected (Zeebe, 2012). The reason is that a greater concentration of CO₂ in seawater decreases the concentration of carbonate (Equation 5) and increases the dissolution of calcium carbonate (Equation 6, Mackie et al., 2011). Comeau, Carpenter, Lantz and Edmunds (2015), for example, found a 59% reduction of calcification in a coral reef community under high concentrations of CO₂, ~1300 µatm.



Despite their close relation to the carbon cycle, the phosphorus and silicon cycles have not shown significant alterations due to elevated CO₂ (e.g., Milligan, Varela, Brzezinski, & Morel, 2004; Tanaka et al., 2008). For instance, Tanaka et al. (2008) did not find significant differences in total particulate phosphorus concentration and phosphate turnover time at three seawater CO₂ treatments, 350, 700 and 1050 μatm. These authors concluded that the future seawater carbonate climate is not likely to alter the biogeochemistry of phosphorus. Moreover, Milligan et al. (2004) found no significant difference in the molar quantity of silica in diatoms (silica quota) between atmospheric and high CO₂ partial pressure cultures. The diatom investigated was *Thalassiosira weissflogii* Frixel & Hasle, 1977 grown under high (750 μatm) and atmospheric (370 μatm) CO₂ partial pressures. The authors concluded that ocean acidification would not alter the silica cycle. Widdicombe and Needham (2007) supported this conclusion. These authors found no significant changes in silicate sediment fluxes at different seawater pH treatments, of 5.6, 6.5, 7.3 and 7.9.

One nutrient cycle that may change under the future carbonate climate is the nitrogen cycle (Hutchins et al., 2009). In this cycle, the future elevated concentration of CO₂ may have a positive effect on biological N₂ fixation. For example, cyanobacteria of the genus *Trichodesmium* were abundant in environments with elevated CO₂ and showed high nitrogen fixation rates (Hutchins et al., 2007; Kranz et al., 2010; Shetye et al., 2013). Gazeau et al. (2014), however, demonstrated no significant differences in denitrification rates in sediments exposed to CO₂-supplied seawater. These authors incubated sediments collected near the harbour in Kongsfjorden, a glacial fjord in the Arctic (Svalbard), in seawater supplied with 317, 540, 760, 1120 and 3000 μatm of CO₂. They found a decrease in nitrite and ammonium release, which was attributed to an enhanced anammox activity. Yet this enhanced activity was found only in the most concentrated CO₂ treatment, which was an extreme scenario since there are no projections for this CO₂ concentration for the next 300 years (IPCC, 2014). Therefore, although anammox activity was altered at this extreme scenario, neither denitrification nor anammox were affected by the projected seawater pCO₂ for the next century, that of 760 μatm. In contrast, nitrification rates might decrease in the future carbonate climate because the availability of ammonia, which is the substrate for the first step of nitrification, decreases at a lower pH (Suzuki et al., 1974; Stein et al., 1997). Decreased pelagic nitrification rates in acidified seawater were confirmed by Beman et al. (2011); Beman, Popp, and Alford (2012); Bowen et al. (2013); Fulweiler, Emery, Heiss, and Berounsky (2011); and Huesemann, Skillman, and Creclius (2002). The effect of acidified seawater on benthic nitrification, however, is still unclear.

Kitidis et al. (2011) conducted the first systematic study on the effect of seawater pH on benthic nitrification, and more specifically, on benthic ammonia oxidation. These authors demonstrated in a laboratory experiment, and in the environment of a natural CO₂ vent, that benthic ammonia oxidation rates were not significantly altered when exposed to acidified seawater. The laboratory experiment included two types of sediment exposed to seawater pH treatments, ranging from 6.1 to 7.9 and a control at 8.0. At the natural CO₂ vent, the sediments were investigated at three sites ranging from pH 7.6 to 8.2. Kitidis and co-workers concluded that the reason for the non-significant effect of seawater acidification on benthic ammonia oxidation rates in the laboratory experiment could be that the seawater pH perturbation was buffered within the sediments. In addition, the microbial ammonia-oxidising assemblages could be already adapted to occasional low pH conditions. To explain the absence of differences in ammonia oxidation rates in the sites investigated at the natural CO₂ vent, the authors concluded that the ammonia-oxidising assemblage could have been adapted through genetic adaptation or adjustments in the microbial assemblage over time.

Given that bioturbation enhances the sediment–seawater exchange of nutrients (Kristensen, 2000), Laverock et al. (2013) investigated the effect of pH decreases on ammonia oxidation rates in sediments inhabited by the mud lobster *U. deltaura*. They incubated such sediments in seawater at pH 8.10, 7.90, 7.70, 7.35 and 6.80. Ammonia oxidation rates were inhibited in the sediment surrounding the burrows by >79% at pH ≤7.9 but not in surface sediment. Yet in the control, ammonia oxidation rates were five times higher in the sediment surrounding the burrows than in surface sediment, suggesting that bioturbation was stimulating nitrification. Laverock and co-workers explained the inhibition of ammonia oxidation rates in the sediment surrounding the burrows as a possible change in the behaviour of *U. deltaura* due to the seawater pH treatments that could have altered the physicochemical conditions within the burrows. For instance, over-beating of appendages to increase oxygen supply (Donohue et al., 2012) or flushing of metabolic waste may have increased the concentration of toxic nutrients, such as sulfides that have been shown to inhibit nitrification (Joye & Hollibaugh, 1995). Laverock and co-workers concluded that the relationship between bioturbation and benthic microorganisms would have a significant effect on the benthic ecosystem response to ocean acidification.

In contrast to the findings by Kitidis et al. (2011) and Laverock et al. (2013), Braeckman et al. (2014) determined a 94% reduction in benthic nitrification rates in two types of sediment exposed to seawater at pH 7.7. The sediments investigated were fine sandy and coarse permeable sediments, which were collected from two sites in the Belgian part of the North Sea

before an annual phytoplankton bloom. However, no significant reduction in such rates was found in sediments sampled from the same sites during a phytoplankton bloom. Braeckman and co-workers argued that the variability among replicates in the latter could have prevented the decrease in nitrification rates observed from being statistically significant. These authors also argued that comparing their results with those of Kitidis et al. (2011) and Laverock et al. (2013) was difficult because of seasonal differences during sampling and differences in the types of sediments investigated. For instance, Kitidis et al. (2011) collected muddy and permeable sediments before and after an annual phytoplankton bloom, respectively. Laverock et al. (2013) collected muddy sediments after the phytoplankton bloom.

Laverock et al. (2013) also investigated the effect of the acidified seawater on the abundance of archaeal and bacterial *amoA* genes and found no significant differences in either the sediment surrounding the burrows or surface sediment. The lack of changes in microorganisms' abundance, along with the low ammonia oxidation rates in the sediment surrounding the burrows, suggested an inhibition of metabolic activity. Such low metabolic activity could be a result of decreased transcription or a post-transcriptional modification that yielded lower rates as pH declined.

Similar to Laverock et al. (2013), Tait et al. (2014) found no significant differences in the abundance of *amoA* genes of ammonia-oxidising archaea and bacteria in Arctic Ocean sediment exposed to acidified seawater. Tait et al. incubated sediment cores in seawater at pH 8.1 (control), 7.8, 7.7, 7.6 and 7.2 (380, 540, 760, 1120, and 3000 μatm of pCO_2 , respectively). These authors, however, presented for the first time evidence for an effect of ocean acidification on ammonia oxidiser gene function. They found that the abundance of *amoA* transcripts in ammonia-oxidising bacteria at pH 7.7 was significantly lower than that under conditions of pH 7.8 and 8.1. Because the abundance of *amoA* genes did not change, they suggested there was either less transcription or the transcripts degraded faster at that specific pH. Yet, there was no difference between the abundances of *amoA* transcripts of ammonia-oxidising archaea at any pH treatment. Tait and co-workers also found that the structure of the ammonia-oxidising bacterial assemblage at pH 7.8 and pH 7.7 differed from that at pH 7.2, 7.6 and 8.1. The ammonia-oxidising archaeal assemblage, however, did not change. The authors concluded that benthic ammonia-oxidising bacteria were more susceptible to pH decreases than ammonia-oxidising archaea.

More recent evidence from Watanabe et al. (2015) revealed no significant changes in benthic ammonia oxidation rates at the injection zone of a controlled sub-seabed CO_2 leakage experiment that was conducted at the west coast of Scotland. They injected CO_2 *in situ*

through a pipe during one month, reaching a maximum reduction of 0.84 pH units in the surface sediment. The lack of significant differences in benthic ammonia oxidation rates at the injection zone was consistent before, during and after the injection. Although they found no significant changes at the injection zone, they found a reduction in ammonia oxidation rates at zones 25, 75 and 450 m away from the injection zone during and after the injection. However, such reduction was due to seasonal changes rather than the CO₂ injection. Sediment from the injection zone was later exposed in the laboratory to seawater containing high CO₂ partial pressures: 50,000 and 200,000 μatm (pH 6.1 and 5.5, respectively). Benthic ammonia oxidation rates decreased significantly at both CO₂ concentrations. Watanabe and co-workers (2015) suggested that a pCO₂ of 50,000 μatm surpassed the pore water buffering capacity. They concluded that the effect of a leakage in CO₂ would depend on the amount of CO₂ released and the pore water buffering capacity.

Watanabe et al. (2015) also found that the relative abundances of archaeal and bacterial *amoA* genes and transcripts changed overtime. The abundance of archaeal *amoA* genes was higher after the injection than before and during the injection. In contrast, the abundance of bacterial *amoA* genes was higher before the injection than during and after the injection. This trend, which was attributed to seasonal changes rather than CO₂ leakage, was consistent among the injection zone and 25, 75 and 450 m away from the injection zone.

In the most recent study in this field, Raulf et al. (2015) determined that the relative abundance of benthic nitrifying bacteria was lower in sites with high, than in sites with low, partial pressure of CO₂ at a natural CO₂ vent. Conversely, the relative abundance of benthic nitrifying archaea, Thaumarchaeota, was high in sites with elevated CO₂ concentrations. Benthic nitrifiers appear to be somewhat resistant to elevated concentrations of CO₂ (e.g., Tait et al., 2014). Raulf et al. (2015) demonstrated, however, that such resistance might change after years of exposure to elevated concentrations of CO₂.

Perturbation experiments for ocean acidification research

To increase our ability to predict how CO₂ emissions could change marine ecosystem functioning, researchers have conducted experiments *in situ* (e.g., Calosi et al., 2013; Gordon, Beaumont, MacDiarmid, Robertson, & Ah Yong, 2010; Martz, Daly, Byrne, Stillman, & Turk, 2015; Raulf et al., 2015, Watanabe, 2015) and in the laboratory (e.g., Braeckman et al., 2014; Gazeau et al., 2014; Tait et al., 2014; Widdicombe & Needham, 2007). Perturbation experiments are one of the most common approaches used to investigate possible responses of organisms to ocean acidification (Gattuso, Gao, Lee, Rost, & Schulz, 2010). For that purpose,

various methods are used to decrease the seawater pH, either *in situ* or in laboratory experiments. In one such method, automated instruments open and close a valve to control the addition of CO₂, or a mixture of pure CO₂ and air, to seawater and the seawater pH is monitored continuously with a pH electrode. Although this is an efficient method to maintain the partial pressure of CO₂ within a narrow range, one disadvantage is that the pH electrode could drift and thus it must be calibrated frequently (Gattuso et al., 2010). Other methods involve the addition of acids or bases, such as hydrogen chloride or sodium hydroxide, or the addition of sodium carbonate or bicarbonate. According to Gattuso et al. (2010), however, gas bubbling is one of the most effective methods to increase the concentration of dissolved inorganic carbon without changing the total alkalinity.

One drawback common to these methods is that the carbonate chemistry required for the experiment can only be achieved at the beginning of the perturbation in recirculation systems. The metabolism of organisms can alter such carbonate chemistry over time, due to photosynthesis, respiration, and nutrient uptake and release (Gattuso et al., 2010). To avoid these alterations, flow-through systems have been used to discard the seawater containing metabolic products through an outflow; while an inlet replaces this seawater with fresh seawater (e.g., Gazeau et al., 2014; Widdicombe & Needham, 2007).

In situ perturbation experiments involve the manipulation of carbonate chemistry to investigate the response of organisms in their natural habitat (Barry, Hall-Spencer, & Tyrrell, 2010). Although *in situ* perturbation provides a more realistic response of organisms than laboratory experiments do, most environmental variables cannot be controlled and the variance in the response of the organisms studied is usually high (Barry et al., 2010).

Laboratory experiments have been conducted in single-species cultures or in multiple-species mesocosms (Widdicombe, Dupont & Thorndyke, 2010). In single-species cultures, the isolated individuals or species are exposed to one or more controlled variables. The advantage of such experiments is that the response of the organisms studied is not confounded by other variables, such as biological interactions. In addition, replication is easy to achieve, thus increasing the statistical power. However, because the organisms are not in their natural habitat, their response to the treatment might be different to that in their natural environment (Widdicombe et al., 2010).

In mesocosm experiments, undisturbed samples collected from a natural ecosystem are exposed to controlled perturbation in the laboratory (Widdicombe et al., 2010). In contrast to single-species experiments, multiple-species mesocosms allow biological interaction, which

increases the realism in the experiment, but replication is more difficult to achieve. Widdicombe et al. (2010) summarised some of the potential pitfalls researchers may encounter in laboratory experiments, either single- or multiple-species experiments. For instance, experimental stress could have an effect on the response of the organisms being investigated. Organisms may alter their behaviour or physiology after an environmental change, and such alteration may depend on the speed at which the environmental change occurred. Although there is no current consensus on the duration, a period of acclimatisation should be reported on and considered for the interpretation of results.

To elucidate the effect of ocean acidification on microbially-mediated ecological processes, researchers have used perturbation experiments to investigate changes in pore water pH and oxygenation (e.g., Braeckman et al., 2014; Widdicombe et al. 2013), sediment–seawater nutrient fluxes (e.g., Gazeau et al., 2014; Widdicombe et al., 2009; Widdicombe & Needham, 2007), and metabolic activity and microbial assemblages using chemical and molecular techniques (e.g., Laverock et al., 2013; Tait et al., 2014; Watanabe et al., 2015; Raulf et al., 2015). These approaches complement each other and increase our understanding to predict potential future changes in the biogeochemistry of sediments due to ocean acidification.

Section II

Molecular techniques to assess metabolic activity and assemblage composition

In recent years, molecular techniques have broadened the range of approaches in ecology research. From the classic polymerase chain reaction (PCR) to contemporary high-throughput technologies, the application of such approaches has provided scientists with information to elucidate ecological processes. In this section, I review the molecular approaches that I have used to study the potential effect of ocean acidification on ammonia oxidation.

Polymerase chain reaction (PCR)

Since the introduction of PCR (Mullis et al., 1986; Saiki et al., 1988), this technique has been used to amplify fragments of deoxyribonucleic acid (DNA). PCR is a step-wise process in which a double-stranded DNA (dsDNA) fragment is denatured (separated) with heat. One PCR requires two primers, which are short sequences of DNA designed to amplify the region of interest. Each primer is complementary to one of the two DNA strands. After denaturation, each primer anneals to its corresponding denatured strand and the DNA polymerase synthesises the rest of the complementary strands. This step is known as extension and gives

rise to two dsDNA fragments identical to the original (Garibyan & Avashia, 2013).

In a second cycle, the two new dsDNA fragments are denatured and the steps repeated to produce four dsDNA fragments. This is repeated 20 to 50 times to produce millions of copies or 'amplicons'. In metagenomics, these amplicons are frequently used as a first step to other techniques requiring large amounts of DNA. For example, PCR amplification is a common prerequisite for DNA sequencing (e.g., Dinsdale et al., 2008; Lejzerowicz et al., 2015; Tait et al., 2014).

The typical reaction mix to run a PCR comprises the primers, DNA polymerase active at elevated temperatures (e.g., *Taq* polymerase), magnesium, deoxyribonucleotide triphosphates (dNTPs), buffer and water (Mullis et al., 1986; Saiki et al., 1988). Other reagents have been used to increase the efficiency of the reaction and mitigate PCR-inhibiting contaminants. For example, interfering substances present in DNA templates, such as extraction residues, often inhibit PCR reactions (Schrader, Schielke, Ellerbroek, & Johne, 2012). Bovine serum albumin (BSA) has been used to overcome the presence of contaminants in DNA from stool (Höss, Kohn, Pääbo, Knauer, & Schröder, 1992), bloodstains (Akane, Matsubara, Nakamura, Takahashi, & Kimura, 1994), ancient bones (Höss, & Pääbo, 1993), sediment and soil (Rojas-Herrera, Narvaez-Zapata, Zamudio-Maya, & Mena-Martinez, 2008; Romanowski, Lorenz, & Wackernagel, 1993).

Exogenous DNA commonly contaminate PCR reagents, which is a particular concern when amplifying 16S rRNA genes. Contaminating DNA can amplify alongside the DNA of interest, creating misleading results. Many strategies have been used to eliminate this contamination from the PCR reagents; for example, UV inactivation (Sarkar & Sommer, 1991), restriction enzymes (Mohammadi, Reesink, Vandenbroucke-Grauls, & Savelkoul, 2003), or the use of commercial enzymes such as DNase I (Life Technologies). A method that Rueckert and Morgan (2007) developed consists of the treatment of the PCR reagents with ethidium monoazide. When exposed to intense light (wavelength >400 nm), this molecule intercalates with the dsDNA molecules, disabling them from being PCR amplified.

DNA sequencing

Since the first DNA nucleotide sequence elucidated by Sanger et al. (1977), developers have worked on faster and more accurate instruments to sequence DNA fragments or genomes. The Ion Torrent's principle is based on voltage changes (Rothberg et al., 2011). In this technique, the DNA fragments attach to microbeads. Such microbeads deposit into one of the millions of wells contained in a semiconductor chip. A solution containing one of the four

nucleotides fills the wells. Whenever the nucleotide finds its complementary nucleotide, this nucleotide attaches to the DNA chain releasing one H^+ . This H^+ release changes the pH and thus the voltage in the solution. The instrument reads and interprets this voltage change and the same procedure is repeated for the other three nucleotides.

Ion Torrent and other high-throughput sequencing approaches have been used to investigate the structure of microbial assemblages in numerous environments. For example, Aravindraja, Viszwapriya, and Pandian (2013) investigated the structure of bacterial assemblages of geographically similar but diverse marine environments: sediment, seawater, seaweed, and seagrass. In the study of ocean acidification, sequencing has been used to study the response of microbial assemblages to elevated pCO_2 . For instance, Kerfahi et al. (2014) and Raulf et al. (2015) sequenced samples of sediment to investigate changes in the structure of benthic microbial assemblages in natural CO_2 vents.

The 16S rRNA gene is the gene most commonly sequenced to assess the composition of microbial assemblages in environmental samples (Olsen, Lane, Giovannoni, & Pace, 1986). Nine hypervariable regions flanked by highly conserved regions comprise this gene (Baker, Smith, & Cowan, 2003). The sequence of these hypervariable regions is unique to each species and thus can be used for identification. The conserved regions are easily targeted with universal primers enabling PCR amplification. Sequencing of this region has not only retrieved information of the structure of the microbial assemblages in environmental samples (e.g., Aravindraja et al., 2013) but has also enabled scientists to elucidate the role of unculturable microorganisms in marine biogeochemistry, such as the importance of archaea in ammonia oxidation (Schleper, Jurgens, & Jonscheit, 2005).

Quantitative polymerase chain reaction (qPCR)

Quantitative PCR or 'real-time PCR' measures the amplification of PCR product and estimates the number of gene copies prior to amplification (Heid, Stevens, Livak, & Williams, 1996). For that, serially diluted DNA of known concentrations and DNA templates to be quantified are run in one set of reactions. A fluorescent probe hybridises to dsDNA to increase the fluorescence with each amplification cycle. The fluorescence at a given threshold cycle is plotted for each of the standards to build a standard curve. The actual concentration of DNA of each sample is obtained by interpolation of the standard curve. SYBR green is one of the most commonly used fluorescent dyes and Ririe, Rasmussen and Wittwer (1997) used it for the first time in a qPCR assay.

In the study of sediments, qPCR has been used to determine the abundance of species

in an assemblage based on a gene sequence (e.g., Grüntzig, Nold, Zhou, & Tiedje, 2001; Leloup et al., 2009; Magalhães, Machado, & Bordalo, 2009; Park, Park, & Rhee, 2008; Schippers & Neretin, 2006; Tait et al., 2014). For example, by determining the abundance of *amoA* genes, Tait et al., 2014 determined the abundance of ammonia-oxidising microorganisms in sediment.

The high sensitivity of this technique could be as much a weakness as a strength. Small amounts of contamination can be translated into large amounts of contamination after amplification (Garibyan & Avashia, 2013). In addition, as in PCR, several compounds inhibit qPCR reactions. Opel, Chung and McCord (2009), for instance, have demonstrated inhibition by calcium, humic acids, collagen, melanin, hematin, and tannic acids. One more limitation is that DNA is present in the environment as active and inactive genes (e.g., Levy-Booth et al., 2007; Ogram, Sayler, GustIn, & Lewis, 1988). Inactive genes can be amplified causing misleading results. The results from qPCR must be studied in conjunction with an approach seeking for active genes if studying functional pathways, such as reverse transcription quantitative polymerase chain reaction.

Reverse transcription quantitative polymerase chain reaction (RT-qPCR)

Researchers use RT-qPCR to determine the abundance of active genes, or the relative expression of such genes (Gibson, Heid, & Williams, 1996). For that purpose, the primary analyte is RNA, which is the template to synthesise complementary DNA (cDNA). The synthesis of DNA from an RNA template is known as reverse transcription (Baltimore, 1970; Temin & Mizutani, 1970). The principle of detection of the abundance of RNA transcripts is the same as explained in the qPCR section. In this case, the instrument detects the signal from the amplified cDNA.

RT-qPCR can be performed as a one-step or a two-step assay. In a one-step RT-qPCR, both reverse transcription and qPCR occur in the same reaction tube (Gibson et al., 1996). In a two-step approach, the RNA is first reverse transcribed and the cDNA is then quantified in a separate reaction (Wacker & Godard, 2005). In the study of sediments, RT-qPCR has been used to assess the abundance of 16S rRNA subunit or mRNA transcripts (e.g., Freitag & Prosser, 2003; Ketil & Andreas, 2006; Nogales, Timmis, Nedwell, & Osborn, 2002; Tait et al., 2014). Comparison between qPCR and RT-qPCR results retrieve information on the activity of genes and cells. For example, Tait et al. (2014) found low *amoA* transcripts at an acidified treatment compared to a control but *amoA* genes remained unchanged. Comparing these results the authors suggested a repressed transcription or degradation of transcripts.

Comparing one-step RT-qPCR with two-step RT-qPCR, the latter is cheaper and

minimises manipulation, thus contamination or human error decrease. Two-step RT-qPCR allows the storage of cDNA for further repetitions or different analysis (Wong & Medrano, 2005). Wacker and Godard (2005) found that both approaches yielded similar efficiencies and had similar accuracy and linearity in standard curves. These authors showed, however, that one-step RT-qPCR had higher sensitivity than two-step method in certain genes, such as PolR2A, a commonly used reference gene (e.g., Saviozzi et al., 2006).

Research questions and hypotheses

Few studies (Braeckman et al., 2014; Kitidis et al., 2011; Laverock et al., 2013; Tait et al., 2014) on the effect of ocean acidification on benthic ammonia oxidation had been published prior to the development of my research questions. These studies presented contrasting evidence on such effect. The design of my study was influenced by the evidence presented by Tait et al. (2014) who showed an effect of a seawater pH decrease on bacterial ammonia oxidation in Arctic sediment. Benthic ammonia-oxidising archaea, however, did not seem to be altered by any of the pH treatments investigated (Tait et al., 2014).

I thus developed two research questions based on the projection that seawater pH will decrease by ~0.3 units during the next century (IPCC, 2014) and considering that:

(1) Ammonia oxidation is catalysed by the archaeal and bacterial enzyme ammonia monooxygenase (Alzerreca et al., 1999);

(2) Ammonia rather than ammonium is the actual substrate for this enzyme (Suzuki et al., 1974; Stein et al., 1997);

(3) A pH decrease favours the ionised ammonium form so that ammonia becomes less available; and

(4) Low seawater pH inhibits pelagic ammonia oxidation (e.g., Beman et al., 2011; Beman et al., 2012; Bowen et al., 2013; Fulweiler et al., 2011; Huesemann et al., 2002) but the effect of low seawater pH on benthic ammonia oxidation is less understood (Braeckman et al., 2014; Kitidis et al., 2011; Laverock et al., 2013; Tait et al., 2014).

I asked the following two questions:

Question 1: Does an experimental decrease in seawater pH alter the composition of the microbial assemblage of ammonia-oxidising archaea and bacteria in coastal sediment?

Question 2: Does an experimental decrease in seawater pH alter the expression level of the ammonia monooxygenase gene in archaea and bacteria in coastal sediment?

For the development of the hypotheses, I considered two additional aspects:

(1) The study by Tait et al. (2014) was performed in sandy mud sampled at a 4-m depth in a different climate region from ours. I chose to study two types of coastal sediment that were contrasting in regard to their granulometry, and water and organic matter content, and

(2) Due to the large size of the ammonia monooxygenase gene, I sought for alterations in the subunit A of the gene (*amoA*).

I thus hypothesised that:

Hypothesis 1: An experimental decrease in the pH of the sediment-overlying seawater will change the structure of the assemblage of ammonia-oxidising archaea and bacteria in two types of coastal sediment.

Hypothesis 2: An experimental decrease in the pH of sediment-overlying seawater will lower the expression level of the *amoA* gene in ammonia-oxidising archaea and bacteria in two types of coastal sediment.

To test both hypotheses, I needed to establish a new facility to incubate sediment cores. To test hypothesis 1, I sequenced DNA extracted from the sediment with Ion Torrent sequencing. To test hypothesis 2, I determined the abundance of archaeal and bacterial *amoA* genes and transcripts using qPCR and RT-qPCR assays, respectively. I used the fluorescent probe SYBR green for both assays.

The aim of my research was to contribute to a better understanding of the effect of ocean acidification on nitrogen cycling in coastal sediment. Such understanding would be of relevance to predict the functioning of the future coastal ocean, to develop strategies to minimise the effects of ocean acidification and to develop countermeasures to help prevent the potentially negative projections from becoming a future reality.

Material and methods

Experimental design

I simulated the carbonate chemistry of the future seawater in the laboratory where I incubated sediment cores of two types. One type of sediment was collected from the Tauranga Harbour estuary; the other type was coastal sediment from Man O'War Bay. In the following text, I refer to sediment cores collected from Tauranga Harbour as estuarine sediment and sediment cores collected from Man O'War Bay as coastal sediment.

I collected a total of 31 sediment cores, 15 estuarine and 16 coastal cores (one of the 16 coastal cores was sacrificed and used for a trial of molecular analyses). I submerged half of them in each of two seawater-circulating systems (hereafter, experimental units) under controlled conditions for two weeks. The pH of the seawater in both experimental units was maintained at 8.1. I then sacrificed five cores of each type of sediment and investigated them (hereafter, time-zero analyses), leaving five estuarine and five coastal sediment cores in each experimental unit. In the course of two weeks, I stepwise lowered the pH of the seawater by 0.02 units per day in the Treatment unit, until a pH of 7.8 was reached. The sediments' incubation continued for one more month before I sacrificed and investigated the remaining sediment cores (hereafter, final analyses). The goal was to compare the response of the sediments incubated in the Treatment unit with that of the sediments incubated in the Control unit. A comparison of the results from time-zero and final analyses provided information on changes over time in each of the two experimental units.

During the sediment incubation, I measured the following seawater carbonate chemistry parameters: Dissolved inorganic carbon, total alkalinity and pH. The sediment properties investigated in each type of sediment were: microbial assemblage structure and *amoA* gene expression during time-zero and final analyses; sediment particle size distribution, organic matter content and water content during final analyses. In coastal sediment, time-zero and final pore water pH profiles provided information on how a change in the pH of the seawater affected the pH of the sediment pore water (Table 1).

Study sites

To conduct preliminary trials of molecular analyses in estuarine sediment I collected five cores of sediment from the large tidal inlet of Tauranga Harbour during low tide on February 27th 2015. The sampling site is located in a mid-intertidal sandflat in the northern basin of Tauranga Harbour, at the northeast coast, Tauranga, New Zealand, 80 m east of

Taupiro Channel (S 37° 29' 29", E 175° 56' 51", Fig. 2). Tauranga Harbour is a 40 km long estuary, one of the largest in New Zealand. Waves and tidal currents dominate the hydrodynamics of this estuary, although other minor movement, such as wave surge and seiche occur. The poorly sorted sediment is mainly sand, with an average shell content of 30% (Davies-Colley & Healy, 1978).

For the laboratory incubation experiment I collected sediment from two sites. I collected 16 cores of soft subtidal sediment on May 10th 2015, at 12 m water depth in Man O'War Bay, the Hauraki Gulf, New Zealand, at the east coast of Waiheke Island (S 36° 47' 38", E 175° 10' 14" Fig. 3). I also collected 15 estuarine sediment cores from Tauranga Harbour, as described above, on May 12th 2015.

The Hauraki Gulf is a semi-enclosed bay, which encompasses nearly 4,000 km², where the water reaches a depth of 50 m (Constantine et al., 2015). Calm currents, wind and tides dominate the hydrodynamics of this Gulf. The distribution of grain size varies greatly across the Gulf; some sites are dominated by coarse sand, whereas other sites contain silts and clays (Sikes, Uhle, Nodder, & Howard, 2009).

Sediment sampling

To collect a sediment core, I vertically pushed an acrylic tube (height = 30 cm, diameter = 10 cm) into the sediment until two-thirds of the tube was filled with sediment. I then closed the lower end of the tube with a stopper. I pushed a lid into the upper end of the tube with the valve of the lid open. Once the lid was in place, I closed the valve to seal the tube. The distance from the sediment surface to the lower edge of the lid in each tube ranged from 5.6 to 11.5 cm. A boat skipper and SCUBA divers assisted in the collection of coastal sediment.

The sediment cores were then transported to the laboratory at Auckland University of Technology within four hours, stored in an insulated bin containing crushed ice. After arrival in the laboratory, I labelled all coastal (C1 to C16) and estuarine sediment cores (E1 to E15). I immediately submerged the estuarine sediment cores in the seawater of the two experimental units (8 and 7 sediment cores, respectively). Transport of the coastal sediment cores suspended fine sediment particles in the sediment-overlying seawater. To allow these particles to settle, I placed these sediment cores on the bench of the laboratory overnight. I submerged them in the morning of the next day (8 sediment cores in each experimental unit).



Figure 2. Map showing the location of the estuarine sediment sampling site, Tauranga Harbour (S 37° 29' 29", E 175° 56' 51"). The red squares indicate the sampling site; the yellow line represents 200 m. Retrieved from <http://maps.stamen.com> and <https://earth.google.com/>.

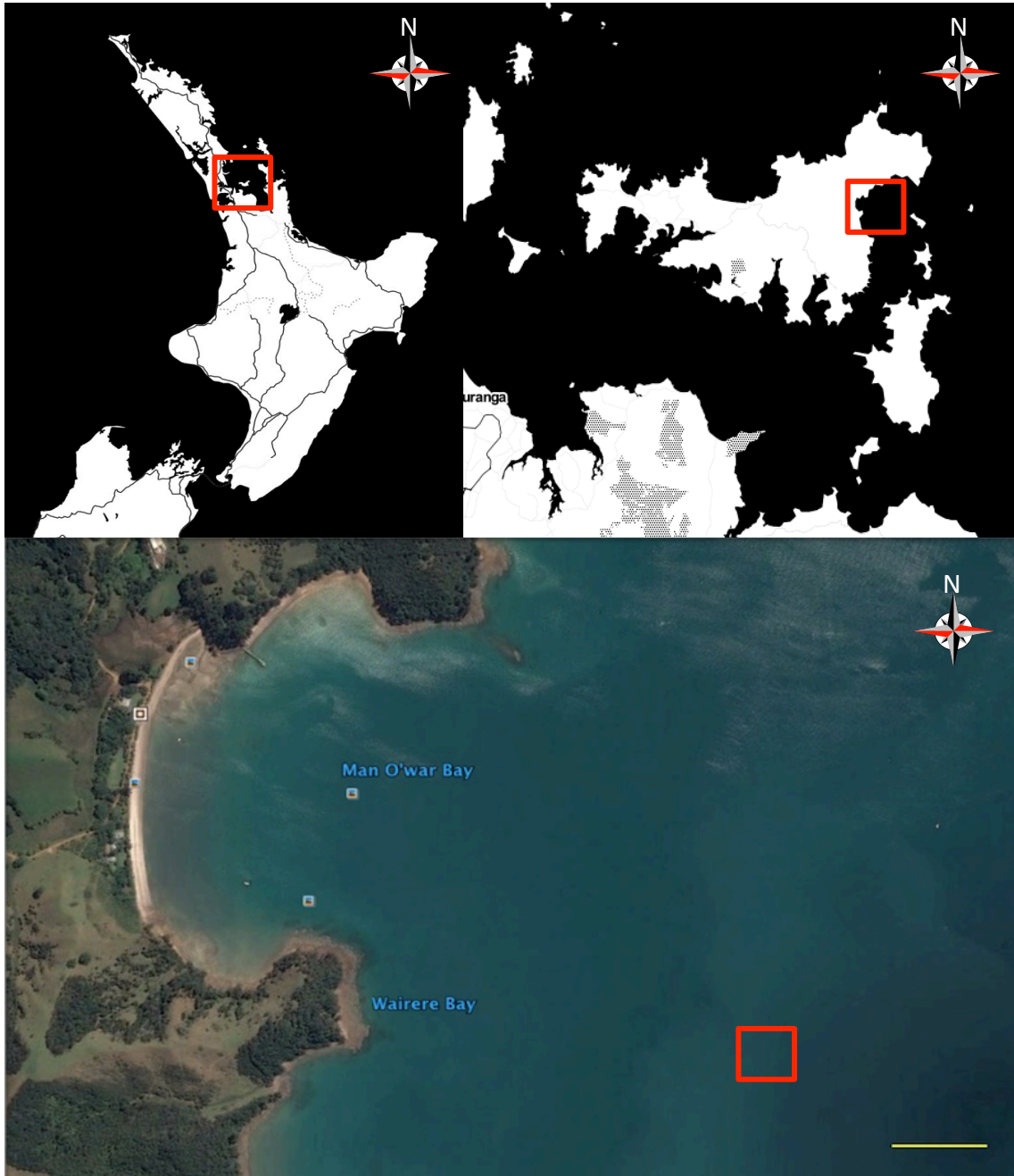


Figure 3. Map showing the location of the coastal sediment sampling site, Man O'War Bay (S 36° 47' 38", E 175° 10' 14"). The red squares indicate the sampling site; the yellow line represents 200 m. Retrieved from <http://maps.stamen.com> and <https://earth.google.com/>.

Sediment incubation

Experimental units

Each of the two experimental units consisted of a 112 × 72 × 60 cm plastic incubation tank (length × width × height), one 60.6 × 89.3 cm mixing barrel with screw lid (diameter × height), a seawater cooler (HC Chiller 300A, Hailea), a 5 Watt UV steriliser (ClearTec, Pond One), a particle filter (Aquis Canister Filter 1200, Aqua One) and a pump (3260, Eheim).

Each experimental unit circulated ~560 L synthetic seawater (351 L in the incubation tank plus 209 L in the mixing barrel) at a rate of ~540 L h⁻¹. To prepare the synthetic seawater, I used a commercial salt mixture: Red Sea Coral Pro Salt (Table 2, www.redseafish.com). I dissolved the salt in tap water, until a salinity of 35 was achieved (~22 kg per each experimental unit). The salinity was measured with a conductivity meter (Portamess 913, Knick International).

Table 2

Red Sea Coral Pro Salt product specification (www.redseafish.com)

Salinity	pH	Alkalinity (mEq L ⁻¹)	Calcium (mg L ⁻¹)	Magnesium (mg L ⁻¹)	Potassium (mg L ⁻¹)
35.0	8.2–8.4	4.4–4.5	455–475	1360–1420	390–410

The seawater was pumped from the incubation tank through the water cooler and UV steriliser into the mixing barrel from which seawater returned by gravity. Seawater was also circulated between the particle filter and the bin. Both seawater jets, one returning seawater from the mixing barrel and one returning seawater from the particle filter, caused sufficient turbulence to avoid stagnation of the seawater overlying the sediment cores (Fig. 4).

One LED floodlight per experimental unit provided photosynthetically active radiation (PAR) to the surface of the submerged sediment cores from 7 am to 7 pm. The intensity of downwelling PAR incident at the sediment surface, measured with a planar underwater quantum sensor (LI-192, LICOR) flush with the sediment surface was 80–130 $\mu\text{mol quanta m}^{-2} \text{ s}^{-1}$. The total exposed sediment surface in each experimental unit was 1,177 cm².

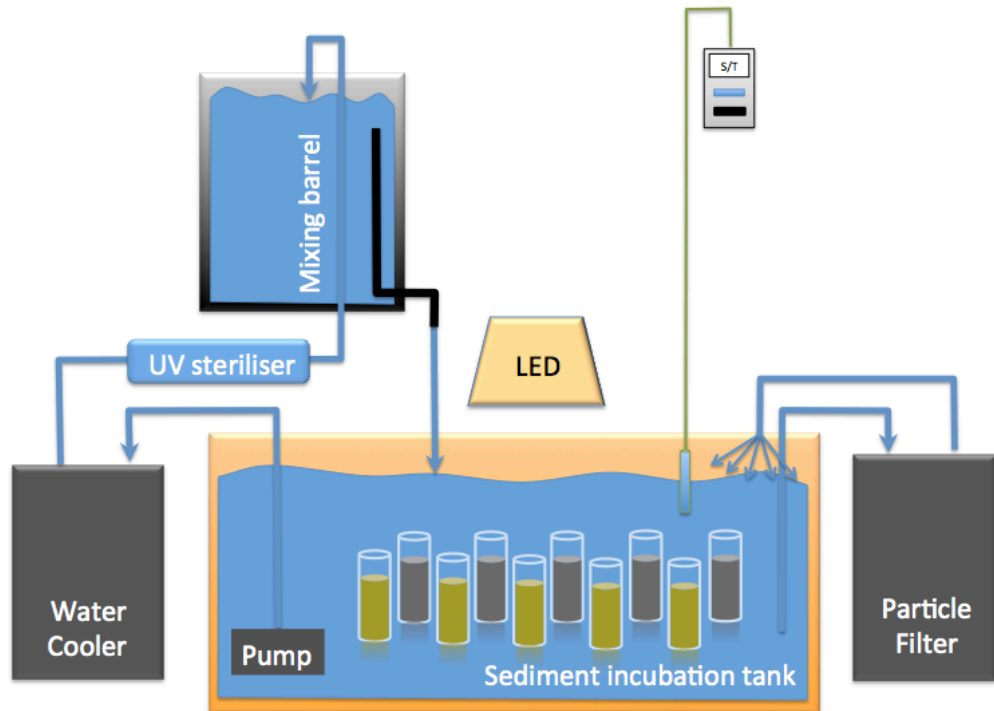


Figure 4. Diagram showing the flow of seawater in one experimental unit. The unit circulated ~560 L of synthetic seawater between a mixing barrel and an incubation tank. Seawater was pumped from the incubation tank through the water cooler and UV steriliser into the mixing barrel from which it returned by gravity. Jets returning seawater from the mixing barrel and a particle filter caused turbulence to avoid stagnation. One LED floodlight provided a 12-hour cycle of photosynthetically active radiation. The salinity was measured with a conductivity meter.

Environmental control

Before the commencement of the experiment, I ran a trial in the experimental units to determine the optimal temperature and pH settings and to understand what temperature and salinity fluctuations to expect. I monitored salinity over a 24-hour period in an incubation tank recording conductivity every 20 minutes with a Portamess 913 (Knick International, Appendix 1 A).

The electrical equipment used in the experimental units produced heat in the room. To establish the optimal temperature to prevent the overheating of air in the laboratory, I monitored the air and seawater temperature using a set of sensors. I also determined whether the temperature of the seawater in both experimental units was the same. One sensor was

placed in each incubation tank and mixing barrel and a fifth sensor monitored the air temperature in the room (Appendix 1 B).

The seawater cooler's setpoint was 19 °C; my objective was to maintain the temperature at 19.5 ± 0.5 °C. I determined that the ideal room temperature was ~ 2 °C above the coolers' setpoint to prevent the coolers from heating the air in the laboratory. The temperature of this air was controlled with an air conditioner (Super Wave, Fujitsu) adjusted to Level 7. When the air temperature outside the laboratory was >10 °C, the air conditioner was set to cool. When the air temperature outside the laboratory was <10 °C the air conditioner was set to heat. Although the seawater coolers of the two experimental units were the same brand and model, they were not maintaining the same seawater temperature at identical setpoints. Therefore, I had to lower and raise, respectively, the setpoints for the Treatment and Control units by 0.2 °C.

The pH in both experimental units was monitored for three months before the experiment. This monitoring enabled us to assess the ability of the system to maintain the seawater pH within a narrow range. I also studied differences in seawater pH between mixing barrel and incubation tanks. This difference resulted from the alteration of the equilibrium between seawater and atmospheric CO₂. As expected for an open seawater circulation system, seawater degassed to restore the equilibrium with the atmosphere (Equation 2). This degassing explained why the pH of the seawater in the incubation tanks was slightly higher than that of the seawater in the mixing barrel.

To control the seawater pH, I used a commercial pH regulator system. The system recorded and adjusted the seawater pH by injecting CO₂-enriched air (5% carbon dioxide, 21% oxygen in nitrogen) into the mixing barrel. This system consisted of a DAQ-M instrument (Loligo Systems); a CapCTRL software (version 1.3.0, Loligo Systems); a gas control set including solenoid valves; air stone and tubing; pH meters (pH 3310, WTW); and pH electrodes (SenTix HWD, WTW). The pH electrode inside the mixing barrel measured the seawater's pH and temperature and submitted these readings to the CapCTRL software installed on a laptop. CapCTRL recorded the readings and sent a signal to the DAQ-M instrument, which controlled the solenoid valve. If the pH was above the setpoint, the solenoid valve opened. CO₂-enriched air flowed from the cylinder to the air stone at the bottom of the mixing barrel. This flow decreased the pH of the seawater in the barrel. When the pH in the mixing barrel reached the setpoint, the solenoid valve closed, preventing the CO₂-enriched air from continuing to flow. The seawater pH then gradually increased over time and when it was above the setpoint, the cycle repeated (Fig. 5).

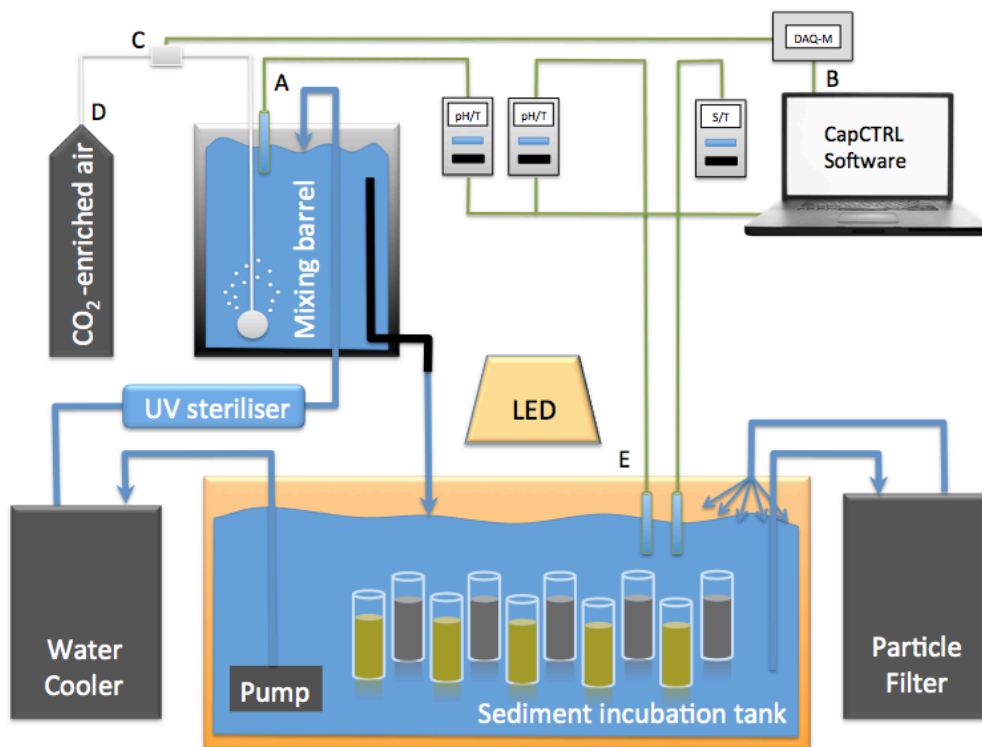


Figure 5. Functioning of the pH regulation system. The (A) pH electrode inside the mixing barrel submitted the pH (and temperature) readings to the CapCTRL software. CapCTRL recorded the readings and (B) sent a signal to the DAQ-M instrument, which controlled the (C) solenoid valve. The solenoid valve opened to (D) allow CO₂-enriched air to flow from the cylinder to the mixing barrel. When the pH in the mixing barrel reached the setpoint, the solenoid valve closed. Degassing increased the pH over time and once the pH was above the setpoint the cycle repeated. A second set of pH meter and electrode (E) measured and registered the pH (and temperature) in the incubation tank.

A second set of pH meter and electrode measured the pH and temperature in the incubation tank. These measurements were also transmitted to the CapCTRL software. They were not, however, used to control the CO₂-air flow but to assess the stability of seawater pH in the incubation tank. The initial settings I established for both systems are listed in Table 3.

To ensure reliable pH control, I isolated the pH meters from the laptop with an optical USB isolator (AC10125, Loligo Systems). The laptop was also isolated from the main power supply with an isolation transformer.

Table 3

Initial settings for the CapCTRL pH regulation system

Component	Setting	Description
Main valve pressure	~13, 000 kPa	Pressure of the CO ₂ -air tank valve
Mode	Auto	This CapCTRL setting enables the automatic regulation of pH
Setpoint	8.1	The pH aimed. To lower down the pH for the treatment system, I adjusted this feature to 0.02 units lower every day
Hysteresis	0.001	The tolerance at which the DAQ-M sends the signal to open or close the solenoid valve
Decreasing	Enabled	The pH is downward regulated
Ramp setpoint	Disabled	A feature that can be used to stepwise lower the pH in automatic mode.

To calibrate the pH meters, I used standard pH calibration buffers for a three-point calibration at pH 4, 7 and 9 (Tables 4 and 5). Following this calibration I measured the pH of certified seawater TRIS buffer prepared as described in Dickson, Sabine and Christian (2007d) SOP 6a (Batch # 26, packaged 25/06/2014, Prof. Andrew G. Dickson's Laboratory at University of California, Dickson, 2009). With the "DeValls & Dickson pH calc" Excel file (Appendix 2), I determined the theoretical pH of the seawater TRIS buffer. Based on this theoretical pH, I established an offset with the difference between the theoretical pH and the electrode reading. Such difference was expected because the ionic strength of the standard calibration buffers is lower than that of seawater (Riebesell et al., 2010). I repeated the same procedure with all four pH electrodes to establish an electrode-specific offset which was set in the General window of the CapCTRL software.

The UV sterilisers of the experimental units supported a maximum flow rate of 1,000 L h⁻¹ (<http://www.pondone.co.uk/>). Their UV light limited the growth of bacteria and algae. The particle filters supported a maximum flow rate of 1,200 L h⁻¹ (<http://www.aquaone.com.au/>). During the experiment I cleaned these particle filters every three weeks.

Table 4

Standard buffers used for the calibration of pH meters and probes

Buffer pH at 25 °C	Brand	Catalogue N ^o	Batch
4.00	Pronalys (LabServ)	BSPA97.1	KJ1942
7.00	Pronalys (LabServ)	BSPA98.1	KL1376
9.14	LabChem	2492-1L	1004005

Table 5

Calibration parameters of the pH sensors

pH meter measuring	6-May-15		22-May-15		12-Jun-15	
	Slope (mV/pH)	Sensor ¹	Slope (mV/pH)	Sensor ¹	Slope (mV/pH)	Sensor ¹
Treatment mixing barrel	-58.9	+++	-58.1	+++	-58.8	+++
Control mixing barrel	-59.0	+++	-58.6	+++	-58.8	+++
Treatment incubation tank	-58.6	+++	-58.0	++	-58.6	+++
Control incubation tank	-58.8	+	-58.8	+++	-58.9	+++

¹ Calibration evaluation according to pH meter (pH 3310, WTW): +++, ++, +, -, from maximum to minimum.

Seawater analyses

During the incubation of sediments, I measured salinity, temperature and pH of the seawater in the experimental units. I measured and recorded salinity with the conductivity meter in each incubation tank every weekday (Appendix 3 A).

The CapCTRL system recorded the seawater pH (total scale) and temperature every second (Appendix 4 A). To keep the resulting files at a manageable size, I stopped the logging and created a new file three times a week (Mondays, Wednesdays and Fridays).

To determine the carbonate chemistry parameters dissolved inorganic carbon and total alkalinity, I took samples from each incubation tank following the instructions in the SOP 1 (Dickson, Sabine, & Christian, 2007a). Briefly, for each experimental unit, I filled a 1-L glass bottle (Schott Duran) with seawater from the incubation tanks, leaving a 10-mL headspace and then added 200 μ L of a saturated mercuric chloride solution. Samples were taken twice a week during the first four weeks of the experiment and once a week for the remaining five weeks

(Table 1). At the end of the experiment, I sent all samples for analyses to the Department of Chemistry at the University of Otago, Dunedin. The analytical method used for the determination of dissolved inorganic carbon was based on SOP 2 (Dickson, Sabine, & Christian, 2007b). The analyst used a Single Operator Multiparameter Metabolic Analyser assembled at the University of Otago. This instrument consists of a computer-controlled system for the extraction of dissolved carbon coupled to a Coulometer. For the determination of total alkalinity, the analyst used a closed-titration system following the SOP 3a (Dickson, Sabine, & Christian, 2007c).

Sediment analyses

Pore water pH

I measured a total of 40 vertical microprofiles of the sediment pore water pH in one coastal sediment core from each of the two experimental units (core C2 from the Treatment and C15 from the Control). Ten of these microprofiles were measured under conditions of darkness, whereas the other 10 were measured under conditions of light for the time-zero analyses. The other 20 profiles were measured under the same conditions for the final analyses, using the Unisense hard- and software (www.unisense.com). I recorded these microprofiles at a resolution of 0.2 mm normal to the sediment surface from a position in the turbulent seawater above the diffusive boundary layer (~3 mm above the sediment surface) to a maximum depth of 12 mm. I calibrated the Unisense microelectrodes once a day before commencement of a measurement series as described above.

To conduct the above measurements, I transferred one sediment core at a time from the incubation tank to a bucket filled with synthetic seawater. An LED floodlight provided photosynthetically active radiation (80–150 $\mu\text{mol photons m}^{-2} \text{ s}^{-1}$ measured with a LI-192 Underwater Quantum Sensor, LI-COR, in place of the sediment surface), and a stream of compressed air directed to the surface of the sediment-overlying seawater provided sufficient seawater advection. I returned the sediment core to the incubation tank after the measurements.

Granulometry, large fauna and microbial mats

I observed the macroscopic attributes of the sediment before I sacrificed each core. I took pictures and registered larger bivalves, polychaetes, sea snails, sea urchins (*Echinocardium* sp.) and the presence or absence of mat-forming diatoms.

For analyses of the sediment particle size distributions, I randomly chose three cores of each sediment type from each treatment. I collected ~9 mL of homogenised sediment of these three cores in a 15 mL-polypropylene centrifuge tube each. Finally, I collected and mixed the remaining homogenised sediments in plastic containers for the analyses of organic matter and water content: one container for the Control, and one container for the Treatment per each type of sediment.

The sediment particle size distributions were analysed with a Mastersizer 2000 (Malvern Instruments Ltd.) at the Faculty of Science and Engineering, The University of Waikato, Hamilton. I determined the water and organic matter content of the sediments in quintuplicate. To do so, I weighed previously cleaned and dried crucibles before and after adding ~15 g of wet sediment, after drying the sediment at 90–100 °C for 24 hours, and after combustion at 400 °C in a muffle furnace (Perfect Fire III, Canadian Instrumentation Company) for six hours.

Molecular analyses

This section describes the methods used for the final analyses as they were optimised in the course of the experiment. I have explained the protocol development and troubleshooting in the Results section.

For the time-zero and final molecular analyses of both the estuarine and coastal sediment, I sanitised with 70% ethanol aluminium trays, a metal spoon and a stainless steel spatula. I gravity siphoned the overlying seawater and transferred the top 1-cm sediment layer to a tray with the spoon. I homogenised this sediment and transferred ~5 mL to a 15-mL sterile RNase-free DNase-free centrifuge tube (Nest Biotechnology Co., Ltd.) in triplicate with the spatula. The tubes were immediately buried in dry ice inside a polystyrene container. I transported them to the Thermophile Research Unit at The University of Waikato, Hamilton, within three hours.

DNA and RNA extraction

After arrival at the Thermophile Research Unit, I thawed one of the triplicate samples on wet ice. The other two samples were stored at -80 °C to serve as backup samples. To extract the DNA and RNA, I used a modified version of the RNA extraction method described in Biddle et al. (2006). DNA is usually extracted alongside RNA, after an RNA extraction. For that reason, I decided to use this method to extract both nucleic acids. After the initial extraction, I treated half of the extract with DNase to recover RNA and the other half with RNase to recover DNA.

The pH of the phenol solutions used during the extractions P4557 and P4682 (Sigma-Aldrich) was adjusted by replacing the aqueous phase with 5× extraction buffer. I shook, allowed to settle and repeated the same procedure numerous times until reaching pH ~5. I transferred 2 g of a 1:1 mixture of 0.1 and 2.5-mm silica–zirconia beads to the tube containing the recently thawed sediment. I added 4 mL of 5× extraction buffer (250 mM sodium acetate/50 mM EDTA, pH 5), 0.5 mL of 20% sodium dodecyl sulfate (SDS) and 4 mL of phenol pH 5. I horizontally shook the samples in a Vortex Genie 2 (MO BIO Laboratories Inc.) with a 15-mL tube adapter at top speed for 10 minutes. The tubes were centrifuged at $3,810 \times g$ for 20 min at 4 °C. I transferred the aqueous phase to a new sterile 15-mL tube and added an equal volume of phenol pH 5. I horizontally shook the tubes for 30 seconds at top speed and centrifuged 20 min ($3,810 \times g$; 4 °C). Again, I transferred the aqueous phase to a new 15-mL tube and added an equal volume of 1:1 phenol/chloroform, shook for 30 seconds and centrifuged 20 min. I transferred the aqueous phase to a new 15-mL tube and added an equal volume of chloroform, shook and centrifuged using the same conditions. Finally, I transferred the last aqueous phase to a new 15-mL tube and added 0.5 volumes of 7.5 M ammonium acetate and 1 volume of isopropanol. I shook for 30 seconds and stored at -20 °C for overnight precipitation. The next morning, I centrifuged these tubes for 20 min, discarded the supernatant and added 1.5 mL of cold 70% ethanol. I resuspended and homogenised the pellet with a pipette and transferred this resuspended pellet to a 1.5-mL centrifuge tube. I centrifuged for 5 min at $18,890 \times g$, discarded the supernatant and dried the pellet in a speed vacuum concentrator (Thermo Scientific). Finally, I resuspended the DNA–RNA pellet in 50 µL of UV-irradiated Milli-Q water (Millipore).

To treat the nucleic acids with the corresponding nuclease, I transferred 21.5 µL of the extracted nucleic acids to a 0.5-mL tube in duplicate. I added 2.5 µL of 10× TURBO DNase buffer (TURBO DNA-free Kit, Ambion) to each tube. I then transferred 1 µL of TURBO DNase to one tube to digest DNA and 1 µL of a 1 mg mL⁻¹ solution of bovine pancreatic Ribonuclease A R5125-100MG (Sigma-Aldrich) to the other tube to digest RNA. I briefly mixed using a vortex, spun down and incubated at 37 °C for 30 minutes. After incubation, I stored the DNA (RNase-treated tube) in ice and added 2.5 µL of DNase inactivation reagent (TURBO DNA-free Kit, Ambion) to the RNA (DNase-treated tube). I incubated with the inactivation reagent at room temperature, gently mixing the tube every ~1.5 min. After a total of 5 minutes, I centrifuged at 10,000 rpm for 1.5 min and transferred the supernatant containing the RNA into a new tube. To determine the final concentration of the nucleic acid and to test the effectiveness of the two treatments, I quantified both DNA and RNA, using the QuBit dsDNA BR and RNA BR Assay

kits in the QuBit fluorometer (Invitrogen). I also ran a PCR control on the RNA extract to confirm that DNA residues would not amplify.

DNA sequencing

To generate the library of 16S rRNA gene PCR amplicons, I used primers to amplify the V4 hypervariable region of the 16S rRNA gene sequence: forward primer 515f and reverse primer 806r (Bergmann et al., 2011). For Ion Torrent sequencing, these primers contain appropriate adapters, adapter A for the forward primer and adapter P1 for the reverse primer. In between the adapter A and the 515f sequence, the forward primer also contains a library key, an IonXpress barcode (Ion Torrent) and the barcode adapter:

Forward primer:

A adapter **library key** + IonXpress barcode + **Barcode adapter** + **515f primer**

5' CCATCTCATCCCTGCGTGTCTCCGACT**TCAG**XXXXXXXXXX**GATGTGCCAGCMGCCGCGGTAA** 3'

Reverse primer (ITR_V4):

P1 adapter + **806f primer**

5' CCACTACGCCTCCGCTTCTCTCTATGGGCAGTCGGTGAT**GGACTACHVGGGTWTCTAAT** 3'

I amplified the sediment DNA using these primers (Tables 6 and 7) and confirmed the amplification of the V4 region running the PCR amplicons in a 1% agarose gel at 65 V for ~25 min. To clean the PCR products, I used the SPRIselect reagent kit (Beckman Coulter) following the vendor's instructions and quantified the cleaned products with QuBit dsDNA HS kit (Invitrogen). The amplicons were then diluted to 26 pM and an equal volume of each sample was pooled into one tube. The library was sequenced on an Ion Torrent PGM DNA sequencer following manufacturer protocols for the Ion PGM Hi-Q Sequencing Kit (400 bp).

Table 6

Temperature, time and cycle conditions for the PCR to generate the library of DNA fragments for sequencing

Step	Temperature (°C)	Time (s)	Number of cycles
Initial denaturation	94	180	Hold
Denaturation	94	30	30
Annealing	50	30	30
Extension	72	110	30
Final extension	72	300	Hold
Hold	4	∞	Hold

Table 7

PCR reactions setup to generate the library of DNA fragments for sequencing

Reagent	Volume (μL) for 25- μL reaction
UV-irradiated Milli-Q water	11.23
BSA (0.8 mg mL ⁻¹)	0.5
dNTPs (2 mM)	3
Buffer 10×	3
MgCl ₂ (50 mM)	3
Reverse primer ITR_V4	0.5
Taq Platinum (5 U μL^{-1})	0.12
Forward primer (1 to 65) ¹	0.5
EMA (5 $\mu\text{L mL}^{-1}$) ²	1.15
DNA (0.5 ng μL^{-1})	2

¹ The master mix was aliquoted in separate master mixes for each triplicate (triplicate master mix). Forward primers were individually added to each triplicate master mix.

² Each triplicate master mix was treated with ethidium monoazide as in Rueckert and Morgan (2007).

Quantitative polymerase chain reaction

To determine the abundance of *amoA* genes, I used two primer sets, which are described in Table 8. To prepare standards, I extracted DNA from soil collected from The University of Waikato using the MO BIO Power Soil DNA isolation kit (MO BIO Laboratories Inc.). I amplified using the standard PCR with the archaeal and bacterial *amoA* primers, and purified using the QuickClean 5M PCR purification kit (GenScript). The stock concentration of each standard is described in Table 9. From each standard I made 1:10 serial dilutions, and included on each assay the corresponding dilutions later described in this section.

Table 8

Primers used to target bacterial and archaeal amoA genes, melting temperature (T_m), sequences and fragment size.

Organism	Primer	T _m (°C)	Sequence	Fragment size (bp)
Archaea ¹	Arch-amoAF	57.5	5' STAATGGTCTGGCTTAGACG 3'	635
	Arch-amoAR	52.6	5' GCGGCCATCCATCTGTATGT 3'	
Bacteria ²	amoA1F-new	53.9	5' GGGGHTTYTACTGGTGGT 3'	489
	amoA2R-new ³	54.1	5' CCTCBGSAAAVCCTTCTTC 3'	

¹ Francis et al. (2005)

² Laverock et al. (2013)

³ I removed the first two C's at the 5' end (originally 5' CCCCTCBGSAAAVCCTTCTTC 3') as in a similar version of the primer, amoA2R (Tait et al., 2014)

Table 9

Concentration of archaeal and bacterial standards

Standards	Amount of DNA (ng μL^{-1})	Concentration (amplicons μL^{-1})
Archaeal	1.96	2.96×10^9
Bacterial	4.09	7.98×10^9

Because the sediment DNA carried inhibitors that prevented it from being amplified in qPCR assays, the DNA was diluted according to the following rule:

If the concentration of estuarine or coastal DNA was $\geq 5 \text{ ng } \mu\text{L}^{-1}$, I diluted the DNA to a final concentration of $0.5 \text{ ng } \mu\text{L}^{-1}$. If the concentration of estuarine DNA was $< 5 \text{ ng } \mu\text{L}^{-1}$, I diluted the DNA 1:10. If the concentration of coastal DNA was $< 5 \text{ ng } \mu\text{L}^{-1}$, I diluted the DNA 1:100. The dilution for coastal sediment is higher because inhibition was greater in this type of sediment.

Finally, I setup the qPCR reactions as follows: To target the archaeal gene, I ran an assay that comprised a duplicate standard curve containing 10^4 , 10^5 , 10^6 and 10^7 amplicons L^{-1} ; the diluted coastal and estuarine DNA in triplicates; and a no-template control (NTC) in duplicate. For the assay targeting the bacterial gene, the assay comprised the same components, except for the standard curve, which contained 10^6 , 10^7 , 10^8 and 10^9 amplicons L^{-1} . I ran standard curves with low concentration of amplicons because I expected low abundance of *amoA* genes due to the dilution of DNA templates. For each target gene (archaeal or bacterial), I used a SYBR green based qPCR. For each individual reaction, I added 9 μL of the master mix (Table 10) and 1 μL of the template (or water for NTCs) to each tube. The temperature, time and cycle conditions are described in Table 11. The instrument used for both qPCR and RT-qPCR assays was a Corbett Rotor-Gene 6000 (QIAGEN).

Table 10

Composition of the qPCR master mix

Component	Volume (μL) for 10 μL reactions
UV-irradiated Milli-Q water	3.6
2 \times KAPA SYBR FAST qPCR Master Mix Universal ¹	5
Fwd Primer (10 μM)	0.2
Rev Primer (10 μM)	0.2

¹KAPA Biosystems

Table 11

Temperature, time and cycle conditions for the archaeal and bacterial qPCR assays

Step	Temperature (°C)	Time (s)	Number of cycles
Enzyme activation	95	180	Hold
Denaturation	95	3	45
Annealing/extension/data acquisition	49	60	45

Reverse transcription quantitative polymerase chain reaction

To determine the abundance of *amoA* transcripts, I used the same primer sets and standards described above. Likewise, I diluted the sediment RNA applying the same rule:

If the concentration of estuarine or coastal RNA was $\geq 5 \text{ ng } \mu\text{L}^{-1}$, I diluted the RNA to a final concentration of 0.5 ng. If the concentration of estuarine RNA was $< 5 \text{ ng } \mu\text{L}^{-1}$, I diluted the RNA 1:10. If the concentration of coastal RNA was $< 5 \text{ ng } \mu\text{L}^{-1}$, I diluted the RNA 1:100.

For the RT-qPCR analyses, I ran a total of three assays per type of sediment. In the first assay, I targeted both the archaeal and bacterial transcripts and included two RNA templates. The standard curves contained 10^4 , 10^5 , 10^6 and 10^7 amplicons L^{-1} for estuarine RNA and 10^5 , 10^6 , 10^7 and 10^8 amplicons L^{-1} for coastal RNA. The second assay targeted archaeal transcripts and I included the remaining RNA templates. The standard curve contained 10^5 , 10^6 , 10^7 and 10^8 amplicons L^{-1} for estuarine RNA and 10^6 , 10^7 , 10^8 and 10^9 amplicons L^{-1} for coastal RNA. Finally, the third assay targeted bacterial transcripts and the configuration used was the same as in the second assay (same standards and RNA templates). For the three assays, I ran the samples in triplicates; whereas the standard curves, no-reverse transcriptase (NRT) controls and NTCs were run in duplicate. Similarly to the qPCR assays, I ran the standard curves with low concentration of amplicons, because I expected a low abundance of *amoA* transcripts, due to the dilution of RNA templates.

The preparation of the master mix was a two-step preparation. First, I mixed the following components (per reaction tube): 5 μL KAPA SYBR FAST qPCR Master Mix (2 \times) (KAPA Biosystems), 0.2 μL Fwd primer (10 μM), and 0.2 μL Rev primer (10 μM). I then transferred 5.4 μL of this mix to the NRT reaction tubes and added to the remaining master mix: 0.2 μL KAPA RT Mix (50 \times) (KAPA Biosystems) and 3.4 μL UV-irradiated Milli-Q water. Finally, I transferred 9 μL of the mix to the rest of the reaction tubes, added 1 μL of template (or 1 μL of water to the NTCs) and added 3.6 μL of water to the NRTs. The temperature, time and cycle conditions are described in Table 12.

Table 12

Temperature, time and cycle conditions for the archaeal and bacterial RT-qPCR assays

Step	Temperature (°C)	Time (s)	Number of cycles
cDNA synthesis	42	300	Hold
Inactivate RT	95	300	Hold
Denaturation	95	3	45
Annealing/extension	49	60	45
Data acquisition	72	30	45

Data analysis

For the CapCTRL temperature and pH readings I filtered all files to display these readings every minute instead of every second. I gathered all these minutely-readings in one Excel file (Appendix 4 B). These readings were used to estimate the average, maximum, minimum and standard deviation of temperature and pH readings. I further filtered this file to retrieve an hourly-readings file (Appendix 4 B), which I used to create the scatter plots. The gap in scatter plots corresponds to a lost file, which contained the readings from 19 June to 22 June 2015.

I used the dissolved inorganic carbon concentrations, total alkalinity, salinity and CapCTRL temperature readings to estimate the partial pressure of CO₂ and pH in USGS CO₂calc Application v1.3.0 (Robbins, Hansen, Kleypas, & Meylan, 2010). The CO₂ constants were K1, K2 from Mehrbach et al. (1973) refit by Dickson and Millero (1987), pH scale was Total scale (mol kg⁻¹-SW).

To analyse the particle size distribution results, I averaged the volume distributions of the six replicates per each type of sediment (three Control and three Treatment replicates). I estimated the Phi (Φ) number: $\Phi = -\log_2$ of the particle size in mm. I summed the volumes corresponding to each range of Φ for the distribution graphs (e.g., volume distributions corresponding to $\Phi = 0.00, 0.25, 0.49$ and 0.76 were categorised as $\Phi = 0$). For the cumulative volume distributions, I left all readings separate and drew scatter plots. I estimated $\Phi_{50}, \Phi_{25}, \Phi_{75}$, etc. in the cumulative curves and such Φ values were used to compute the median, quartile deviation, inclusive graphic quartile deviation, graphic skewness and to classify the sorting according to Higgins and Thiel (1988).

Water and organic matter content were calculated applying the following formulas to each replicate and computing the average of the final percentages:

Water content = $100 - (\text{dry weight} \div \text{wet weight} \times 100)$

Organic matter content = $100 - (\text{combusted weight} \div \text{dry weight} \times 100)$

Of the coastal sediment incubated in the Control experimental unit, I excluded replicate 4 from these calculations because of its high organic matter content compared to the rest of the replicates (Appendix 5 A).

The relative position of the sediment surface in the pore water pH was detected by a change in the slope. The readings from the pH profiles, expressed as H⁺ ion concentration, were averaged and then converted to pH.

Sequence processing and generation OTU abundance table were carried out by Dr Charles Lee using Waikato DNA Sequencing Unit's standardised protocols for 16S rRNA gene PCR amplicons developed for Ion Torrent PGM. Approximately 20% of the raw reads were removed due to the length (shorter than 275 bp or longer than 359 bp) or presence of long homopolymers (>6). Approximately 2% of the remaining reads were removed due to mismatches to the PCR primers; of the remaining reads, approximately 5% were removed due to high (>1%) estimated error rates. All remaining sequences were used in the analysis. Briefly, sequence data were quality-trimmed based on length and homopolymer counts using Mothur 1.17.0. (Schloss et al., 2009). The resulting high quality sequences were dereplicated, ranked by abundance, binned into operational taxonomic units (OTUs), and checked for PCR chimeras using UPARSE (Edgar 2013). The abundance of each OTU in all samples was calculated and stored in an Excel spreadsheet for downstream analyses. Representative sequences of each OTU were analysed using the Ribosomal Database Project (RDP) Classifier to analyse and determine phylogeny to provide automatic taxonomic assignments. Classification at each taxonomic level was assigned a percentage confidence score, where a higher number indicates a higher level of certainty that the taxonomic assignment is accurate.

Results of the sequencing analysis were filtered to manually classify all results with <80% Phyla confidence as 'unknown'. I converted abundances to frequencies and the frequencies <0.01% were manually changed to 'zero'. The replicates of relative abundances per treatment were averaged for each type of sediment; and these abundances were used to build the abundance graphs. For the abundance graphs built for the classes of *Proteobacteria*, I classified those results <80% confidence as 'unknown' but did not exclude frequencies <0.01%. The OTUs corresponding to genera that were suspected to be nitrifying organisms (*Nitrosococcus*, *Nitrosospira*, *Nitrosopumilus* and *Nitrososphaera*) were further identified in the Basic Local Alignment Search Tool with a BLASTn search

(<http://blast.ncbi.nlm.nih.gov/Blast.cgi>). Likewise, the 20 most abundant OTUs were identified with BLASTn. The database used was the 16S rRNA sequences (archaea and bacteria). When this search retrieved <98% identity, I ran a second BLASTn search with the Nucleotide collection (nr/nt) database to confirm that the sequences were true amplification of the 16S gene and not an artefact or chimera.

To determine the abundance of *amoA* genes and transcripts, I firstly determined the concentration of amplicons in the archaeal and bacterial standards. For that, I calculated the molecular weight of the dsDNA fragment considering the molecular weight of each base. With that molecular weight, the total amount of amplicon DNA and the Avogadro number, I calculated the concentration of amplicons. For the standard curves, I used the average of the C_T replicates for each standard dilution. With the C_T and the logarithm of the concentration of amplicons, I computed the slope, efficiency, correlation coefficient r , r^2 and y -intercept. To determine the genes and transcripts copies per gram of sediment, I averaged the C_T of the 3 replicates per template. This average was used to calculate the logarithm of the concentration (and then the concentration with the antilog) considering the slope and y -intercept. I calculated the copies g^{-1} sediment with the following formula:

$$\text{Copies } g^{-1} \text{ sediment} = (\text{Concentration of copies} \times \text{Dilution factor} \times \text{Total volume of extraction}) \div \text{g of sediment}$$

I computed the average and standard deviation of the replicates per treatment, per type of sediment, to construct the column graphs. Results for E7 and E11 sediment cores were not considered for the analyses of the abundance of bacterial *amoA* genes in estuarine sediment, due to their proximity to the C_T value of the no-template control. For the RT-qPCR analysis of coastal RNA, I ran a parametric correlation analysis between the dilution factors and the number of copies per template. Because of the strong correlation found between such dilution factors and the number of transcripts for g^{-1} sediment ($r^2 = 0.8582$ for archaeal transcripts; $r^2 = 0.9759$ for bacterial transcripts), I did not contemplate the results from the highest and lowest dilutions used. The RNA template from sediment C13 was not contemplated for the statistical analysis, because of being outside of the range of the standard curve.

Statistical analysis

To determine whether the differences in copy number abundances of genes and transcripts were of statistical significance, I ran an f -test to compare the variances between treatments. Considering such variances, I then ran a two-tailed t -test in RStudio (RStudio

Team, 2015). With the average of the abundance of genes and transcripts determined and their standard deviation, I computed a retrospective power *t*-test in RStudio (RStudio Team, 2015). This power *t*-test revealed whether the probability to detect a true difference with the number of samples analysed was of statistical significance.

The results from the sequencing analysis were normalised to 2,500 reads (shown in Appendix 6 A) and I ran a similarity profile analysis of the time-zero, pH 8.1 and pH 7.8 treatments for both types of sediment. The number of similarity profiles was 999, the cluster method used was average, and the Euclidean distance method had an alpha = 0.05. I also ran a hierarchical cluster analysis to find statistically significant clusters (*p*-value <0.05). To compare different distance methods I used a correlation method, and a bootstrap of 1,000 replications. Both the similarity profile and hierarchical clustering were executed in RStudio (RStudio Team, 2015). I determined the diversity indices: Shannon-Weaver and Simpson (Hill, 1973) using the Vegan package in RStudio. Evenness was estimated with the Shannon-Weaver index, divided by the natural logarithm of the species richness. Finally, normalised readings were used to compute a permutational multivariate analysis of variance (PERMANOVA) and an analysis of similarity (ANOSIM) with 999 permutations in Qiime (<http://qiime.org/>).

Results

Performance of experimental units

Temperature and salinity

My objective was to maintain the seawater temperature at 19.5 ± 0.5 °C. This temperature was maintained within such a range most of the time during the experiment. During the incubation of sediments, including the acclimatisation period, the average seawater temperature in the two incubation tanks was 19.8 °C (Table 13, Fig. 6 A, B). Four excursions of seawater temperature were registered, reaching a minimum of 17.5 °C in the Control and 17.0 °C in the Treatment incubation tanks. The highest seawater temperatures registered were 21.0 and 22.0 °C in the Control and Treatment incubation tanks, respectively. These excursions were related to the changing weather conditions that presented during those days. Excluding these excursions, which lasted less than 24 hours each, the seawater temperature ranged within 19.4 and 20.0 °C in both incubation tanks. The differences in temperature between the two incubation tanks remained ≤ 1.0 °C throughout the experiment (Fig. 6 C).

Table 13

Temperature and salinity of incubation tanks during the experiment; SD, standard deviation

	Control incubation tank		Treatment incubation tank	
	Temperature (°C)	Salinity	Temperature (°C)	Salinity
Average	19.8	35.0	19.8	35.0
Maximum	21.0	35.7	22.0	35.7
Minimum	17.5	34.4	17.0	34.5
SD	0.3	0.3	0.4	0.3

The seawater salinity increased over time due to evaporation. The goal was to keep it within the range of 35.0 ± 0.5 . To do so, I added in average ~ 1 L of tap water to each incubation tank per weekday (Fig. 7). During the incubation of sediments, including the acclimatisation period, the average salinity was 35.0 for both incubation tanks. In the Control incubation tank, the salinity ranged from 34.5 to 35.7; similarly, the salinity ranged from 34.4 to 35.7 in the Treatment incubation tank (Fig. 7, Table 13).

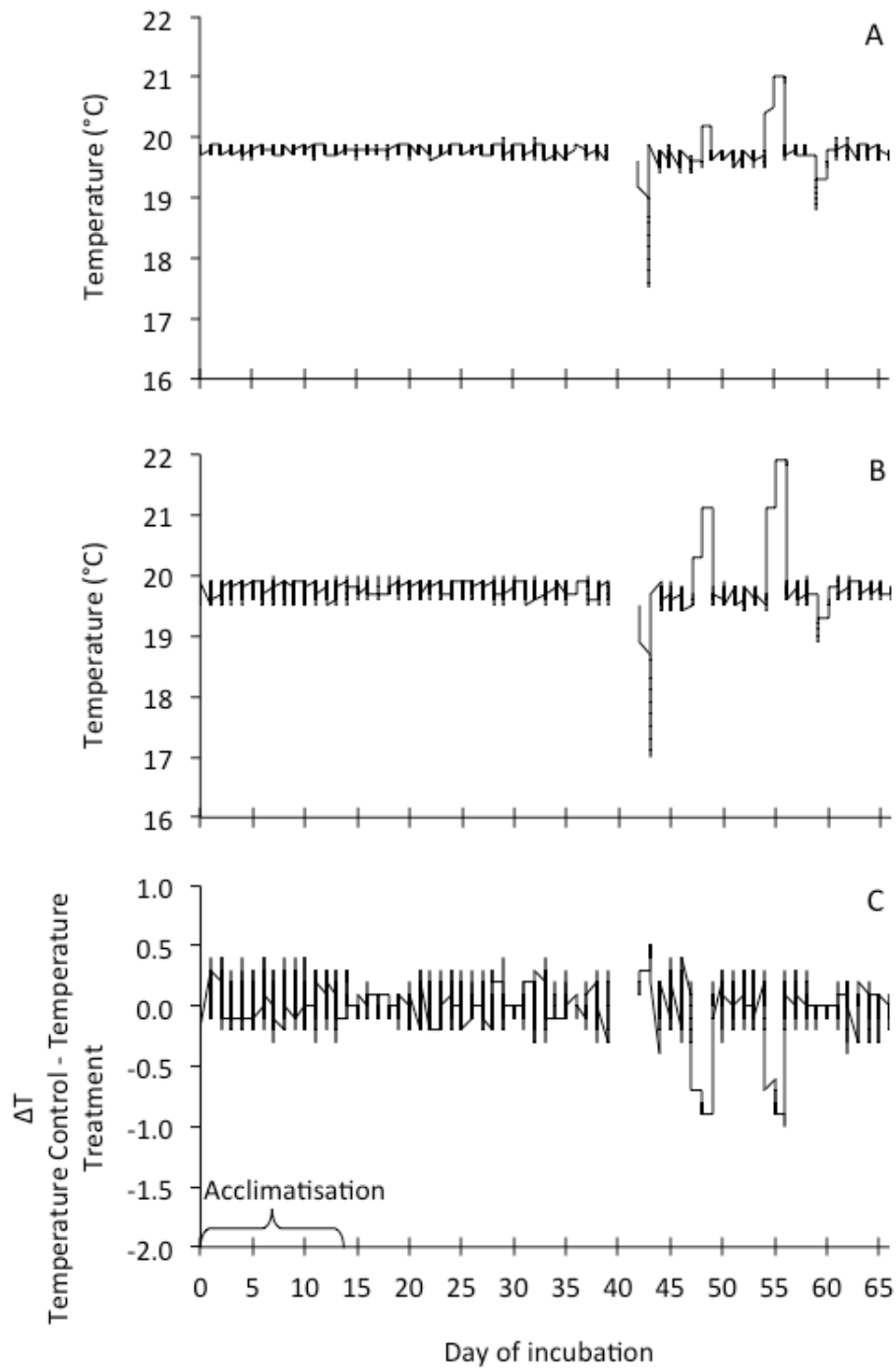


Figure 6. Temperature of seawater in the incubation tanks. (A) Control incubation tank; average temperature = 19.8 °C, maximum = 21.0 °C, minimum = 17.5 °C. (B) Treatment incubation tank; average temperature = 19.8 °C, maximum = 22.0 °C, minimum = 17.0 °C. (C) The differences in temperature between the two incubation tanks remained ≤ 1.0 °C. The gap in readings corresponds to a lost file containing readings from 19 June to 22 June 2015.

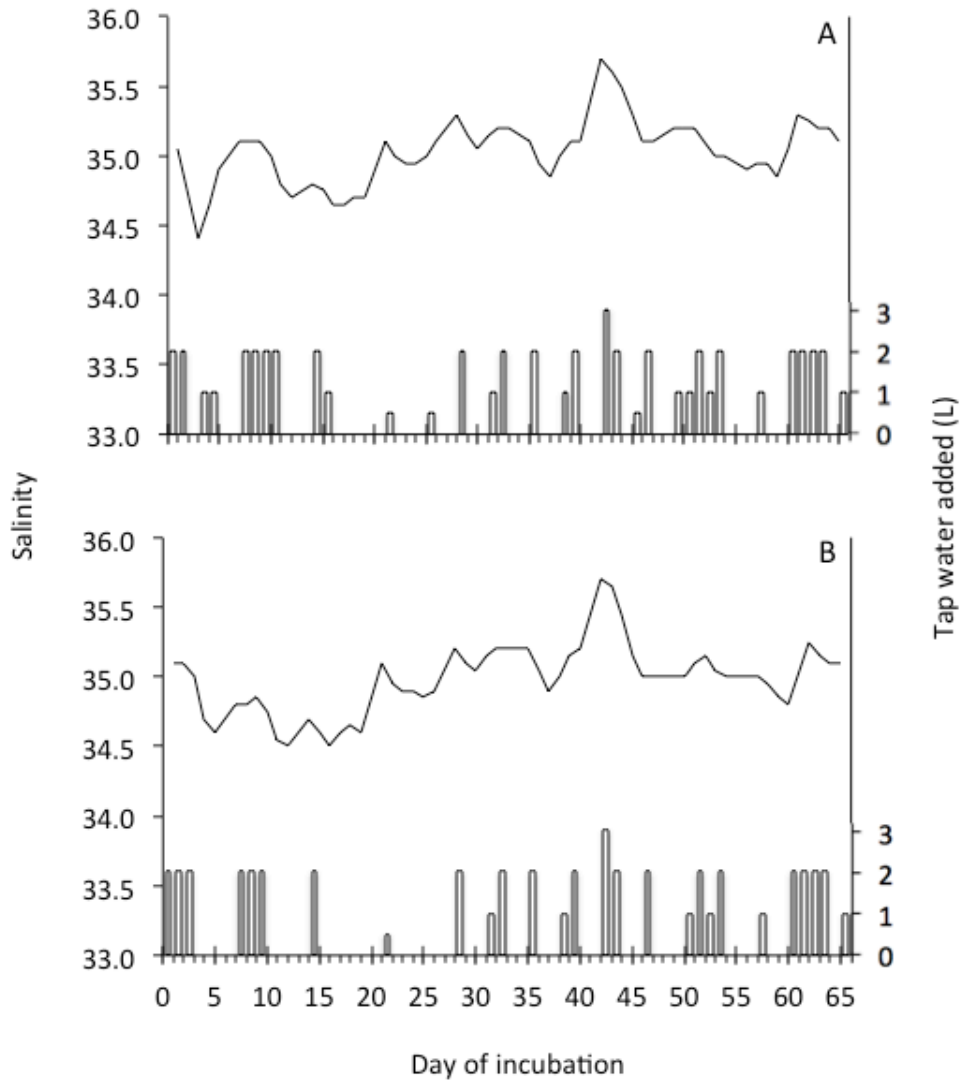


Figure 7. Salinity of the seawater in incubation tanks. (A) Control incubation tank; average salinity = 35.0, maximum = 35.7, minimum = 34.4. (B) Treatment incubation tank; average salinity = 35.0, maximum = 35.7, minimum = 34.5. The average volume of water added was 1 L per weekday. Lines: salinity, left axis; bars: tap water added (L), right axis.

Seawater carbonate chemistry

The first attempts to control the seawater pH with pure CO₂ were challenging. The valve that released CO₂ into the mixing barrel was highly sensitive to inlet pressure and so fine control of the CO₂ input was difficult to achieve. After experiencing such difficulties, I tried a different gas mixture with a lower percentage of CO₂. Using a mixture of 5% CO₂ in oxygen enabled us to apply higher pressure and adjust the seawater pH more precisely. This gas mixture was different from the one used during the experiment, which is described in the Material and Methods section. The proportion of CO₂, however, was the same and I could maintain the pH within a smaller range over greater periods of time.

Inspection of pH recordings during those trials confirmed the expected difference in pH between the mixing barrel and incubation tank due to degassing. Such difference was greater when the pH setpoint was lower, because of greater loss of CO₂ to the atmosphere (Fig. 8). Inspection of the time-series in Figure 9 showed an overall seawater pH stability during the experiment. Yet some unexpected trends and excursions occurred. As opposed to what I expected from the evidence from the trials, the seawater pH recordings in the incubation tanks were below the setpoint (mixing barrel) during the first 11 days of acclimatisation (Fig. 9, Table 14). Recalibration of the pH sensors, however, rectified the pH measurements showing the expected pH after such recalibration. Closer inspection of the time-series of the Control experimental unit, which was set to maintain the seawater pH at 8.1, revealed that a peak occurred on day 46 (Fig. 9 A). That day I swapped the CO₂-enriched air cylinders, and therefore I attributed such peak to this activity. Two excursions occurred during days 56 and 58, due to failures of the solenoid valve that controlled the CO₂ flow to the Control mixing barrel. These failures lowered the seawater pH in the incubation tank temporarily to 7.805 and 7.146, respectively (Fig. 9 A). To avoid further excursions, I decided to manually control the pH for the remaining week of incubation, which resulted in greater pH fluctuations (Fig. 9 A, Table 14).

In the Treatment experimental unit, the objective was to gradually lower the pH from 8.1 to 7.8 and then to maintain that pH. Following the stepwise decrease, the seawater pH remained stable and above the setpoint. The pH recordings of the mixing barrel remained close to the setpoint. The difference between the pH recordings in the mixing barrel and incubation tank, however, increased towards the end of the experiment (Fig. 9 B, Table 14).

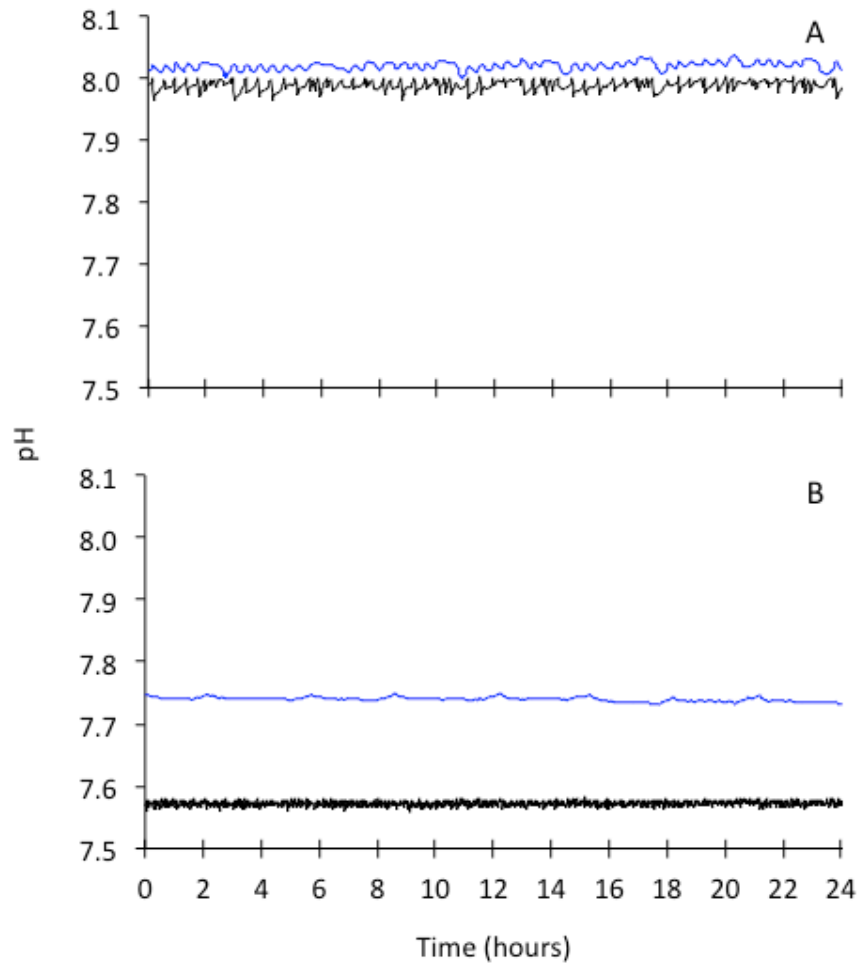


Figure 8. 24-hour monitoring of seawater pH in one experimental unit using a 5% CO₂ in oxygen gas mixture. (A) setpoint = 8.000; the average pH difference between mixing barrel (black solid line) and incubation tank (blue solid line) was 0.032 units; (B) setpoint = 7.575; the average pH difference between mixing barrel and incubation tank was 0.166 units.

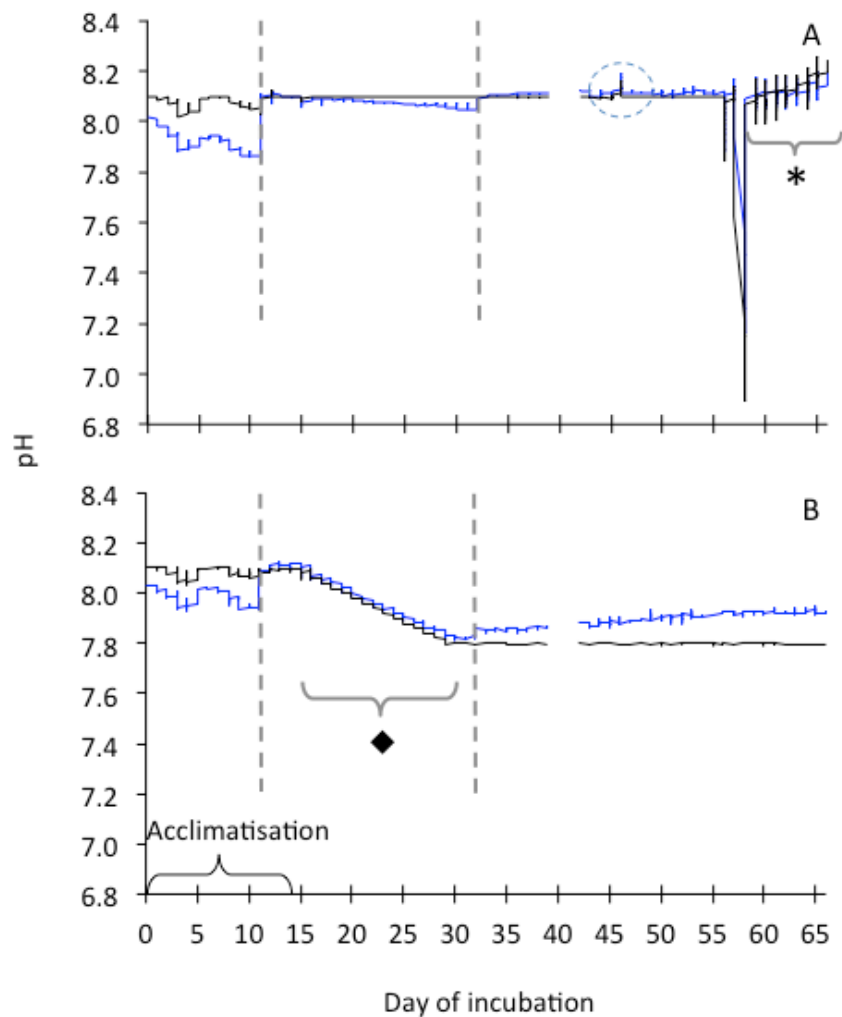


Figure 9. Time-series of seawater pH in the mixing barrel (black lines) and incubation tank (blue lines) in two experimental units. (A) Control unit. The peak on day 46 corresponds to a swap of the CO₂-enriched air cylinders (blue dashed circle). Seawater pH excursions during days 56 and 58 were due to failures of the solenoid valve. These failures lowered the seawater pH in the incubation tank temporarily to 7.805 and 7.146. During the last week of manual control of pH (*), the average pH was 8.118 (maximum = 8.204; minimum = 8.041). (B) Treatment unit. During the stepwise decrease of seawater pH in the treatment experimental unit, the maximum difference between the setpoint and the seawater pH was 0.042 units. After this stepwise decrease, the average seawater pH was 7.889 (maximum = 7.958; minimum = 7.809). The gap in readings corresponds to a lost file containing readings from 19 June to 22 June 2015. The grey dashed lines indicate the days of recalibration of pH electrodes.

Table 14

Seawater pH of experimental units during the experiment. SD, standard deviation; NA, not applicable

Period		Control experimental unit		Treatment experimental unit	
		Mixing barrel	Incubation tank	Mixing barrel	Incubation tank
Acclimatisation (15 days)	Average	8.081	7.965	8.087	8.014
	Maximum	8.125	8.125	8.144	8.129
	Minimum	8.012	7.828	8.023	7.902
	SD	0.021	0.084	0.017	0.058
First 30 days or after stepwise decrease (37 days) ¹	Average	8.096	8.084	7.797	7.889
	Maximum	8.101	8.128	7.842	7.958
	Minimum	8.060	8.034	7.731	7.809
	SD	0.004	0.019	0.003	0.034
Manual control (10 days)	Average	8.134	8.118	NA	NA
	Maximum	8.262	8.204	NA	NA
	Minimum	7.932	8.041	NA	NA
	SD	0.053	0.040	NA	NA

¹ First 30 days for the Control experimental unit; after stepwise decrease for the Treatment experimental unit.

The seawater total alkalinity in the two incubation tanks was stable, with a slight decrease of ~5% towards the end of the experiment (Fig. 10 A, Table 15, Appendix 3 B). As expected, the concentration of dissolved inorganic carbon increased during the stepwise decrease of the seawater pH in the Treatment experimental unit. Thereafter, it remained above that in the seawater of the Control experimental unit (Fig. 10 B, Table 15, Appendix 3 B). Estimation of the seawater pCO₂ from the total alkalinity and concentration of dissolved inorganic carbon confirmed that the pCO₂ in the Treatment incubation tank was higher than that in the Control (Table 15). Estimation of the pH computed with the same carbonate chemistry parameters also confirmed the difference between the Control and Treatment average pH, which had an average pH of ~8.1 and ~7.8 after the stepwise decrease, respectively (Table 15). Excluding the first 11 days of acclimatisation, the estimated pH and the pH CapCTRL recordings were similar. However, the upward trend in the Treatment incubation tank mentioned above was not confirmed with the estimated pH, which did not show such a trend (Fig. 11).

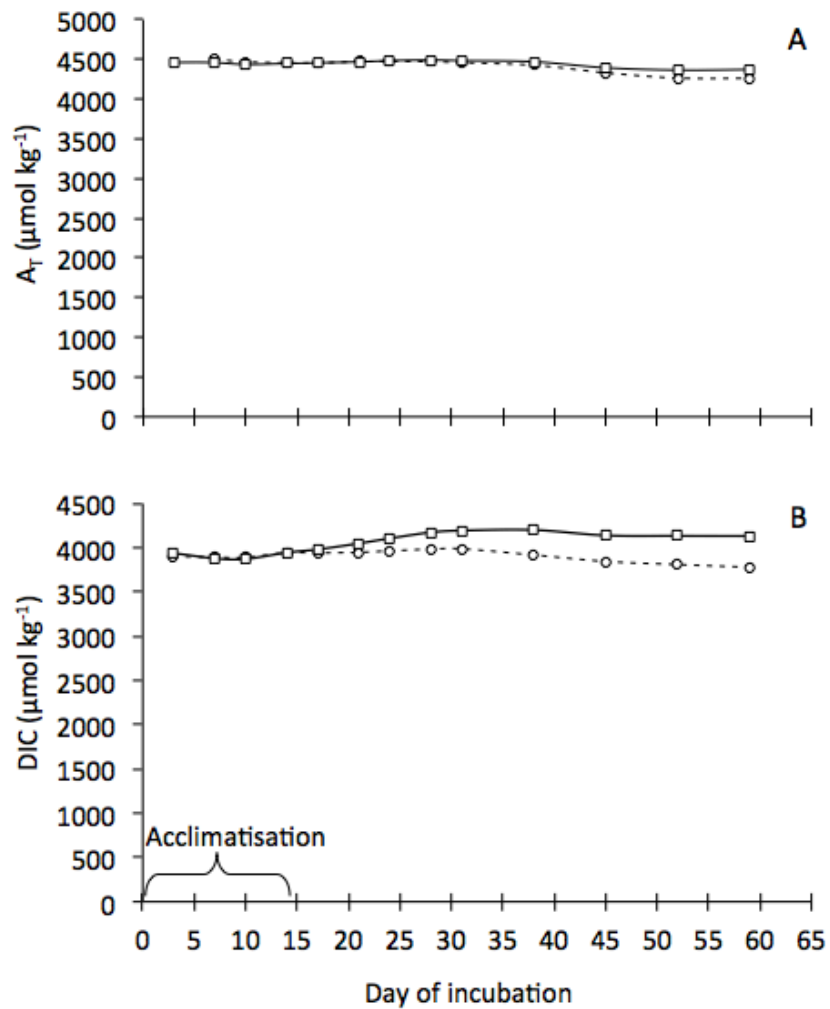


Figure 10. Time-series of seawater (A) total alkalinity (A_T) and (B) concentration of dissolved inorganic carbon (DIC) in the Control (circles, dashed line) and Treatment (squares, solid line) incubation tanks.

Table 15

Carbonate chemistry of incubation tanks during the experiment. SD, standard deviation

Analysis		Acclimatisation		After stepwise decrease	
		Control	Treatment	Control	Treatment
Alkalinity ($\mu\text{mol kg}^{-1}$)	Average	4476.5	4454.6	4350.4	4402.2
	Maximum	4502.0	4468.4	4461.0	4472.7
	Minimum	4457.1	4438.7	4263.0	4366.7
	SD	23.0	12.9	91.4	48.6
DIC ($\mu\text{mol kg}^{-1}$)	Average	3907.7	3908.9	3867.2	4150.4
	Maximum	3943.2	3944.1	3987.0	4199.5
	Minimum	3890.3	3871.9	3778.4	4131.2
	SD	24.6	39.4	84.6	32.9
pCO ₂ (μatm)	Average	539.6	558.1	631.8	1350.5
	Maximum	613.4	622.6	690.6	1419.1
	Minimum	487.4	506.4	589.9	1289.1
	SD	65.7	55.4	40.4	55.1
Estimated pH	Average	8.185	8.172	8.118	7.838
	Maximum	8.221	8.205	8.137	7.862
	Minimum	8.137	8.132	8.094	7.815
	SD	0.043	0.035	0.021	0.020

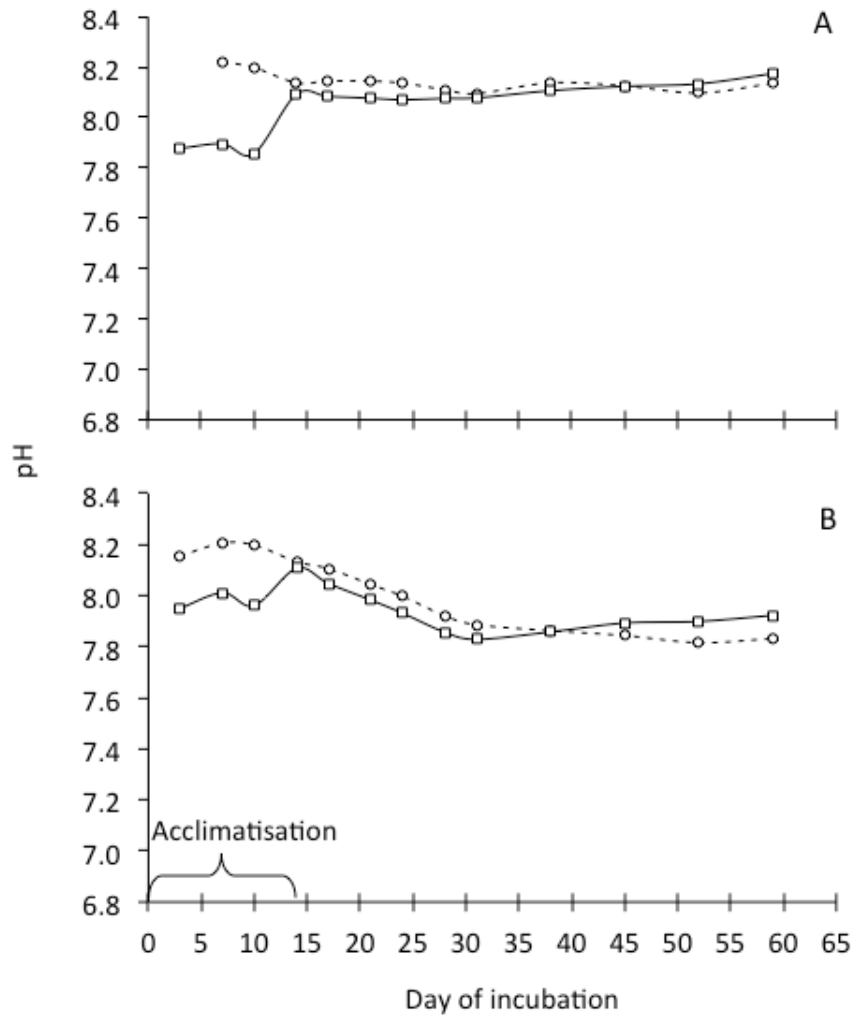


Figure 11. Time-series of estimated (circles, dashed line) versus measured (squares, solid line) pH of the seawater in the (A) Control and (B) Treatment incubation tanks.

Physicochemical sediment characteristics

The macroscopically observable biota in the coastal sediment was comprised of snails, bivalves, the irregular sea urchin *Echinocardium* sp., and mat-forming diatoms. The biota in the estuarine sediment comprised bivalves (mostly cockles), polychaetes and mat-forming diatoms (Table 16, Fig. 12).

Table 16

Large fauna and microbial mats found in sediment cores

Sediment	Analysis	Name	Macroscopic biota
Coastal	Time-zero	C1	None
	Time-zero	C3	None
	Time-zero	C4	<i>Echinocardium</i> sp.
	Time-zero	C5	<i>Echinocardium</i> sp.
	Time-zero	C8	None
	Final Control	C7	Diatom biofilm
	Final Control	C10	Small <i>Echinocardium</i> sp. (~1.7 cm)
	Final Control	C11	Small <i>Echinocardium</i> sp. (~1.2 cm)
	Final Control	C14	2 big <i>Echinocardium</i> sp. (~2.5, ~3.5 cm)
	Final Control	C15	1 small <i>Echinocardium</i> sp. (~1.5 cm)
	Final Treatment	C2	None
	Final Treatment	C9	None
	Final Treatment	C12	1 snail, diatom biofilm
	Final Treatment	C13	2 small bivalves, diatom biofilm
	Final Treatment	C16	Diatom biofilm
	Estuarine	Time-zero	E1
Time-zero		E2	>2 cockles
Time-zero		E3	Shell particles
Time-zero		E4	1 big cockle, 2 small cockles
Time-zero		E5	9 cockles
Final Control		E6	1 polychaete, 1 cockle, shell particles
Final Control		E7	2 polychaetes, 1 big cockle
Final Control		E8	1 polychaetes, 1 big cockle, 2 small cockles
Final Control		E9	Shell particles
Final Control		E10	>7 cockles
Final Treatment		E11	3 cockles
Final Treatment		E12	1 dead cockle, 2 polychaetes, 2 small cockles
Final Treatment		E13	1 big cockle, 2 polychaetes, 2 small cockles
Final Treatment		E14	1 polychaete, 1 cockle
Final Treatment		E15	1 cockle, diatom biofilm

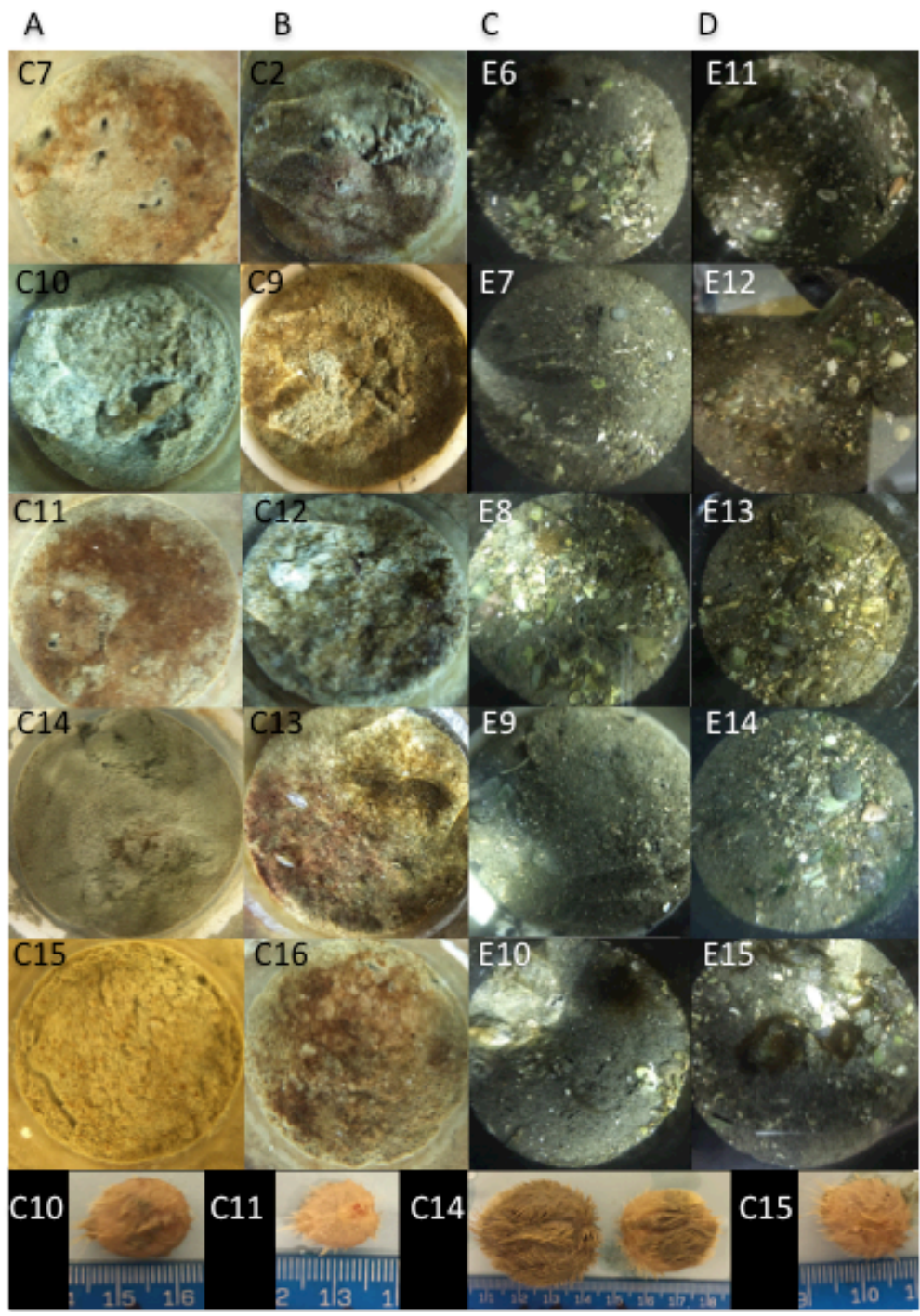


Figure 12. Photographs of Treatment and Control sediment cores' surface. Panel A, coastal control sediment cores; panel B, coastal treatment sediment cores; panel C, estuarine control sediment cores; panel D, estuarine treatment sediment cores. Bottom of image, photographs of *Echinocardium* sp. found in the sediment cores C10, C11, C14 and C15.

I chose to study two contrasting types of sediment; subtidal mud (coastal sediment) and estuarine sand (estuarine sediment). Inspection of the sediments' particle size distribution, water content and organic content confirmed such contrast; the median size of the estuarine sediment particles was one order of magnitude greater than that of the coastal sediment particles (Fig. 13, Table 17, Appendix 5 B, C); the coastal sediment contained 50% more water than the estuarine sediment; and the organic matter content of the coastal sediment was five times higher than that of the estuarine sediment (Table 17, Appendix 5 A).

Table 17

Granulometric indices, water content and organic matter content for coastal and estuarine sediments

Granulometric index	Coastal sediment		Estuarine sediment	
	Control	Treatment	Control	Treatment
Median Md (µm)	30 Silt	28 Silt	350 Medium sand	350 Medium sand
Lower Quartile Q1 (µm)	63	61	500	550
Upper Quartile Q3 (µm)	10	10	213	225
Inclusive Sorting Coefficient QD ₁	1.95 Poorly sorted	1.88 Poorly sorted	1.20 Poorly sorted	1.24 Poorly sorted
Inclusive Graphic Skewness Sk ₁	0.07	0.01	0.21	0.17
Water content (%)	73.8	74.1	24.6	24.4
Organic matter content (%)	5.6	6.4	1.2	1.3

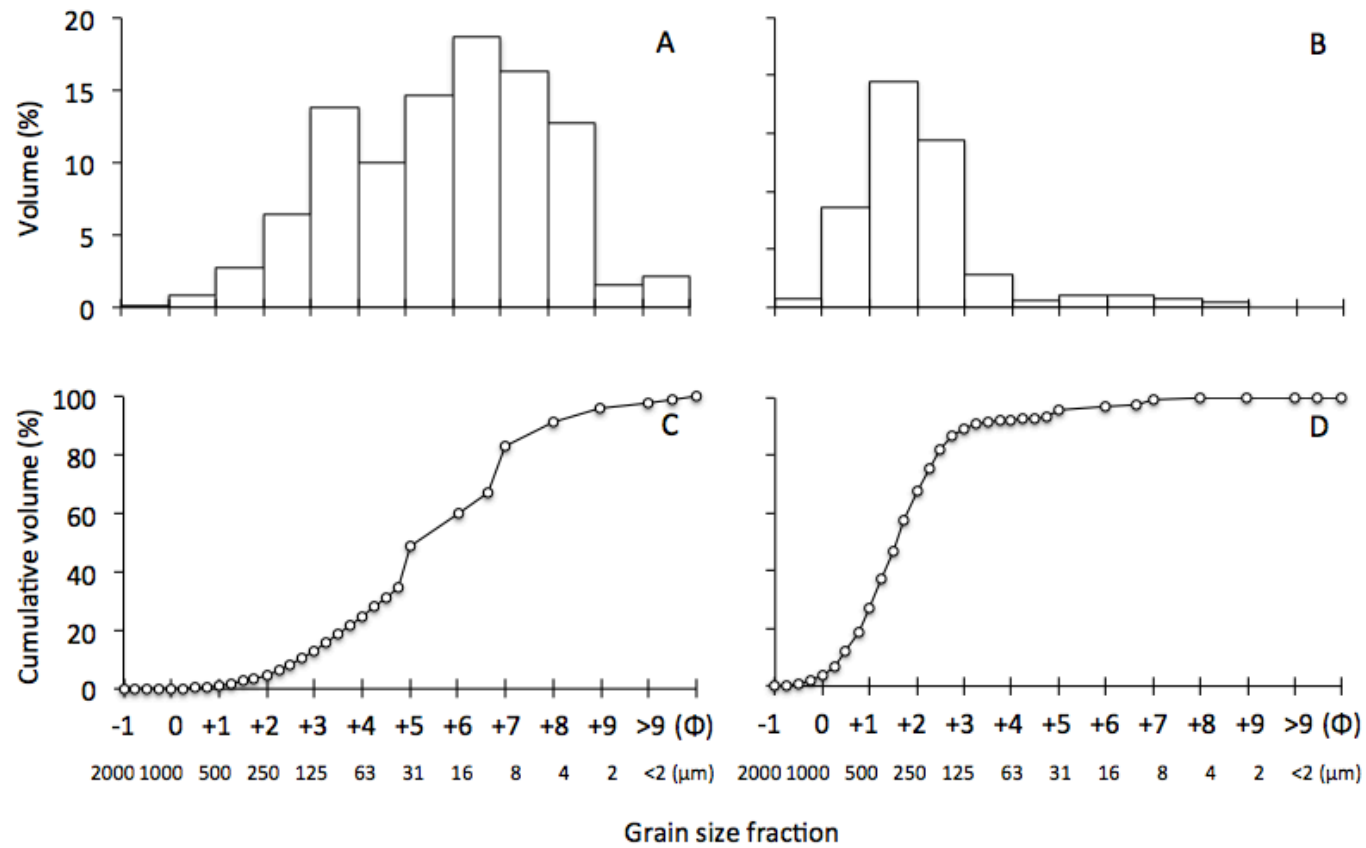


Figure 13. Sediment particle size distribution. Left panel, coastal sediment; right panel estuarine sediment. (A and B) Sediment grain size fractions, (C and D) Granulometric curves. Very coarse sand = 1000–2000 μm; coarse sand = 500–1000 μm; medium sand = 550–500 μm; fine sand 125–250 μm; very fine sand = 63–125 μm; silt = <63 μm; clay = <2 μm.

Modulation of pore water pH

I recorded pH microprofiles in two coastal sediment cores to investigate the effect of a decrease in the pH of the sediment-overlying seawater on the pore water pH. All average microprofiles shared the same overall shape. In light and darkness, the pH of the sediment-overlying seawater was close to that of the seawater in the incubation tanks (Fig. 14 A, B). In darkness, it decreased towards the sediment surface whereas under conditions of light, it increased to a maximum just below the sediment surface. Further down, the pH decreased to reach a stable value (7.49–7.54, Fig. 14 A–C) at 5–8 mm depth under conditions of light. Below this zone, the pore water pH continued to decrease. Inspection of the average dark profiles revealed that the pH decreased below the sediment surface to reach a stable value (Fig. 14 A, C, D) or a zone of less steep decrease (Fig. 14 B) at a shallower depth of ~4–6 mm. Further down, the pH continued to decrease as observed under conditions of light.

Comparing the average pH profiles measured in the Control (C15) and Treatment (C2) sediment core at time-zero revealed that the sediment core C2 appeared to have more photosynthetic activity than C15, because the subsurface maximum was more pronounced (Table 18).

Table 18

Median, maximum and minimum pore water pH readings at the upper 2 mm during time-zero and final time-point analyses for the Control and Treatment sediment in darkness and light conditions

		Control C15		Treatment C2	
		Light	Dark	Light	Dark
Time-zero	Median	8.12	7.90	8.28	7.94
	Maximum	8.27	8.04	8.37	8.05
	Minimum	7.87	7.79	7.99	7.79
Final time-point	Median	8.18	7.83	8.12	7.51
	Maximum	8.31	8.01	8.43	7.73
	Minimum	7.89	7.67	7.73	7.43

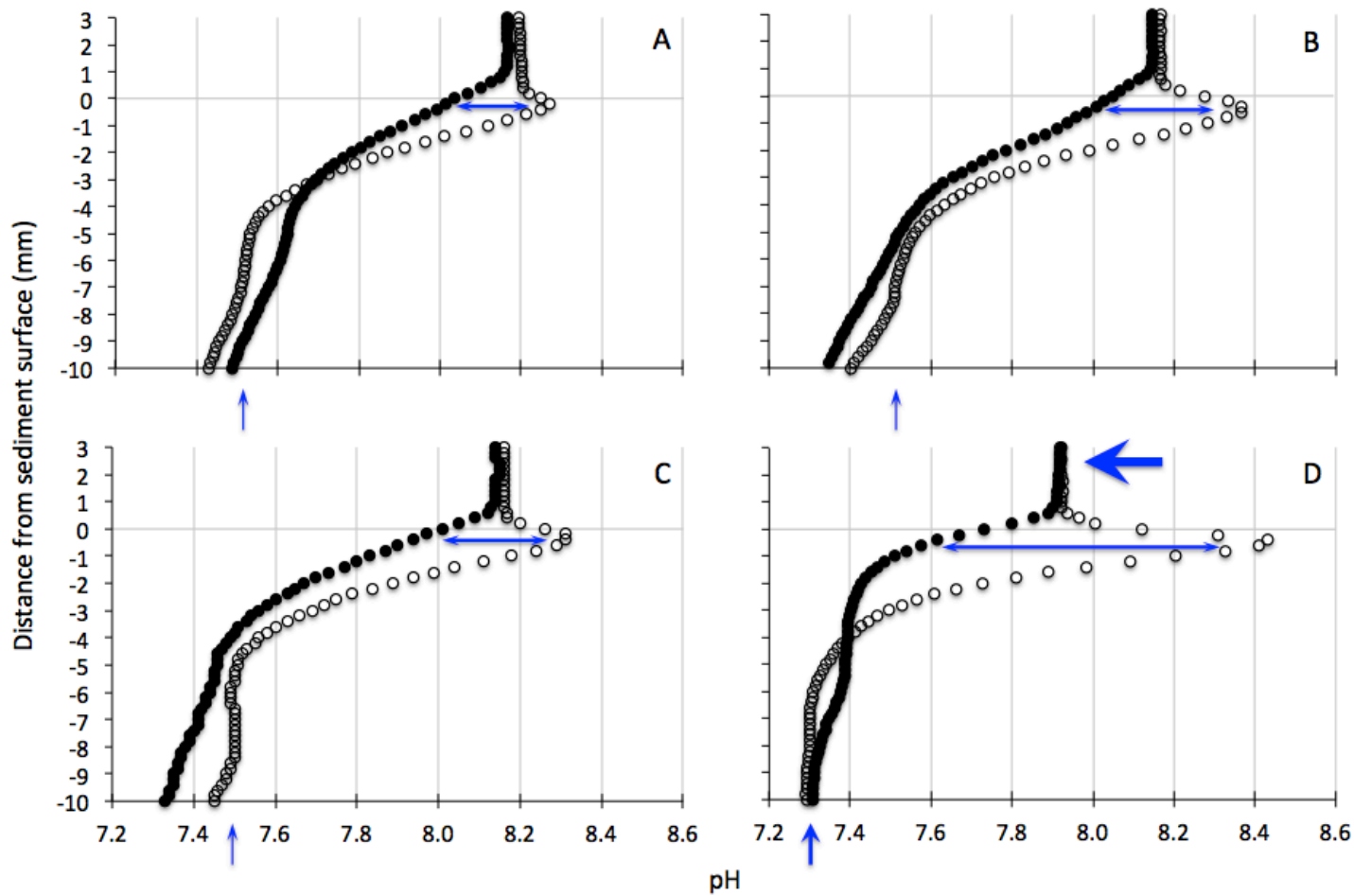


Figure 14. Average pore water pH profiles in coastal sediment in (A) Control sediment C15 time-zero, (B) Treatment sediment C2 time-zero, (C) Control sediment C15 final time-point, (D) Treatment sediment C2 final time-point. Filled circles: darkness, empty circles: light conditions. Horizontal double-headed lines indicate the increased amplitude of diel variations in the pH of the Treatment sediment subsurface with overlying acidified seawater (large arrow); vertical arrows indicate the decrease in the pH of the suboxic sediment layer

The pH of the seawater overlying the sediment core, C2, was then lowered over the course of two weeks and another set of microprofiles was recorded in both cores in Week 7. Inspection of the average profiles (Fig. 14 C, D) confirmed the treatment; that is, the pH of the sediment-overlying seawater in C2 was 0.23 units lower than that of the seawater overlying the sediment core C15 (big arrow in Fig. 14 D). This decrease in the pH of the sediment-overlying seawater was not paralleled by a decrease in the pH of the subsurface pore water. In contrast, the subsurface pH maximum was more pronounced, reaching an average value of 8.43. Also, under darkness the subsurface decrease in pH became steeper. That is, the differences between dark and light variations became larger (compare Fig. 14 B with Fig. 14 D, Table 18). A similar trend was apparent in core C15, but the changes over time were less pronounced. In addition to an increase over time in the light-induced variability of the subsurface pH, the pH of the suboxic sediment layer also decreased. Under conditions of light, the pH of the pore water in this layer was constant at ~7.5 (Fig. 14 A–C). In the Treatment sediment (Fig. 14 D), however, the pH of this pore water was ~7.3. That is, a decrease in the pH of the sediment-overlying seawater appeared to have decreased the pH of the deeper, suboxic sediment layer.

Composition of microbial assemblages

The purpose of investigating the composition of microbial assemblages in the sediments was to determine whether the seawater pH decrease had an effect on their structure. I hypothesised I would find a significant difference between the Treatment and Control sediments in the structure of the assemblage of ammonia-oxidising archaea and bacteria. A total of 6,238 OTUs were detected among the 30 DNA templates analysed, including five time-zero and 10 final time-point samples for both types of sediment (Appendix 6 B, C). A limited number of OTUs were likely to be ammonia-oxidising bacteria. These were *Nitrosomonas* sp. and *Nitrospira multiformis*, corresponding to 0.0056% and 0.0026% of the total reads, respectively. Three OTUs appeared to be ammonia-oxidising archaea, *Nitrosopumilus maritimus* and two species of uncultured Thaumarchaeota, which collectively represented 0.0383% and 0.0092% of the total reads, respectively. The extremely low relative abundance of potential ammonia-oxidising OTUs was insufficient for meaningful statistical analyses (Table 19).

Table 19

Percentage of reads of ammonia-oxidising archaea and bacteria identified in coastal and estuarine sediment. AOA, ammonia-oxidising archaea; AOB, ammonia-oxidising bacteria

	Coastal			Estuarine		
	Time-zero (%)	pH 8.1 (%)	pH 7.8 (%)	Time-zero (%)	pH 8.1 (%)	pH 7.8 (%)
<i>Nitrosopumilus maritimus</i>	0.0195	0.0035	0	0.0024	0.0105	0.0024
Uncultured Thaumarchaeota	0	0.0039	0.0004	0.0006	0.0004	0
Uncultured Thaumarchaeota	0.0017	0.0004	0.0004	0.0002	0.0006	0.0006
Total AOA	0.0213	0.0078	0.0009	0.0032	0.0116	0.0030
<i>Nitrosospira multiformis</i>	0	0	0	0.0009	0.0013	0.0004
<i>Nitrosomonas</i> sp.	0.0026	0	0	0	0.0006	0.0024
Total AOB	0.0026	0	0	0.0009	0.0019	0.0028

Although I was not able to determine differences in the structure and abundance of potential ammonia-oxidising microorganisms, I investigated the overall response of the microbial assemblages. Cluster analysis and similarity profile did not reveal clustering patterns that distinguish between treatments in any of the two types of sediment (Fig. 15, 16). Likewise, PERMANOVA and ANOSIM analyses revealed no significant differences between the Control and Treatment final time-point assemblages in both types of sediment (Table 20 A). The positive R number in the ANOSIM analysis for estuarine sediment reflected that the variation within treatments was not greater than the variation between treatments. In contrast, the negative R number retrieved for coastal sediment reflected greater variation within than between treatments. Overall, I found no statistical difference between the microbial assemblages in the Control and Treatment sediments. The composition of the microbial assemblages, however, changed over time. PERMANOVA and ANOSIM analyses showed a marginal difference in the composition of such assemblages in the coastal sediment, and a significant difference in the estuarine sediment, between time-zero and final time-point assemblages (Table 20 B).

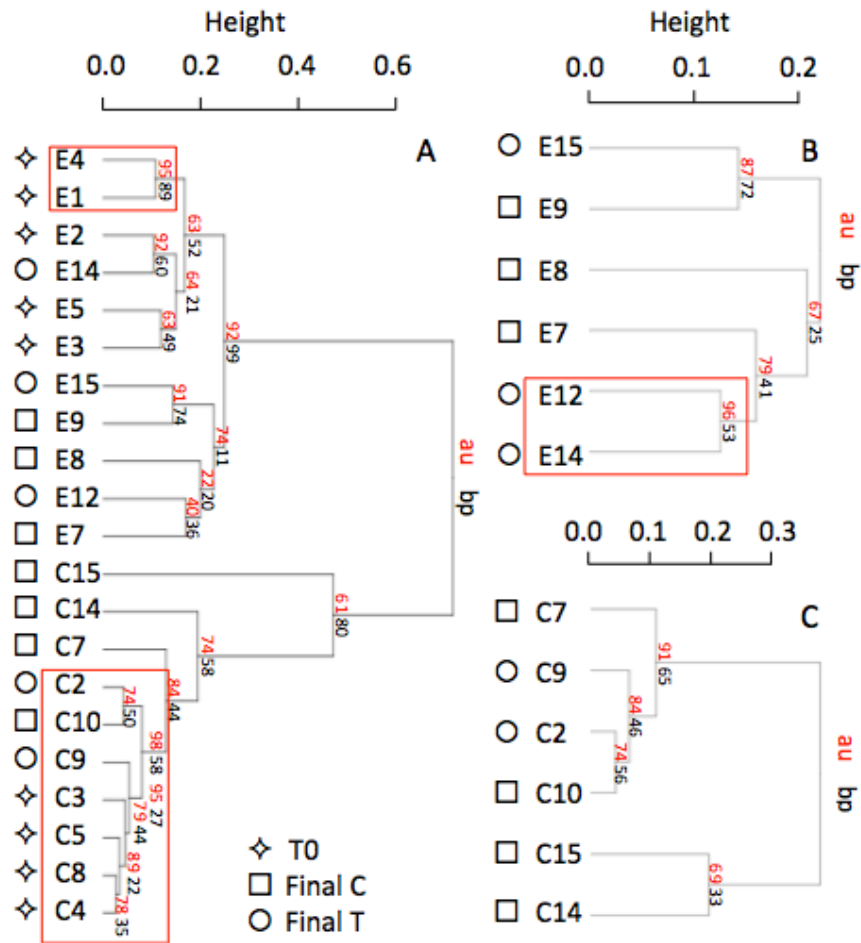


Figure 15. Hierarchical cluster analysis of normalised OTU frequencies at time-zero (T0, pH 8.1) and final analyses (Final C, pH 8.1 and Final T, pH 7.8) showing no defined clustering patterns between treatments in any of the two types of sediment. (A) Estuarine and coastal sediment. (B) Final analysis of estuarine sediment. (C) Final analysis of coastal sediment. AU = Approximately Unbiased p-value; BP = Bootstrap Probability value; red squares = AU > 95% (clusters strongly supported by multiscale bootstrap resampling). Cluster method = average, distance method = correlation, alpha = 0.05, bootstrap replications = 1000.

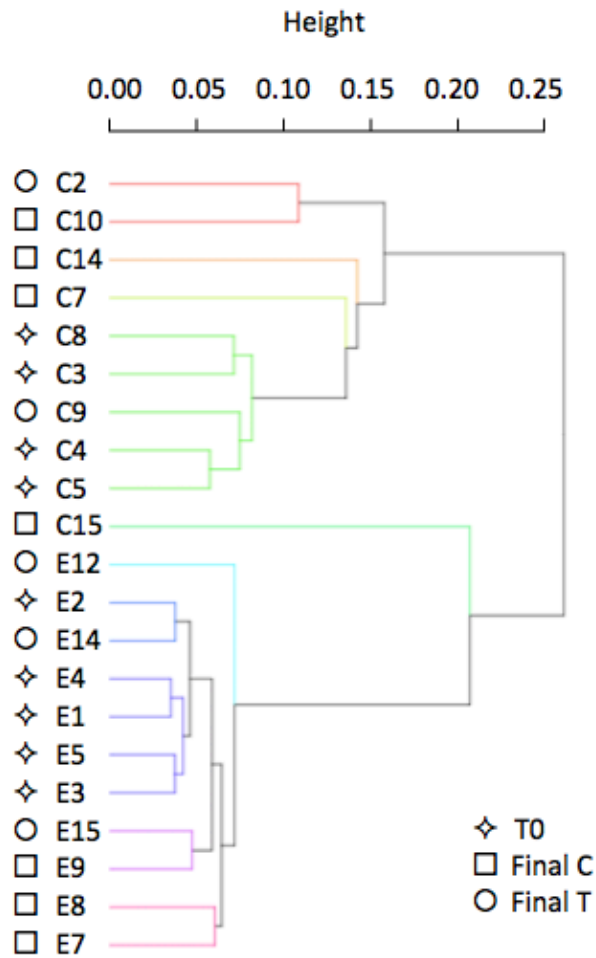


Figure 16. Similarity profile analysis of normalised OTU frequencies at time-zero (T0, pH 8.1) and final analyses (Final C, pH 8.1 and Final T, pH 7.8) showing no defined clustering differences between treatments in any of the two types of sediment. Each colour of branch represents statistically different clusters. Number of similarity profiles = 999, cluster method = average, distance method = Euclidean, alpha = 0.05.

Table 20

Statistical analyses of microbial assemblages in coastal and estuarine sediment. PERMANOVA, permutational multivariate analysis of variance; ANOSIM; analysis of similarity

Statistical analysis	Type of sediment	PERMANOVA		ANOSIM	
		Pseudo-F	<i>p</i> -value	R	<i>p</i> -value
A. Control vs. treatment	Coastal	1.0913	0.333	-0.1429	0.656
	Estuarine	1.0636	0.292	0.0555	0.308
B. Time-zero vs. control vs. treatment	Coastal	1.6009	0.045	0.2740	0.049
	Estuarine	1.7925	0.002	0.7228	0.001
C. Coastal vs. estuarine sediment	Both	26.1053	0.001	1.0000	0.001

I was expecting differences in the structure of microbial assemblages between the two types of sediment because of their contrasting characteristics. This expectation was confirmed by the defined clustering for each type of sediment, the significant difference found in PERMANOVA and ANOSIM analyses and the differences in diversity and species' richness (Fig. 15 A, 16, Tables 20 C, 21).

Diversity, evenness and richness appeared to have decreased from time-zero to final analysis in the Treatment coastal sediment. In the latter, however, only two replicates were considered, because of the low number of readings in the other three replicates (<500 reads). Although not of statistical relevance, comparing only two replicates randomly chosen in each time-point and treatment revealed a similar diversity, evenness and richness (Table 21).

Similarly, in estuarine sediment, diversity and richness appeared to have decreased from the time-zero to final analyses. However, five replicates were considered for the time-zero analyses, compared to three replicates for both the Control and Treatment final analyses. Comparing only three replicates randomly chosen retrieved similar diversity, evenness and richness (Table 21).

Inspection of the relative abundance of the microorganisms comprising the assemblages revealed that in both the coastal and estuarine sediment, *Proteobacteria* was the dominant phylum (Fig. 17). Closer inspection showed that the dominant class of this phylum was the *Gammaproteobacteria* for coastal sediment; whereas the *Alphaproteobacteria* dominated estuarine sediment (Fig. 17). As expected from the macroscopically observable biota, diatoms were abundant in both types of sediment. In fact, diatoms were the 16th most

abundant OTU in coastal sediment and the 7th most abundant in estuarine sediment (Table 22) even though the PCR primers used do not explicitly target them.

Table 21

Diversity indices of microbial assemblages in coastal and estuarine sediment including all normalised replicates (above) and identical number of replicates (below, two and three replicates randomly chosen, respectively). OTUs, operational taxonomic units

	Coastal sediment			Estuarine sediment		
	Time-zero	pH 8.1	pH 7.8	Time-zero	pH 8.1	pH 7.8
Replicates	4	4	2	5	3	3
Shannon-Weaver Index	4.002	4.152	3.640	6.351	6.157	6.130
Simpson's index of diversity	0.937	0.945	0.912	0.994	0.992	0.992
Evenness	0.630	0.655	0.624	0.832	0.838	0.836
Species richness (Total OTUs)	575	565	342	2069	1558	1527
Replicates	2	2	2	3	3	3
Shannon-Weaver Index	3.841	3.635	3.640	6.223	6.157	6.130
Simpson's index of diversity	0.936	0.918	0.912	0.994	0.992	0.992
Evenness	0.660	0.624	0.624	0.847	0.838	0.836
Species richness (Total OTUs)	337	340	342	1551	1558	1527

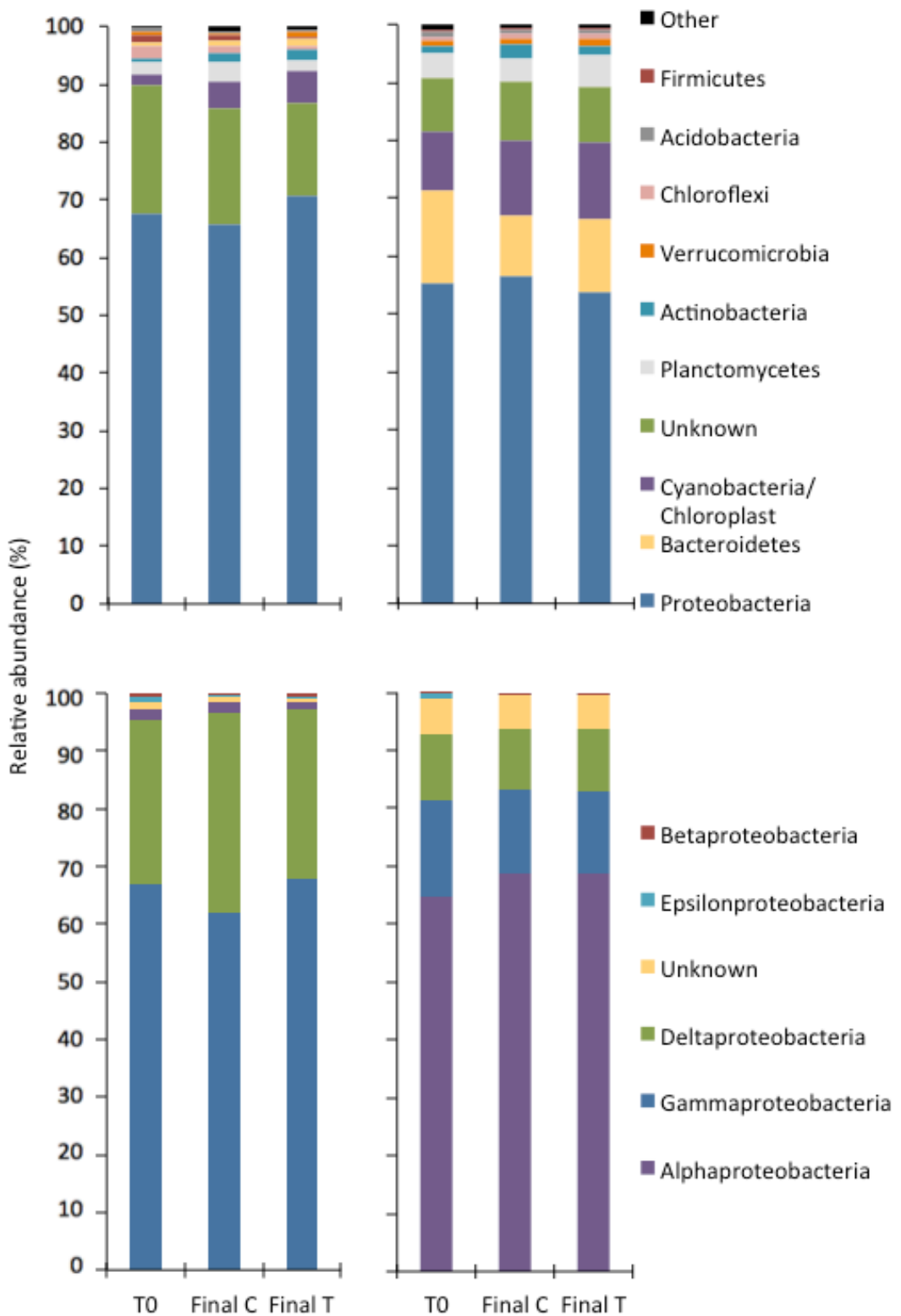


Figure 17. Relative abundance of phyla (above) and *Proteobacteria* classes (below) found in coastal (left) and estuarine (right) sediment in time-zero (T0, pH 8.1) and final analyses (Final C, pH 8.1 and Final T, pH 7.8). Phyla with <80% confidence level of identification were classified as Unknown. Phyla classified as Other constitute <1% of the phyla identified. Classes with <80% confidence level of identification were classified as Unknown.

Table 22.

Twenty most abundant operational taxonomic units in coastal and estuarine sediment identified with a nucleotide BLASTn search. Accession numbers correspond to the most similar sequence found in the database. E value, Expectation value; Ident %, percentage of identity

Coastal sediment				Estuarine sediment			
Microorganism	E value	Ident %	Accession	Microorganism	E value	Ident %	Accession
Uncultured Chromatiales	9E-121	99	AM501626.1	Uncultured δ -Proteobacteria	2E-123	100	JF344024.1
Uncultured γ -Proteobacteria	2E-123	100	JF777025.1	Uncultured Cyanobacteria	2E-123	100	JF929315.1
Uncultured δ -Proteobacteria	2E-123	100	JF344024.1	Uncultured γ -Proteobacteria	2E-123	100	JQ579699.1
Uncultured Latescibacteria	2E-123	100	KR814116.1	<i>Thiopfundum hispidum</i>	6E-119	98	NR_112620.1
Uncultured Desulfobulbaceae	9E-121	99	KR814221.1	<i>Neptuniibacter caesariensis</i>	2E-124	99	NR_042749.1
Uncultured δ -Proteobacteria	2E-123	100	HE803874.1	Uncultured γ -Proteobacteria	2E-123	100	JF344461.1
<i>Marinicella litoralis</i>	2E-124	99	NR_112913.1	Uncultured diatom, chloroplast	3E-120	99	FJ178075.1
Uncultured sediment bacteria	5E-118	98	KC925127.1	Uncultured Desulfobacteraceae	2E-123	100	KR814191.1
<i>Haliae mediterranea</i>	2E-124	99	NR_116976.1	<i>Loktanella maricola</i>	5E-127	100	NR_044163.1
Uncultured γ -Proteobacteria	5E-118	99	EU418464.1	<i>Sulfitobacter guttiformis</i>	5E-127	100	NR_029347.1
Uncultured γ -Proteobacteria	8E-122	99	GQ850559.1	<i>Haliae mediterranea</i>	2E-124	99	NR_116976.1
Uncultured γ -Proteobacteria	2E-117	99	FM211760.1	<i>Ruegeria conchae</i>	1E-122	99	NR_109062.1
Uncultured γ -Proteobacteria	6E-117	98	AB583276.1	<i>Octadecabacter arcticus</i>	5E-120	98	NR_102905.1
Uncultured γ -Proteobacteria	4E-119	99	KR086615.1	Uncultured Cyanobacteria	9E-121	99	AM177396.1
Uncultured ϵ -Proteobacteria	1E-119	99	KC631532.1	Uncultured δ -Proteobacteria	9E-121	99	AM040114.1
Uncultured diatom, chloroplast	3E-120	99	FJ178075.1	Uncultured Bacteroidetes	2E-123	100	JQ580249.1
Uncultured Proteobacteria	1E-113	97	EF651592.1	<i>Oceanicola granulosis</i>	5E-127	100	NR_115900.1
Uncultured mangrove bacteria	4E-94	98	HQ458776.1	<i>Psammodictyon panduriforme</i>	2E-123	100	FJ002157.1
<i>Psammodictyon panduriforme</i>	2E-123	100	FJ002157.1	<i>Actibacter sediminis</i>	2E-124	99	NR_044349.1
Uncultured γ -Proteobacteria	2E-117	99	KR086615.1	Uncultured Planctomycete	2E-123	100	EF215724.1

Abundance of *amoA* genes and transcripts

The methods used to determine the abundance of *amoA* genes and transcripts in this study had not been used before at The University of Waikato. I encountered numerous obstacles during the development of the protocol. In the next section, I will summarise the protocol development and troubleshooting. Following this, I will present the results of my final analyses.

Protocol development and troubleshooting

During the qPCR and RT-qPCR assays, I expected to find amplification in the DNA and RNA templates extracted from sediment. Such amplification would retrieve information about the initial amount of *amoA* genes or transcripts in the reaction tube when analysing against the standard curve. When the instrument did not retrieve a C_T value for a template (below the threshold), this suggested no amplification. C_T values above or very close to the negative controls indicated background fluorescence signal rather than amplification.

Amplification of standards and of one DNA template extracted from the estuarine sediment during trials misled me to believe that the protocol for qPCR assay did not require optimisation before starting time-zero analyses. For the RT-qPCR trials, I was not able to extract RNA from the frozen estuarine sediment. I could only run an RT-qPCR trial until I collected the sediments for the experiment to extract RNA from one coastal sediment core. Although RNA did not amplify in this trial, the fast degradation of RNA did not allow further optimisation assays and I used the same protocol for time-zero analyses.

The initial protocols used for time-zero qPCR and RT-qPCR assays were unsuccessful. The standards amplified, but neither DNA nor RNA templates extracted from the sediment amplified. Again, due to the fast degradation of the RNA, I could not repeat the RT-qPCR assays. I then continued to develop the protocol for the qPCR assays (Fig. 18), expecting to have results for the final analyses. PCR temperatures, times and cycle conditions used during time-zero analyses are listed in Appendix 7.

The annealing temperature is the temperature at which the primers anneal to the template to be amplified. If this temperature is not suitable, amplification becomes less likely to occur. I ran a gradient PCR, which revealed that 49 °C was the most suitable annealing temperature for both *amoA* archaeal and bacterial primers (Fig. 19). The annealing temperature I used during time-zero analyses was 52 °C. Contrary to what I expected, the annealing temperature improvement did not solve the lack of amplification in qPCR assays.

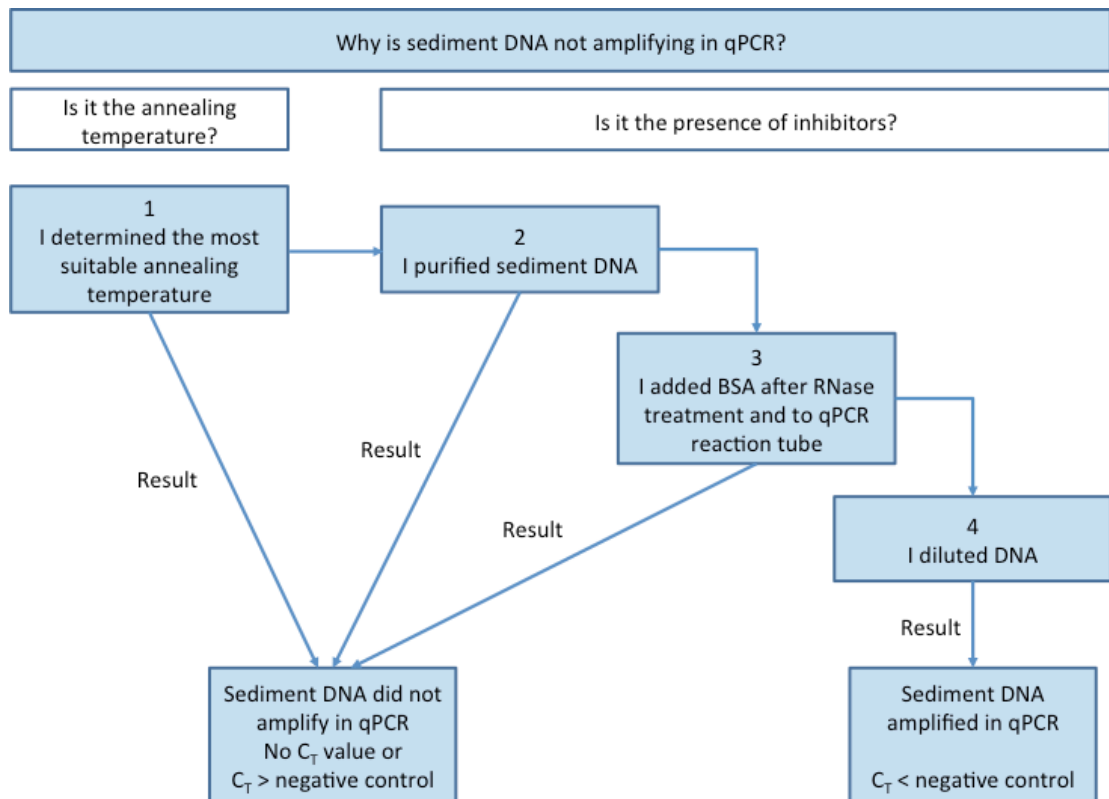


Figure 18. Sequence of steps followed during the protocol development and troubleshooting.

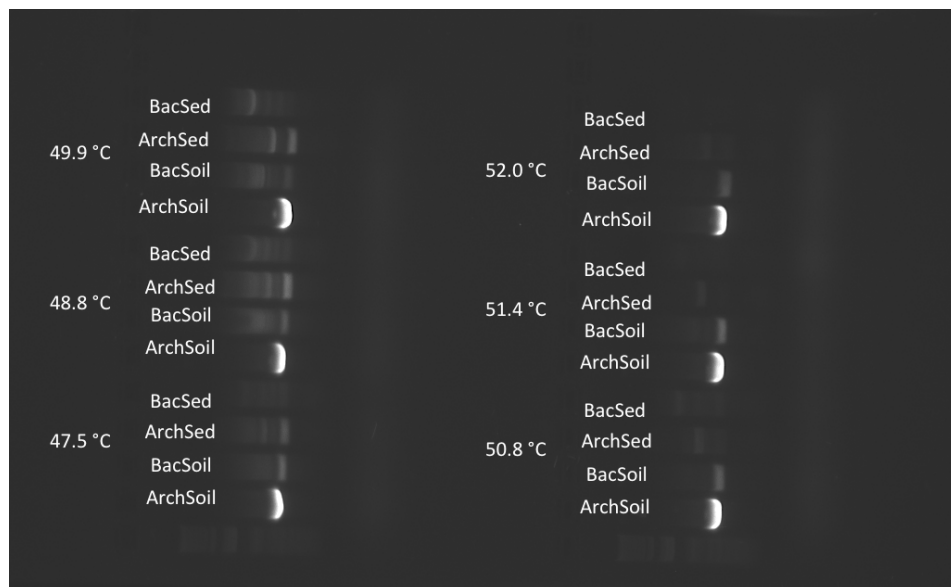


Figure 19. Gradient PCR analysis for *amoA* bacterial and archaeal primers in sediment and soil DNA showing the most suitable annealing temperature is ~49 °C for both primers (most intense, discrete and well-defined bands). BacSed, sediment bacterial amplicon; ArchSed, sediment archaeal amplicon; BacSoil, soil bacterial amplicon; ArchSoil, soil archaeal amplicon

I then hypothesised that sediment extractions contained compounds that inhibited qPCR (e.g., humic substances). To eliminate such inhibitors, I purified the DNA templates with Ultra Clean 15 DNA purification kit (MO BIO). This strategy, however, did not solve the lack of qPCR amplification.

Bovine serum albumin (BSA) has been used to overcome the presence of contaminants in DNA extracted from sediment (e.g., Rojas-Herrera et al., 2008). I ran a qPCR with RNase treated sediment supplied with 4 µg of BSA as a final step of the treatment. I also added 240 ng of BSA in each qPCR reaction tube. I included non-treated sediment as a control to exclude the possibility that the RNase treatment itself were inhibiting amplification. None of these DNA templates amplified, suggesting that the RNase treatment was not inhibiting the amplification, and that the addition of BSA was not an effective strategy to overcome inhibition.

Finally, I diluted the DNA templates, expecting that dilution of the inhibiting compounds would enable DNA to be amplified. Diluting the templates was an effective method to overcome inhibitors. For coastal sediment, the 1:100 diluted DNA templates amplified, whereas estuarine sediment DNA amplified in 1:10 and 1:100 dilutions. The C_T values for the amplified DNA templates were lower than that of the NTCs, suggesting true amplification (Table 23). Considering such dilutions, I assumed the same dilutions

Table 23

Average C_T of diluted DNA templates targeting bacterial and archaeal amoA genes. BT, below the threshold; NTC, no-template control

<i>amoA</i> target gene	Sediment type	Name	Dilution factor	Average C_T
Archaeal	Coastal	C8	10	BT
Archaeal	Coastal	C8	100	35.00
Archaeal	Estuarine	E3	10	31.81
Archaeal	Estuarine	E3	100	33.13
Archaeal	-	NTC	-	41.04
Bacterial	Coastal	C8	10	BT
Bacterial	Coastal	C8	100	31.35
Bacterial	Estuarine	E3	10	26.14
Bacterial	Estuarine	E3	100	29.74
Bacterial	-	NTC	-	34.98

would work for RT-qPCR assays and established the dilution rules specified in the Material and Methods section.

I was aware, however, that diluting DNA and RNA templates to overcome inhibition of amplification could be problematic for two reasons: (1) diluting templates might result in C_T values outside the range covered by the standards; and (2) amplification might become a function of the dilution factor of the inhibitors, rather than the abundance of genes or transcripts. I minimised the effect of using this strategy for the final analyses by: (1) including standards with low amounts of amplicon so as to cover the range of the diluted templates; and (2) determining the correlation between the dilution factor and results to analyse the data accordingly as explained in the Material and Methods section.

Abundance of *amoA* genes and transcripts after incubation

Among all the qPCR and RT-qPCR final analyses, I could only determine the abundance of *amoA* bacterial genes in the estuarine sediment and the abundance of *amoA* archaeal and bacterial transcripts in the coastal sediment. The remaining analyses were not considered to support or reject my hypothesis, because of one of two reasons: they produced C_T values that were so high that they resulted in theoretical concentrations <1 amplicon μL^{-1} in the reaction tube; or, they produced C_T values that were above or very close to the negative controls, indicating background fluorescence signal rather than amplification (Table 24).

The objective of analysing the abundance of *amoA* genes and transcripts was to determine whether the seawater pH decrease would alter the potential for ammonia oxidation. I hypothesised a lower abundance of genes, transcripts or both in sediments incubated in the Treatment tank than in those incubated in the Control tank. A lower abundance of genes would have indicated an alteration in the growth of ammonia oxidisers. A lower abundance of transcripts would indicate a lower expression of the *amoA* gene.

Different from what I hypothesised, analysis of the bacterial *amoA* gene abundances in the estuarine sediment revealed no significant differences between the Treatment and the Control sediments ($p = 0.59$, Fig. 20). The standard deviation of replicates was higher than the average, which indicated high variation among replicates (Table 25). Similarly, inspection of the abundance of archaeal *amoA* transcripts did not reveal significant differences between the Control and the Treatment coastal sediments ($p = 0.11$, Fig. 21, Table 26).

Table 24

Summary of results where the determination of *amoA* genes or transcripts abundance was possible

	Coastal		Estuarine	
	Archaeal	Bacterial	Archaeal	Bacterial
qPCR	No ¹	No ²	No ¹	Yes
RT-qPCR	Yes	Yes	No ²	No ²

¹ Concentration <1 amplicon μL^{-1}

² C_T above or very close to negative controls

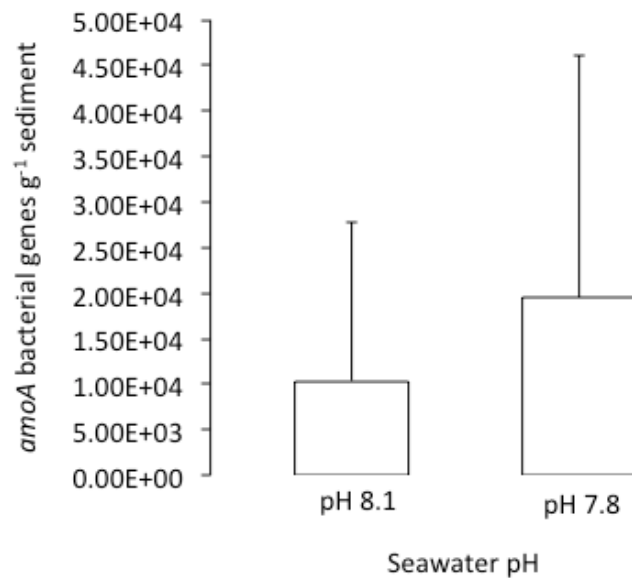


Figure 20. Effect of sediment-overlying seawater pH on the abundance of bacterial *amoA* genes in estuarine sediment. Bars, average number of *amoA* genes g^{-1} sediment at pH 8.1 and pH 7.8, respectively ($n = 4$; $p = 0.59$). Results for E7 and E11 sediment cores were not considered for the analyses due to their proximity to the C_T value of the no-template controls. Error bars represent standard deviation.

Table 25

Relative abundance of bacterial *amoA* genes in estuarine sediment

Bacterial <i>amoA</i> genes	Control (genes g^{-1} sediment)	Treatment (genes g^{-1} sediment)
Average	1.04×10^4	1.94×10^4
SD	1.73×10^4	2.66×10^4

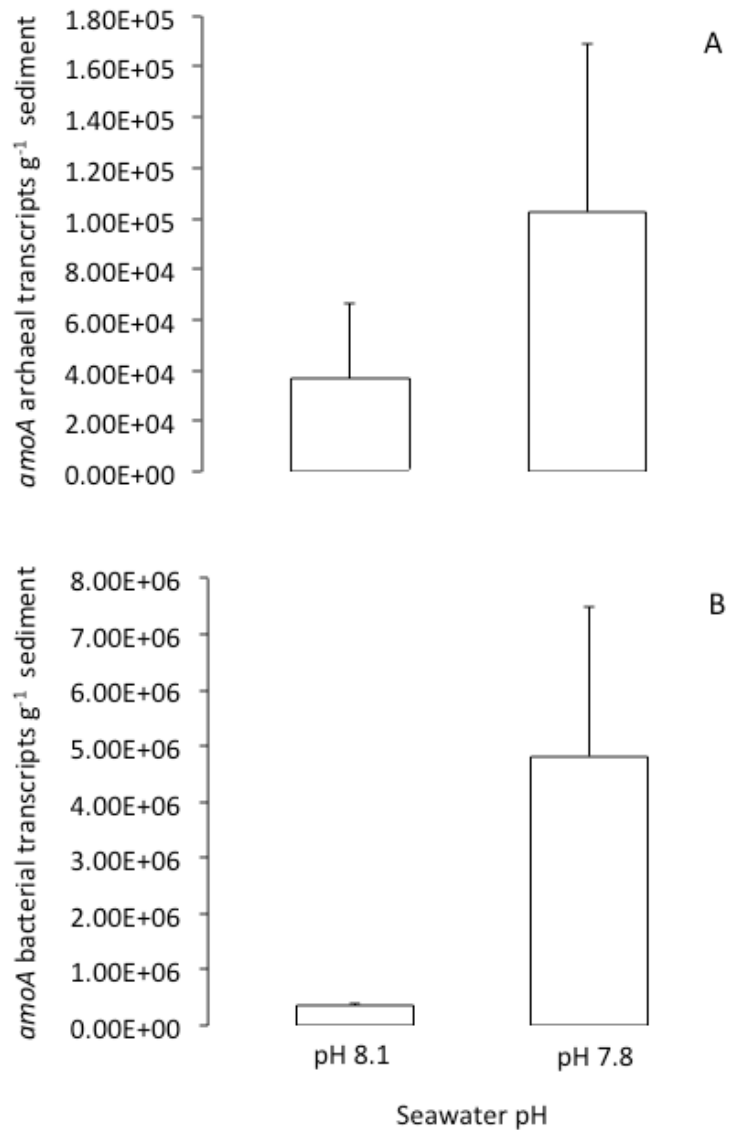


Figure 21. Effect of sediment-overlying seawater pH on the abundance of archaeal and bacterial *amoA* transcripts in coastal sediment. Bars, average number of *amoA* transcripts g⁻¹ sediment at pH 8.1 and pH 7.8, respectively (n = 3, archaeal transcripts $p = 0.14$; bacterial transcripts $p = 0.10$). Results for RNA templates with the lowest and highest dilutions were not considered for the analyses due to a strong correlation between dilution and number of copies ($r^2 = 0.8582$ for archaeal transcripts; $r^2 = 0.9759$ for bacterial transcripts). Error bars represent standard deviation.

Table 26

Relative abundance of archaeal amoA transcripts in coastal sediment

		Control (transcripts g ⁻¹ sediment)	Treatment (transcripts g ⁻¹ sediment)
Archaeal <i>amoA</i> transcripts	Average	3.73 × 10 ⁴	1.10 × 10 ⁵
	SD	2.68 × 10 ⁴	5.63 × 10 ⁴
Bacterial <i>amoA</i> transcripts	Average	3.59 × 10 ⁵	4.82 × 10 ⁶
	SD	4.55 × 10 ⁴	2.67 × 10 ⁶

Although the difference in bacterial *amoA* transcripts' abundance between the Control and Treatment coastal sediments appeared to be significant at first glance (Fig. 21, Table 26), statistical analysis revealed that such differences were not significant ($p = 0.10$). This non-significant difference was due to the variances of each data set, which were significantly different ($p = 0.0006$).

A retrospective statistical power analysis, however, revealed a high probability of falsely rejecting a true difference between the Control and the Treatment samples (type-II error). Such high probability was determined in both the *amoA* genes and transcripts abundances. The statistical power for the *amoA* transcripts' abundance was 0.46, whereas the statistical power for the *amoA* genes' abundance was 0.66. In both cases, the sample size determined to achieve a power of 0.8 was five. This means that considering five replicates for these analyses would have given an 80% probability to detect a true difference between the Control and the Treatment sediments.

A slope of -3.32 in the standard curve translates to a 100% efficiency of the PCR amplification, meaning a 10-fold increase of PCR amplicons every 3.32 cycles. Ideally, such a slope must be accompanied by a linearity $r^2 > 0.99$ and a sensitivity (y -intercept) of ~ 40 . The standard curve of the qPCR assay was relatively efficient, but with low sensitivity and linearity (Table 27). This was attributed to the low concentration of standards used; but all DNA templates were run in the same assay, minimising the margin of error. Standard curves from the first RT-qPCR showed a weak linear correlation and efficiency. This assay included DNA templates from sediment cores C10 and C13, which were not considered to estimate the average of transcripts g⁻¹ sediment. Standard curves for the second RT-qPCR showed good efficiency and linearity, although were low in sensitivity (Table 27).

The no-reverse transcriptase controls had higher C_T values than the no-template controls. This suggested that the DNA that was not fully degraded after DNase treatment did not interfere with the abundance of transcripts found. Table 28 lists the concentration of DNA and RNA extracted from the sediment cores.

Table 27

Standard curve parameters for the final RT-qPCR analyses in coastal sediment. r^2 , correlation coefficient

	qPCR	RT-qPCR 1		RT-qPCR 2	
	Bacteria	Archaea	Bacteria	Archaea	Bacteria
Slope	-3.679	-3.048	-2.026	-3.497	-3.625
Efficiency %	87.0	112.9	211.6	93.2	88.8
r^2	0.9829	0.9127	0.7669	0.9983	0.9928
y intercept	67.0	57.3	51.7	61.8	69.1

Table 28

Concentration of DNA and RNA extracted from coastal and estuarine sediment for final analyses. EBlank, estuarine extraction blank; CBlank, coastal extraction blank

Estuarine sediment	DNA (ng μL^{-1})	RNA (ng μL^{-1})	Coastal sediment	DNA (ng μL^{-1})	RNA (ng μL^{-1})
E6	<0.010	<0.050	C7	<0.010	47.9
E7	2.88	14.1	C10	<0.010	24.7
E8	1.29	8.6	C11	1.03	102
E9	1.57	<0.050	C14	<0.010	56.9
E10	<0.010	<0.050	C15	<0.010	54.7
E11	<0.010	<0.050	C2	1.05	91.7
E12	6.11	7.7	C9	<0.010	26.5
E13	<0.010	<0.050	C12	1.06	247
E14	<0.010	<0.050	C13	1.60	391
E15	2.89	20.1	C16	<0.010	73.8
EBlank	<0.010	<0.050	CBlank	<0.010	<0.050

Discussion

Effect of acidified seawater on the structure of benthic microbial assemblages

I hypothesised that an experimental decrease in the pH of the seawater overlying sediment would change the structure of the sediment assemblage of ammonia-oxidising archaea and bacteria. My results, however, could not support or reject such a hypothesis, due to the low abundances of ammonia-oxidising microorganisms found (Table 19). Although I could not investigate the response of the ammonia oxidising assemblage to acidified seawater, I investigated the response of the overall microbial assemblage. My results were mostly inconclusive. I had planned a robust analysis, with five biological replicates per time-point and treatment; but some of these replicates retrieved <2500 reads, likely due to the low DNA extraction yields (Table 28). These replicates, with a low number of reads, were excluded from the data analysis. For the coastal sediment, this resulted in an inconsistent number of replicates between treatments and time-points and, for the estuarine sediment, between time-points (Table 21). These inconsistencies made it impossible to draw significant conclusions.

For estuarine sediment, however, the number of replicates for final analyses was consistent between the Control and Treatment sediments (three replicates each). Although five replicates would have retrieved a more robust study, three replicates are acceptable for microbial ecology studies (Prosser, 2010). I found no significant differences in the overall microbial assemblages between the Control and the Treatment estuarine sediment. The positive R-value of the ANOSIM analysis confirmed that the failure to detect significant differences between the two treatments was not due to high variability among replicates.

Effect of acidified seawater on coastal sediment pore water pH

I found changes in the temporal variations and spatial distribution of pore water pH in the coastal Treatment sediment after a two-week incubation of the sediment cores in seawater of pH 7.8. Changes in the Control sediments were not as pronounced as in the Treatment sediment.

Temporal variations of pH in the upper oxic zone

Addition of carbon dioxide to the seawater seemed to alter the growth of diatoms, which in turn had an effect on the pore water pH, oxygen concentration and perhaps the microbial assemblage. The pore water pH profiles revealed that microorganisms experienced high pH fluctuations in the oxic zone at a diel scale, mostly in the upper ~2 mm (Fig. 14). In

darkness, diatoms consumed oxygen and released CO₂, decreasing the pore water pH. In light conditions, CO₂ fixation, due to photosynthetic activity, led to oxygen supersaturation and low concentration of CO₂ increasing the pore water pH (Revsbech, Jørgensen, Blackburn, & Cohen, 1983; Kristensen, 2000). These photosynthetic and dark respiration activities intensified in the Treatment sediment, presumably due to the CO₂-stimulation of diatoms' growth resulting in enhanced temporal variability (Fig. 14, double-arrowed lines).

The pH profiles showed that the seawater pH decrease not only shifted the pore water median pH, but the maximum and minimum also shifted towards a higher and lower pH, respectively (Table 18). Although microorganisms inhabiting the oxic zone may be adapted to temporal variability, the pH extremes they experienced may have exceeded their thresholds of optimal performance. For instance, low pH not only favours the ionised form ammonium over ammonia, but also favours nitrous acid over nitrite. In contrast, the concentration of free ammonia and nitrite increases at high pH. Ammonia is the actual substrate of ammonia-oxidising microorganisms, but high concentration of this substrate also inhibits the metabolism of ammonia-oxidising bacteria (Anthonisen, Loehr, Prakasam, & Srinath, 1976). High concentration of free ammonia has also inhibited the metabolism of nitrite-oxidising bacteria (Anthonisen et al., 1976).

Although there is controversy as to whether the actual substrate of nitrite-oxidising bacteria is nitrite or nitrous acid (e.g., Jiménez, Giménez, Ruano, Ferrer, & Serralta, 2011; Kampschreur et al., 2007; Pambrun, Paul, & Spérandio, 2006), high concentrations of both molecular forms have inhibited the nitrifying activity. High concentration of nitrous acid inhibited the metabolism of nitrite-oxidising bacteria (Anthonisen et al., 1976); whereas nitrite inhibited the activity of ammonia monooxygenase (Stein & Arp, 1998).

In addition to the enhanced temporal variations of pH, the activity of diatoms seemed to have shifted the oxic–suboxic boundaries (see stabilisation of pH, Fig. 14 D). The decreased oxygen penetration during the hours of darkness apparently shifted the suboxic zone to a shallower depth (~2–6 mm, Fig. 14 D); whereas the increased concentration of oxygen during light conditions seemed to have shifted the suboxic zone to a deeper layer (~6–10 mm, Fig. 14 D). Shifts in the oxic–suboxic boundaries between day and night are common in coastal sediments (e.g., Garcia-Pichel, Mechling, & Castenholz, 1994; Revsbech, Madsen, & Jørgensen, 1986). Ammonia-oxidising archaea (Blainey, Mosier, Potanina, Francis, & Quake, 2011), ammonia-oxidising bacteria, sulfide-oxidising bacteria (Kristensen, 2000) and filamentous cyanobacteria (McBride, 2001) redistribute under natural conditions when such boundaries shift (Kristensen, 2000). Many of these aerobic microorganisms descend during light hours and

ascend during darkness to meet their oxygen, light and pH requirements. The speed at which these microorganisms move is often less than that at which the boundary shifts (e.g., Garcia-Pichel et al., 1994). With a greater speed of boundary shifts because of the enhanced consumption and production of oxygen by diatoms, it is likely that the oxygen requirements of microorganisms may not have been met for greater periods of time.

Spatial distribution of pH in the suboxic zone

The decrease in the pH of the sediment-overlying seawater exceeded the buffering capacity of the suboxic zone. That is, the excess of protons was transferred to this zone. The stabilisation of pH in the suboxic zone is due to the balance between proton production and consumption (Jourabchi et al., 2005). Dissolution of calcite and reduction of metal oxides, the main processes for proton consumption (Jourabchi et al., 2005), did not seem to consume such excess of protons and the pH decreased. The decrease in pore water pH may have altered the metabolism of microorganisms inhabiting the suboxic zone. For instance, the abundance of transcripts of nitrite reductase has been low in sediments underlying low pH seawater (Tait et al., 2014). Benthic denitrification rates, however, have not shown a significant effect after exposure to low pH seawater (Gazeau et al., 2014).

Similar to the oxic–suboxic boundary, the suboxic–anoxic boundary seemed to have shifted to a deeper zone. In the anoxic zone, the pore water pH is no longer stable and decreases with increasing depth due to sulfate reduction (Jourabchi et al., 2005). The suboxic–anoxic boundary seemed to be at a ~8 mm depth in sediment, under conditions of light exposed to pH-8.1 overlying seawater (Fig. 14 A, B, C). Such a boundary was not visible in the Treatment profile, suggesting a shift to a layer deeper than 10 mm (Fig. 14 D). The presence of oxygen or reactive oxygen species, such as hydrogen peroxide and superoxide radicals, may have affected strict anaerobes that inhabited the anoxic zone before the shift (>8 mm), such as sulfate-reducing bacteria (Cypionka, 2000; Cypionka, Widdel, & Pfennig, 1981), and methanogenic archaea (Whitman, Bowen, & Boone, 2014). Although some sulfate-reducing bacteria are not strict anaerobes, others have been shown to be sensitive to oxygen (Cypionka et al., 1981). For instance, *Desulfovibrio* spp. is capable of survival in the presence of oxygen, although not showing sustainable growth in aerobic cultures (Cypionka, 2000); whereas Desulfobacterales have shown inhibited sulfate reduction as a function of oxygen concentration (Marschall, Frenzel, & Cypionka, 1993). Although some Desulfobacterales and methanogenic microorganisms may have migrated to a different depth, not all of them are motile (Brenner, Krieg, Staley, & Garrity, 2005; Whitman et al., 2014).

Similar structure of the microbial assemblage in the Control and Treatment estuarine sediment

I did not detect significant differences in the overall microbial assemblages comprising the oxic, suboxic and part of the anoxic zone of estuarine sediment between the Control and the Treatment sediment. I expected to find the ammonia-oxidising assemblages at the oxic–suboxic boundary (e.g., Zehr & Kudela, 2011) because, although nitrification is coupled to aerobic respiration and thus the reaction needs oxygen to occur, the substrate for nitrification, ammonia, is provided from the suboxic–anoxic zone (Jensen, Revsbech, & Nielsen, 1993). Nitrate, however, is provided from the oxic to the suboxic zone, where denitrification takes place. It was not until I analysed the pore water pH profiles that I had evidence to infer the depth of the oxic–suboxic boundary in my sediment cores: ~2–4 mm. My samples included sediment up to a depth of ~1 cm and the sequencing results confirmed that I sampled deeper zones.

For instance, the most abundant OTU in estuarine sediment was likely to be an anaerobic Deltaproteobacteria. This OTU showed a 100% match to bacteria found during the characterisation of an anaerobic microbial community in oil-polluted subtidal sediments (Acosta-González, Rosselló-Móra, & Marqués, 2013). This OTU also showed a 100% confidence score for belonging to the order Desulfobacterales, which are strict anaerobes capable of sulfate reduction (Rabus et al., 2013), the dominant pathway of anaerobic remineralisation in some coastal sediments (Jørgensen, 1982). The eighth most abundant OTU in estuarine sediment was also likely to be a strict anaerobe (Table 22).

Measuring pore water pH profiles for the estuarine sediment would have helped to understand why the structure of the microbial assemblage in the Treatment sediment did not differ from that in the Control sediment. This similarity, however, could be explained by acknowledging both possibilities; whether or not the decrease in the pH of the seawater decreased the pH in the porewater.

One explanation would be that the pH may not have decreased because the porewater was buffered. If so, the microbial assemblage was not exposed to a lower pH and thus its structure did not change. Changes in pH temporal variations at the oxic zone, however, seem to be possible due to the high abundance of diatoms, which was not specific to coastal sediment. In fact, diatoms were among the 20 most abundant OTUs in both types of sediment (Table 22) and their mats were visible and manually removed from the walls of the experimental units on various occasions. Although the abundance of diatoms was common to

both types of sediment, the pore water pH temporal variations and spatial changes may have been different in the estuarine compared with the coastal sediment. Estuarine sediment, for instance, was clearly rich in shells (Table 16, Fig. 12). Dissolution of calcium carbonate shells may have buffered the excess of protons and may have increased the pH, because a decrease in pH dissolves such carbonate shells consuming CO₂ (Equation 6, Mackie et al., 2011). In fact, dissolution of calcite is the main sink of protons in sediments (Jourabchi et al., 2005) and may have compensated for the excess of protons during the hours of darkness. In contrast, dissolution of calcite may have enhanced the increase in pH during light hours, because dissolution of CaCO₃ is not only a sink of protons, but also a source of CO₂ (Equation 6). Diatoms may have also decreased the oxygenation, availability of CO₂ and nitrogen sources through competitive exclusion, limiting these substrates for other aerobic microorganisms (Henriksen & Kemp, 1988; Risgaard-Petersen et al., 2004). This limitation would have resulted in starvation of such aerobic microorganisms and thus a decrease in their relative abundance. However, the oxic zone perhaps represented the smallest portion of the sediment sampled. Any alteration on the relative abundance of species at this zone could have been masked by a lack of such an alteration at the suboxic and anoxic zones.

If the pH in suboxic sediment decreased because the porewater did not buffer the excess of protons, the pH ranges for optimal growth of the microbiota inhabiting this zone could explain the lack of alterations. Although Tait et al. (2014) found inhibited transcription in denitrifying bacteria as mentioned above, many of these, and other bacteria inhabiting this portion of sediment, have optimal growth pH ranges that may have covered the pH at which the pore water may have shifted. The denitrifying bacterium *Thiobacillus denitrificans* (Beijerinck, 1904) Kelly and Wood, 2000, for instance, has an optimal growth pH of 6.8–7.4 (Brenner et al., 2005). Species of the genus *Desulfuromonas*, capable of reducing metal oxides, have an optimal pH range of between 7.2 and 7.5, although they are capable of growing at pH 6.5–8.5 (Brenner et al., 2005). *Deferribacter thermophilus* (Greene et al., 1997), capable of reducing iron, has a growth pH range of between 5 and 8 (Garrity et al., 2001). Given that the minimum pH registered in the pore water pH profile in coastal sediment was 7.29, I believe it is unlikely that the pH at the suboxic zone would have been below the minimum value of these ranges.

If the oxic–suboxic boundary shifted, as seen in the coastal sediment, redistribution of microorganisms may explain why the structure of the assemblage in the Treatment and Control sediments did not differ. This zone was likely inhabited by aerobes, which may have moved towards the surface of the sediment during darkness and descended a few millimetres

during light hours (e.g., Garcia-Pichel et al., 1994). Such aerobes may have moved to a zone that was included in the analysis and thus sequencing would not detect a change in the structure of the microbial assemblage.

If the suboxic–anoxic boundary shifted to a deeper zone, it is likely that this zone would have been inhabited by anaerobes. If so, formation of bacterial clumps or aerophobic bands by sulfate-reducing bacteria (e.g., Krekeler, Teske, & Cypionka, 1998) may explain the similarity between the Treatment and Control microbial assemblages. Apart from bacterial migration to deeper zones, which may not explain such similarity, sulfate-reducing bacteria form clumps and bands to tolerate oxygen saturation. The bands, for instance, have been found at the suboxic–anoxic boundary and even inside the oxic zone (Eschemann, Köhl, & Cypionka, 1999).

In agreement with my study, Tait et al. (2013), found no significant differences in the composition of microbial assemblages in Arctic sediments exposed to acidified pH treatments for two weeks. As in my study, the depth of sediment sampled was 1 cm. These authors attributed the lack of significant differences to the already low pH that microorganisms experience. They acknowledged, however, that there were no published data with detailed pore water pH profiles for a ~1 cm depth, which could have helped them to fully understand their failure to detect a difference in the composition of microbial assemblages among pH treatments.

Effect of acidified seawater on the potential for ammonia oxidation

I hypothesised a low *amoA* gene expression in sediment, due to the acidified overlying seawater. Results from this study were inconclusive, because of low statistical power. The fact that I could not include the five replicates for the statistical analyses reduced the power of my analyses to 66% and 46% probability to detect a difference in *amoA* genes and transcripts' abundance, respectively.

Strategies to improve the recovery of ammonia-oxidising microorganisms for future research

Investigating the oxic–anoxic boundary

One possible reason for the low abundance of ammonia-oxidising microorganisms in the present study was the depth of sediment sampled. Investigating the position of the oxic–suboxic boundary to inform the sampling depth should prevent excessive dilution of the ammonia-oxidising community with microorganisms inhabiting the suboxic–anoxic zone.

Increasing nucleic acids extraction yields

Another possible reason for the low abundance of ammonia-oxidising archaea and bacteria found in this research could be the low DNA and RNA extraction yields. On various occasions, the amount of nucleic acids extracted was below the limit of detection of the QuBit system.

The ability to recover detectable amounts of DNA or RNA appeared to be partly related to the phenol's pH. According to Pilcher, Gaudet, Fey, Kowal, and Chisholm (2007), the ideal pH to extract RNA is 4.7. Such acidic pH degrades DNA, which is partitioned to the phenolic phase, and the RNA remains in the aqueous phase. In the last extraction of coastal sediment, for instance, I could have adjusted the phenol's pH at <5. This could have caused the high RNA but low DNA yields (Table 27). Adjusting the phenol at pH 5 is difficult to achieve, mostly because the resolution of pH strips is not fine enough to differentiate between, for instance, pH 4.7 and 5. Having separate bottles of phenol, one at pH 4.3 and another at pH 8.0, which is the optimal pH for DNA extractions (e.g., Schneegurt, Dore, & Kulpa, 2003) should solve the problem of having low extraction yields due to phenol's pH. Both pH values of phenol are commercially available (e.g., Sigma-Aldrich).

In addition, the low amounts of nucleic acids extracted from sediment could be due to over-drying of extraction pellets. After discarding the 70% ethanol supernatant in the last steps of the extraction, I dried the pellet in a speed vacuum concentrator. The time in which the pellets are dried in depends on a visual inspection, to determine whether more time is needed. After drying it is difficult to see whether the pellet is still there, especially when the amount of nucleic acids extracted is already low. Leaving the tubes opened to air-dry after discarding the 70% ethanol supernatant rather than centrifuging would mitigate the risk of losing pellets.

Trying other methods to overcome inhibitors

Diluting DNA and RNA templates was the only possible strategy to overcome qPCR inhibition for this research, because of time and budgetary limitations. Yet, dilutions had undesirable implications. The strong correlation between the dilution factor and the abundance of transcripts limited the number of replicates for the statistical analysis, thus reducing the statistical power.

Coastal sediment contained more organic matter than estuarine sediment and perhaps more humic substances, such as humic acids, fulvic acids and humin. If so, inhibition by humic substances would explain why the coastal sediment needed higher dilution factors to amplify, compared to the estuarine sediment. Humic substances are known to inhibit PCR and

qPCR reactions (Schrader et al., 2012; Sidstedt et al., 2015). Sediments contain large amounts of humic substances, especially those rich in organic matter (Cronin & Morris, 1981; Sidstedt et al., 2015).

In addition, PCR was not inhibited; only the qPCR and RT-qPCR assays were. One possibility is that the fulvic acid did not inhibit amplification, but the humic acid inhibited fluorescence. According to Sidstedt et al. (2015), fulvic acid inhibits qPCR amplification and humic acid quenches the fluorescence of SYBR green. Various alternatives could be tried for further studies to overcome or prevent the presence of inhibitory compounds. For instance, the use of commercial kits to extract DNA and RNA from sediments; such as the MO BIO RNA Power Soil isolation kit and the DNA elution accessory kit (MO BIO Laboratories Inc.). Such extraction kits are designed to eliminate inhibitors, including fulvic and humic acids and have been used by other authors (e.g., Bowen et al., 2013; Magalhães et al., 2009; Tait, Stahl, Taylor, & Widdicombe, 2015). In addition, extraction yields would likely be higher than the ones obtained in this research.

Despite the benefits of using extraction kits, such extraction kits are expensive. Other strategies could be attempted to mitigate the effect of inhibitory compounds if using the extraction method described in this study. For instance, the purification of DNA through gel filtration chromatography, such as Sephadex G-200 saturated with Tris-EDTA buffer (Tsai & Olson, 1992), or the addition of extra Taq polymerase (Sutlovic, Gojanovic, Andelinovic, Gusic, & Primorac, 2005), are strategies that have been used to overcome inhibition by humic acid in sediment in PCR and qPCR assays, respectively. Moreover, according to Sidstedt et al. (2015), although humic acid quenches fluorescence of SYBR green, this acid does not quench hydrolysis probe fluorescence. Thus using probe-based kits for qPCR and RT-qPCR assays (e.g., TaqMan) instead of SYBR green could solve the lack of amplification signal in these assays.

Inhibition by residues of phenol from the extraction could also explain the higher dilution factor needed for the coastal sediment. The volume of phenol added to the coastal sediment was greater than the volume added to the estuarine sediment during nucleic acid extractions. That was because the aqueous phase was larger in coastal sediment than in estuarine sediment and I added an equal volume of phenol. Phenol is another organic compound known to inhibit PCR by degrading DNA polymerases (Katcher & Schwartz, 1994). Inhibition by phenol, however, would not explain that amplification was possible in PCR but not in the qPCR and RT-qPCR assays.

Benthic mesocosms for ocean acidification research

One of the goals of this experiment was to establish a new facility for acidification experiments with cores of sediment. The aim was to maintain each experimental unit under controlled conditions to (1) minimise the organisms' stress and (2) have confidence that any differences found between the Control and Treatment sediments were a function of the overlying seawater pH and not variations in other physicochemical parameters.

Despite the seawater pH excursions, I proved that the experimental units could maintain the pH within a narrow range. The fluctuations were similar and in some cases narrower than that of some published experimental units (Table 29).

Overall, the unexpected pH trends during the experiment could be explained by malfunction of parts of the experimental units. For instance, the fluctuations in pH measurements during the first 11 days of acclimatisation were attributed to electrical interference. I was expecting variations in the incubation tanks during this period because of the biological activity in the sediments. However, the seawater pH fluctuations followed the same pattern in the incubation tanks and mixing barrels of both experimental units (Fig. 9). This pattern disappeared after recalibration of the pH sensors, suggesting that the interference was mitigated after such recalibration.

Table 29

Ranges of seawater pH in three published experimental units for ocean acidification research and in the present study

Source	Aimed pH	Range	Days of incubation
Widdicombe and Needham (2007)	7.9	7.880 ± 0.040	35
Widdicombe and Needham (2007)	7.3	7.255 ± 0.045	35
Braeckman et al. (2014)	8.0	7.955 ± 0.115	14
Braeckman et al. (2014)	8.0	8.075 ± 0.035	14
Braeckman et al. (2014)	7.7	7.800 ± 0.210	14
Braeckman et al. (2014)	7.7	7.715 ± 0.045	14
Gazeau et al. (2014)	8.1	8.130 ± 0.080	14
Gazeau et al. (2014)	7.8	7.840 ± 0.110	14
Mixing barrel (present study)	8.1	8.081 ± 0.021	30
Mixing barrel (present study)	7.8	7.787 ± 0.056	37

A drift of the pH sensor likely caused the upward trend in the Treatment incubation tank towards the end of the experiment. The pH sensors were not recalibrated during the last month of incubation, thus it is possible that during this time sensor drift caused such trend. This is supported by the fact that the seawater pH, estimated from total alkalinity and dissolved inorganic carbon concentration, did not show such a trend (Fig. 11). In addition, after the stepwise decrease of the seawater pH in the Treatment experimental unit, the concentration of dissolved inorganic carbon did not seem to increase (Fig. 10). This further supports that the seawater pH did not increase, but rather the upward trend observed was due to a drift in the pH sensor.

I acknowledge that another option, although less likely, could be a change of the seawater carbonate chemistry. The slight decrease in seawater total alkalinity during the second half of the experiment would support this possible explanation. According to observations by Goldman and Brewer (1980) and Wolf-Gladrow et al. (2007), an elevated uptake of ammonia by photoautotrophs could cause a decline in seawater alkalinity. As Henriksen and Kemp (1988) and Risgaard-Petersen et al. (2004) found, the mat of diatoms that developed over time could have increased the rates of ammonia uptake. Mats of diatoms were not only found in sediment but over the walls of the experimental units. They could have had an effect on the seawater of the experimental unit. However, a change of the carbonate chemistry would not explain why the estimated pH and concentration of dissolved inorganic carbon did not increase.

Setting the CapCTRL system setpoint at pH 8.1 seemed to be appropriate to maintain the pH in the Control experimental unit at such pH. But because of degassing, the pH in the Treatment incubation tank remained above the setpoint. The time-series recorded after the stepwise decrease in pH showed that the seawater pH was ~ 0.05 units above the aimed pH. Therefore, an offset should be considered for future research.

One improvement for future research in the experimental units could be a programmed partial replacement with fresh synthetic seawater. Recirculation of the same seawater may result in accumulation of nutrients that could promote the growth of diatoms. A number of studies, for example, Braeckman et al. (2014), Gazeau et al. (2014), and Widdicombe and Needham (2007) used flow-through systems that discarded (or recycled as in Braeckman et al., 2014) the outflow; whereas the inlet circulated natural seawater.

Another option could be the use peristaltic pumps to pump seawater into each sediment core and this seawater flowing to waste. The incubation tank could be used as a

reservoir of synthetic seawater and it would also solve the problem of pseudoreplication. In the current setup, the cores cannot be treated as replicates because they are connected (not independent) through the circulated seawater. Pumping seawater from the tank into individual cores would make these cores independent; thus avoiding pseudoreplication (Hurlbert, 1984).

Finally, I acknowledge that any sediments' alterations or lack of alterations found in this study in response to the CO₂-enrichment of the seawater column should not be taken as a prediction of the effect of ocean acidification on the future coastal sediment. It is clear that ocean acidification is a process of years that cannot be replicated in laboratory conditions. This mesocosm experiment, however, was an attempt to increase our understanding of the link between the microenvironment, in terms of the porewater pH, and the structure of the microbial assemblage.

Conclusion

The decreasing seawater pH has raised numerous questions seeking to understand how the ecosystem could respond in the near future. I conducted this study to investigate the effect of a seawater pH decrease on the potential for benthic ammonia oxidation, a key process of organic matter remineralisation and nutrient cycling in coastal ecosystems.

The majority of results from this study were inconclusive. I have provided evidence, however, that a pH decrease of 0.3 units in seawater overlying estuarine sediment did not show significant alterations of the microbial assemblage structure at the upper 1-cm. This finding is in line with previous findings (Tait et al., 2013) and motivates further research questions to understand the mechanism underlying such non-significant alterations.

I have provided detailed pore water pH profiles of the upper 1-cm of muddy coastal sediment, showing alterations on temporal variations and spatial distribution of pH due to the seawater pH decrease. Such alterations seemed to be a consequence of diatoms' CO₂-growth stimulation, which may in turn have implications in the microbiota inhabiting the oxic, suboxic and upper anoxic zones. The diatoms' intensified respiration and photosynthesis shifted the pore water median pH, oxygen concentration and likely altered part of the microbial assemblages.

Although pore water pH profiles have been examined in the past to determine alterations due to overlying acidified seawater (e.g., Braeckman et al., 2014; Widdicombe et al., 2013), further work should focus on increasing the detail at the upper millimetres of sediment. The profiles in the present study were perhaps the first step towards improving our understanding on the importance of interactions between diatoms and associated microbiota to elucidate the possible effect of the future acidified ocean on the biogeochemistry of coastal sediment. The results presented in this thesis are encouraging and should be validated by a larger sample size of biological replicates.

I have succeeded in establishing a facility for ocean acidification research to incubate sediment cores in recirculating seawater. Despite instrument failures, I have demonstrated that this facility was capable of maintaining the seawater pH within narrow pH fluctuations, and temperature and salinity under controlled perturbation. This facility enabled us to investigate important biological interactions underlining the importance of multiple-species mesocosm experiments.

References

- Acosta-González, A., Rosselló-Móra, R., & Marqués, S. (2013). Characterization of the anaerobic microbial community in oil-polluted subtidal sediments: aromatic biodegradation potential after the Prestige oil spill. *Environmental Microbiology*, *15*(1), 77-92. doi:10.1111/j.1462-2920.2012.02782.x
- Ahmed, M. G., Elhassan, B. M., & K.E. Bashar. (2012). Modeling of oil spill in the Sudanese Red Sea coastal water. *Sudan Engineering Society Journal*, *58*(2), 45-53.
- Akane, A., Matsubara, K., Nakamura, H., Takahashi, S., & Kimura, K. (1994). Identification of the heme compound copurified with deoxyribonucleic acid (DNA) from bloodstains, a major inhibitor of polymerase chain reaction (PCR) amplification. *Journal of Forensic Sciences*, *39*(2), 362-372.
- Aller, R. C. (1994). Bioturbation and remineralization of sedimentary organic matter: effects of redox oscillation. *Chemical Geology*, *114*, 331–345. doi:10.1016/0009-2541(94)90062-0
- Aller, R. C., & Aller, J. Y. (1998). The effect of biogenic irrigation intensity and solute exchange on diagenetic reaction rates in marine sediments. *Journal of Marine Research*, *56*(4), 905-936. doi:10.1357/002224098321667413
- Allison, S. D., & Martiny, J. B. H. (2008). Resistance, resilience, and redundancy in microbial communities. *Proceedings of the National Academy of Sciences of the United States of America*, *105*, 11512-11519. doi:10.1073/pnas.0801925105
- Alzerreca, J., Norton, J., & Klotz, M. (1999). The *amo* operon in marine, ammonia-oxidizing gamma-proteobacteria. *FEMS Microbiology Letters*, *180*(1), 21-29.
- Anthonisen, A. C., Loehr, R. C., Prakasam, T. B. S., & Srinath, E. G. (1976). Inhibition of nitrification by ammonia and nitrous acid. *Water Pollution Control Federation*, *48*(5), 835-852.
- Aravindraja, C., Viszwapriya, D., & Pandian, K. S. (2013). Ultradeep 16S rRNA sequencing analysis of geographically similar but diverse unexplored marine samples reveal varied bacterial community composition. *PLoS One*, *8*(10), e76724.
- Archer, D. E., Morford, J. L., & Emerson, S. R. (2002). A model of suboxic sedimentary diagenesis suitable for automatic tuning and gridded global domains. *Global Biogeochemical Cycles*, *16*(1), 17. doi:10.1029/2000GB001288
- Arfi, R., & Bouvy, M. (1995). Size, composition and distribution of particles related to wind-induced resuspension in a shallow tropical lagoon. *Journal of Plankton Research*, *17*(3), 557-574. doi:10.1093/plankt/17.3.557
- Baas-Becking, L. G. M., & Parks, G. S. (1927). Energy relations in the metabolism of autotrophic bacteria. *Physiological Reviews*, *7*(1), 85-106.
- Baker, K. M., Gobler, C. J., & Collier, J. L. (2009). Urease gene sequences from algae and heterotrophic bacteria in axenic and nonaxenic phytoplankton cultures. *Journal of Phycology*, *45*(3), 625–634. doi:10.1111/j.1529-8817.2009.00680.x
- Baker, G. C., Smith, J. J., & Cowan, D. A. (2003). Review and re-analysis of domain-specific 16S primers. *Journal of Microbiological Methods*, *55*, 541 – 555. doi:10.1016/j.mimet.2003.08.009
- Balashova, V., & Zavarzin, G. (1979). Anaerobic reduction of ferric iron by hydrogen bacteria. *Mikrobiologiya*, *48*(5), 773-778.

- Baltimore, D. (1970). RNA-dependent DNA polymerase in virions of RNA tumour viruses. *Nature*, *226*, 1209-1211.
- Barry, J. P., Hall-Spencer, J. M., & Tyrrell, T. (2010). *In situ* perturbation experiments: natural venting sites, spatial/temporal gradients in ocean pH, manipulative *in situ* p(CO₂) perturbations. In U. Riebesell, V. J. Fabry, L. Hansson, & J.-P. Gattuso (Eds.), *Guide to best practices for ocean acidification research and data reporting* (pp. 123-136). Luxembourg: Publications Office of the European Union.
- Beijerinck, M. W. (1904). Phénomènes de réduction produits par les microbes. *Archives Néerlandaises des Sciences Exactes et Naturelles*, *9*, 131-157.
- Beman, J. M., Chow, C.-E., King, A. L., Feng, Y., Fuhrman, J. A., Andersson, A., . . . Hutchins, D. A. (2011). Global declines in oceanic nitrification rates as a consequence of ocean acidification. *PNAS*, *108*(1), 208–213. doi:10.1073/pnas.1011053108
- Beman, J. M., Popp, B. N., & Alford, S. E. (2012). Quantification of ammonia oxidation rates and ammonia-oxidizing archaea and bacteria at high resolution in the Gulf of California and eastern tropical North Pacific Ocean. *Limnology and Oceanography*, *57*(3), 711–726. doi:10.4319/lo.2012.57.3.0711
- Bergmann, G. T., Bates, S. T., Eilers, K. G., Lauber, C. L., Caporaso, J. G., Walters, W. A., . . . Fierer, N. (2011). The under-recognized dominance of *Verrucomicrobia* in soil bacterial communities. *Soil Biology and Biochemistry*, *43*(7), 1450-1455. doi:10.1016/j.soilbio.2011.03.012
- Berner, R. A. (1964). Distribution and diagenesis of sulfur in some sediments from the Gulf of California. *Marine Geology*, *1*(2), 117-140. doi:10.1016/0025-3227(64)90011-8
- Biddle, J. F., Lipp, J. S., Lever, M. A., Lloyd, K. G., Sørensen, K. B., Anderson, R., . . . Hinrichs, K. U. (2006). Heterotrophic archaea dominate sedimentary subsurface ecosystems off Peru. *Proceedings of the National Academy of Sciences of the United States of America*, *103*(10), 3846-3851. doi:10.1073/pnas.0600035103
- Biteen, J. S., Blainey, P. C., Cardon, Z. G., Chun, M., Church, G. M., Dorrestein, P. C., . . . Young, T. D. (2016). Tools for the Microbiome: Nano and Beyond. *ACS Nano*, *10*, 6-37. doi:10.1021/acsnano.5b07826
- Blackburn, T. H., & Henriksen, K. (1983). Nitrogen cycling in different types of sediments from Danish waters. *Limnology and Oceanography*, *28*(3), 477-493.
- Blainey, P. C., Mosier, A. C., Potanina, A., Francis, C. A., & Quake, S. R. (2011). Genome of a low-salinity ammonia-oxidizing archaeon determined by single-cell and metagenomic analysis. *PLoS One*, *6*(2), e16626. doi:10.1371/journal.pone.0016626
- Boetius, A., Ravensschlag, K., Schubert, C., Rickert, D., Widdel, F., Gieseke, A., . . . Pfannkuche, O. (2000). A marine microbial consortium apparently mediating anaerobic oxidation of methane. *Nature*, *407*, 623-626.
- Boon, P. I., Moriarty, D. J. W., & Saffigna, P. G. (1986). Rates of ammonium turnover and the role of amino-acid deamination in seagrass (*Zostera capricorni*) beds of Moreton Bay, Australia. *Marine Biology*, *91*(2), 259-268.
- Boone, D. R., Liu, Y., Zhao, Z. J., Balkwill, D. L., Drake, G. R., Stevens, T. O., & Aldrich, H. C. (1995). *Bacillus infernus* sp. nov., an Fe(III)- and Mn(IV)-reducing anaerobe from the deep terrestrial subsurface. *International Journal of Systematic and Evolutionary Microbiology*, *45*(3), 441-448.

- Bowen, J. L., Kearns, P. J., Holcomb, M., & Ward, B. B. (2013). Acidification alters the composition of ammonia-oxidizing microbial assemblages in marine mesocosms. *Marine Ecology Progress Series*, 492, 1-8. doi:10.3354/meps10526
- Braeckman, U., Van Colen, C., Guilini, K., Van Gansbeke, D., Soetaert, K., Vincx, M., & Vanaverbeke, J. (2014). Empirical evidence reveals seasonally dependent reduction in nitrification in coastal sediments subjected to near future ocean acidification. *PLoS One*, 9(10), e108153. doi:10.1371/journal.pone.0108153
- Brenner, D. J., Krieg, N. R., Staley, J. T., & Garrity, G. M. (2005). Volume Two The Proteobacteria Part C The Alpha-, Beta-, Delta-, and Epsilonproteobacteria. In *Bergey's Manual of Systematic Bacteriology* (pp. 1388). doi:10.1007/0-387-29298-5
- Brown, C. M., & Herbert, R. A. (1977). Ammonia assimilation in purple and green sulphur bacteria. *FEMS Microbiology Letters*, 1(1), 39-42. doi:10.1016/0378-1097(77)90107-0
- Brune, A., Frenzel, P., & Cypionka, H. (2000). Life at the oxic–anoxic interface: microbial activities and adaptations. *FEMS Microbiology Ecology*, 24, 691-710.
- Burris, J. E. (1977). Photosynthesis, photorespiration, and dark respiration in eight species of algae. *Marine Biology*, 39(4), 371-379. doi:10.1007/BF00391940
- Bustin, S. A., Shipley, G. L., Vandesompele, J., Wittwer, C. T., Benes, V., Garson, J. A., . . . Pfaffl, M. W. (2009). The MIQE guidelines: minimum information for publication of quantitative real-time PCR experiments. *Clinical Chemistry*, 55(4), 611-622. doi:10.1373/clinchem.2008.112797
- Caccavo, F. J., Coates, J. D., Rossello-Mora, R. A., Ludwig, W., Schleifer, K. H., Lovley, D. R., & McInerney, M. J. (1996). *Geovibrio ferrireducens*, a phylogenetically distinct dissimilatory Fe(III)-reducing bacterium. *Archives of Microbiology*, 165(6), 370-376.
- Calosi, P., Rastrick, S. P. S., Lombardi, C., de Guzman, H. J., Davidson, L., Jahnke, M., . . . Gambi, M. C. (2013). Adaptation and acclimatization to ocean acidification in marine ectotherms: an *in situ* transplant experiment with polychaetes at a shallow CO₂ vent system. *Philosophical transactions of the Royal Society B*, 368:20120444(1-15). doi:10.1098/rstb.2012.0444
- Canadell, J. G., Quéré, C. L., Raupach, M. R., Field, C. B., Buitenhuis, E. T., Ciais, P., . . . Marland, G. (2007). Contributions to accelerating atmospheric CO₂ growth from economic activity, carbon intensity, and efficiency of natural sinks. *PNAS*, 104(47), 18866–18870 doi:10.1073/pnas.0702737104
- Canfield, D. E., Jørgensen, B. B., Fossing, H., Glud, R., Gundersen, J., Ramsing, N. B., . . . Hall, P. O. J. (1993). Pathways of organic carbon oxidation in three continental margin sediments. *Marine Geology*, 113(1-2), 27-40. doi:10.1016/0025-3227(93)90147-N
- Carpenter, E. J., Montoya, J. P., Burns, J., Mulholland, M. R., Subramaniam, A., & Capone, D. G. (1999). Extensive bloom of a N₂-fixing diatom/cyanobacterial association in the tropical Atlantic Ocean. *Marine Ecology Progress Series*, 185, 273-283. doi:10.3354/meps185273
- Carpenter, E. J., & Romans, K. (1991). Major role of the cyanobacterium *Trichodesmium* in nutrient cycling in the North Atlantic Ocean. *Science*, 254(5036), 1356-1358.
- Coates, J. D., Ellis, D. J., Gaw, C. V., & Lovley, D. R. (1999). *Geothrix fermentans* gen. nov., sp. nov., a novel Fe(III)-reducing bacterium from a hydrocarbon-contaminated aquifer. *International Journal of Systematic and Evolutionary Microbiology*, 49(4), 1615-1622.

- Comeau, S., Carpenter, R. C., Lantz, C. A., & Edmunds, P. J. (2015). Ocean acidification accelerates dissolution of experimental coral reef communities. *Biogeosciences*, *12*, 365–372.
- Constantine, R., Johnson, M., Riekkola, L., Jervis, S., Kozmian-Ledward, L., Dennis, T., . . . Soto, N. A. d. (2015). Mitigation of vessel-strike mortality of endangered Bryde's whales in the Hauraki Gulf, New Zealand. *Biological Conservation*, *186*, 149-157. doi:10.1016/j.biocon.2015.03.008
- Corredor, J. E. (1999). Nitrov — An etymology of nitrogen and other related words. *Biogeochemistry*, *46*, 5-6. doi:10.1007/978-94-011-4645-6_1
- Costa, E., Pérez, J., & Kreft, J.-U. (2006). Why is metabolic labour divided in nitrification? *Trends in Microbiology*, *14*(5), 213-219. doi:10.1016/j.tim.2006.03.006
- Couceiro, F., Fones, G. R., Thompson, C. E. L., Statham, P. J., Sivyer, D. B., Parker, R., . . . Amos, C. L. (2012). Impact of resuspension of cohesive sediments at the Oyster Grounds (North Sea) on nutrient exchange across the sediment–water interface. *Biogeochemistry*, *113*(1), 37-52. doi:10.1007/s10533-012-9710-7
- Cronin, J. R., & Morris, R. J. (1981). The occurrence of high molecular weight humic material in recent organic-rich sediment from the Namibia shelf. *Estuarine, Coastal and Shelf Science*, *15*, 17-27.
- Cummings, D. E., Jr., F. C., Spring, S., & Rosenzweig, R. F. (1999). *Ferribacterium limneticum*, gen. nov., sp. nov., an Fe(III)-reducing microorganism isolated from mining-impacted freshwater lake sediments. *Archives of Microbiology*, *171*(3), 183-188. doi:10.1007/s002030050697
- Cypionka, H. (2000). Oxygen respiration by *Desulfovibrio* species. *Annual Review of Microbiology*, *54*, 827-848.
- Cypionka, H., Widdel, F., & Pfennig, N. (1981). Survival of sulfate-reducing bacteria after oxygen stress, and growth in sulfate-free oxygen-sulfide gradients. *FEMS Microbiology Letters*, *31*(1), 39-45. doi:10.1016/0378-1097(85)90045-X
- Dähnke, K., Moneta, A., Veuger, B., Soetaert, K., & Middelburg, J. J. (2012). Balance of assimilative and dissimilative nitrogen processes in a diatom-rich tidal flat sediment. *Biogeochemistry*, *9*, 4059–4070. doi:10.5194/bg-9-4059-2012
- Daims, H., Lebedeva, E. V., Pjevac, P., Han, P., Herbold, C., Albertsen, M., . . . Wagner, M. (2015). Complete nitrification by *Nitrospira* bacteria. *Nature*, *528*, 504–509. doi:10.1038/nature16461
- Davies-Colley, R. J., & Healy, T. R. (1978). Sediment and hydrodynamics of the Tauranga entrance to Tauranga Harbour. *New Zealand Journal of Marine and Freshwater Research*, *12*(3), 225-236. doi:10.1080/00288330.1978.9515747
- Devol, A. H. (2015). Denitrification, anammox, and N₂ production in marine sediments. *Annual Review of Marine Science*, *7*, 403-423. doi:10.1146/annurev-marine-010213-135040
- Dickson, A. G. (2009). *Quality assurance of analytical measurements of CO₂ parameters*. Retrieved 31 Aug 2015, from <http://www.who.edu/files/server.do?id=53883&pt=2&p=58666>
- Dickson, A. G., & Millero, F. J. (1987). A comparison of the equilibrium constants for the dissociation of carbonic acid in seawater media. *Deep Sea Research Part A. Oceanographic Research Papers*, *34*(10), 1733–1743. doi:10.1016/0198-0149(87)90021-5

- Dickson, A. G., Sabine, C. L., & Christian, J. R. (2007a). SOP 1 Water sampling for the parameters of the oceanic carbon dioxide system. In *Guide to Best Practices for Ocean CO₂ Measurements* (pp. 191). Retrieved from http://cdiac.ornl.gov/ftp/oceans/Handbook_2007/sop01.pdf
- Dickson, A. G., Sabine, C. L., & Christian, J. R. (2007b). SOP 2 Determination of total dissolved inorganic carbon in sea water. In *Guide to Best Practices for Ocean CO₂ Measurements* (pp. 191). Retrieved from http://cdiac.ornl.gov/ftp/oceans/Handbook_2007/sop02.pdf
- Dickson, A. G., Sabine, C. L., & Christian, J. R. (2007c). SOP 3a Determination of total alkalinity in sea water using a closed-cell titration. In *Guide to Best Practices for Ocean CO₂ Measurements* (pp. 191). Retrieved from http://cdiac.ornl.gov/ftp/oceans/Handbook_2007/sop03a.pdf
- Dickson, A. G., Sabine, C. L., & Christian, J. R. (2007d). SOP 6a Determination of the pH of sea water using a glass / reference electrode cell In *Guide to Best Practices for Ocean CO₂ Measurements* (pp. 191). Retrieved from http://cdiac.ornl.gov/ftp/oceans/Handbook_2007/sop06a.pdf
- Dinsdale, E. A., Edwards, R. A., Hall, D., Angly, F., Breitbart, M., Brulc, J. M., . . . Rohwer, F. (2008). Functional metagenomic profiling of nine biomes. *Nature*, *452*, 629-632. doi:10.1038/nature06810
- Doney, S. C., Mahowald, N., Lima, I., Feely, R. A., Mackenzie, F. T., Lamarque, J.-F., & Rasch, P. J. (2007). Impact of anthropogenic atmospheric nitrogen and sulfur deposition on ocean acidification and the inorganic carbon system. *PNAS*, *104*(37), 14580–14585. doi:10.1073/pnas.0702218104
- Donohue, P. J. C., Calosi, P., Bates, A. H., Laverock, B., Rastrick, S., Mark, F. C., . . . Widdicombe, S. (2012). Impact of exposure to elevated pCO₂ on the physiology and behaviour of an important ecosystem engineer, the burrowing shrimp *Upogebia deltaura*. *Aquatic Biology*, *15*, 73-86. doi:10.3354/ab00408
- Eschemann, A., Kühl, M., & Cypionka, H. (1999). Aerotaxis in *Desulfovibrio*. *Environmental Microbiology*, *1*(6), 489-494.
- Evans, W., Hales, B., & Strutton, P. G. (2011). Seasonal cycle of surface ocean pCO₂ on the Oregon shelf. *Journal of Geophysical Research*, *116*(C5), C05012. doi:10.1029/2010JC006625
- Fanning, K. A., Carder, K. L., & Betzer, P. R. (1982). Sediment resuspension by coastal waters: a potential mechanism for nutrient re-cycling on the ocean's margins. *Deep-Sea Research*, *29*(8), 953-965. doi:10.1016/0198-0149(82)90020-6
- Feely, R. A., Sabine, C. L., Lee, K., Berelson, W., Kleyppas, J., Fabry, V. J., & Millero, F. J. (2004). Impact of anthropogenic CO₂ on the CaCO₃ system in the oceans. *Science*, *305*(5682), 362-366. doi:10.1126/science.1097329
- Flores, E., Frías, J. E., Rubio, L. M., & Herrero, A. (2005). Photosynthetic nitrate assimilation in cyanobacteria. *Photosynthesis Research*, *83*(2), 117–133.
- Forbes, E. (1841). *A history of British starfishes and other animals of the class Echinodermata*. London, U.K.: John van Voorst.
- Francis, C. A., Roberts, K. J., Beman, J. M., Santoro, A. E., & Oakley, B. B. (2005). Ubiquity and diversity of ammonia-oxidizing archaea in water columns and sediments of the ocean. *Proceedings of the National Academy of Sciences of the United States of America*, *102*(41), 14683-14688. doi:10.1073/pnas.0506625102

- Freitag, T. E., & Prosser, J. I. (2003). Community structure of ammonia-oxidizing bacteria within anoxic marine sediments. *Applied and Environmental Microbiology*, *69*(3), 1359-1371. doi:10.1128/AEM.69.3.1359-1371.2003
- Froelich, P. N., Klinkhammer, G. P., Bender, M. L., Luedtke, N. A., Heath, G. R., Cullen, D., . . . Maynard, V. (1979). Early oxidation of organic matter in pelagic sediments of the eastern equatorial Atlantic: suboxic diagenesis. *Geochimica et Cosmochimica Acta*, *43*(7), 1075-1090.
- Fryxell, G. A., & Hasle, G. R. (1977). The genus *Thalassiosira*: species with a modified ring of central strutted processes. In R. Simonsen (Ed.), *Proceedings from the Fourth Symposium on Recent and Fossil Marine Diatoms* (Vol. 54, pp. 67-98). Oslo: Beihefte zur Nova Hedwigia.
- Fulweiler, R. W., Emery, H. E., Heiss, E. M., & Berounsky, V. M. (2011). Assessing the role of pH in determining water column nitrification rates in a coastal system. *Estuaries and Coasts*, *34*(6), 1095-1102. doi:10.1007/s12237-011-9432-4
- Garcia-Pichel, F., Mechling, M., & Castenholz, R. (1994). Diel migrations of microorganisms within a benthic, hypersaline mat community. *Applied and Environmental Microbiology*, *60*(5), 1500-1511.
- Gardner, W. S., McCarthy, M. J., An, S., & Sobolev, D. (2006). Nitrogen fixation and dissimilatory nitrate reduction to ammonium (DNRA) support nitrogen dynamics in Texas estuaries. *Limnology and Oceanography*, *51*(1), 558-568.
- Garibyan, L., & Avashia, N. (2013). Polymerase chain reaction. *Journal of Investigative Dermatology*, *133*, e6. doi:10.1038/jid.2013.1
- Gattuso, J.-P., Gao, K., Lee, K., Rost, B. r., & Schulz, K. G. (2010). Approaches and tools to manipulate the carbonate chemistry. In U. Riebesell, V. J. Fabry, L. Hansson, & J.-P. Gattuso (Eds.), *Guide to best practices for ocean acidification research and data reporting* (pp. 41-52). Luxembourg: Publications Office of the European Union.
- Gayon, U., & Dupetit, G. (1886). Recherches sur la réduction des nitrates par les infiniment petits. *Mémoires de la Société des Sciences Physiques et Naturelles de Bordeaux*, *3*(2), 201-307.
- Gazeau, F., Rijswijk, P. v., Lara, P., & Middelburg, J. J. (2014). Impacts of ocean acidification on sediment processes in shallow waters of the Arctic Ocean. *PLoS One*, *9*(4), e94068. doi:10.1371/journal.pone.0094068
- Gibson, U. E. M., Heid, C. A., & Williams, P. M. (1996). A novel method for real time quantitative competitive RT-PCR. *Genome Research*, *6*(10), 995-1001.
- Glud, R. N. (2008). Oxygen dynamics of marine sediments. *Marine Biology Research*, *4*, 243-289. doi:10.1080/17451000801888726
- Glud, R. N., Gundersen, J. K., Jørgensen, B. B., Revsbech, N. P., & Schulz, H. D. (1994). Diffusive and total oxygen uptake of deep-sea sediments in the eastern South Atlantic Ocean: *in situ* and laboratory measurements. *Deep Sea Research Part I: Oceanographic Research Papers*, *41*(11-12), 1767-1788. doi:10.1016/0967-0637(94)90072-8
- Goldman, J. C., & Brewer, P. G. (1980). Effect of nitrogen source and growth rate on phytoplankton-mediated changes in alkalinity. *Limnology and Oceanography*, *25*(2), 352-357. doi:10.4319/lo.1980.25.2.0352
- Google earth. (2015, August 24). *Tauranga harbour, [map], S 37° 29' 29", E 175° 56' 51"*. Retrieved from <https://earth.google.com/>

- Google earth. (2015, August 24). *Man O'War Bay, [map], S 36° 47' 38", E 175° 10' 14"*. Retrieved from <https://earth.google.com/>
- Gordon, D. P., Beaumont, J., MacDiarmid, A., Robertson, D. A., & Ahyong, S. T. (2010). Marine biodiversity of Aotearoa New Zealand. *PLoS One*, 5(8), e10905. doi:10.1371/journal.pone.0010905
- Greene, A. C., Patel, B. K., & Sheehy, A. J. (1997). *Deferribacter thermophilus* gen. nov., sp. nov., a novel thermophilic manganese- and iron-reducing bacterium isolated from a petroleum reservoir. *International Journal of Systematic Bacteriology*, 47(2), 505-509.
- Grüntzig, V., Nold, S. C., Zhou, J., & Tiedje, J. M. (2001). *Pseudomonas stutzeri* nitrite reductase gene abundance in environmental samples measured by real-time PCR. *Applied and Environmental Microbiology*, 67(2), 760-768. doi:10.1128/AEM.67.2.760-768.2001
- Gundersen, K. (1966). The growth and respiration of *Nitrosocystis oceanus* at different partial pressures of oxygen. *Journal of General Microbiology*, 42, 387-396.
- Hannides, A. K., Dunn, S. M., & Aller, R. C. (2005). Diffusion of organic and inorganic solutes through macrofaunal mucus secretions and tube linings in marine sediments. *Journal of Marine Research*, 63, 957-981.
- Hansen, L. S., & Blackburn, T. H. (1992). Effect of algal bloom deposition on sediment respiration and fluxes. *Marine Biology*, 112(1), 147-152. doi:10.1007/BF00349738
- Hargrave, B. T. (1973). Coupling carbon flow through some benthic and pelagic communities. *Journal of the Fisheries Research Board of Canada*, 30, 1317-1326.
- Hauri, C., Gruber, N., Vogt, M., Doney, S. C., Feely, R. A., Lachkar, Z., . . . Plattner, G.-K. (2013). Spatiotemporal variability and long-term trends of ocean acidification in the California Current System. *Biogeosciences*, 10, 193-216. doi:10.5194/bg-10-193-2013
- Hedderich, R., & Whitman, W. B. (2013). Physiology and biochemistry of the methane-producing archaea. In E. Rosenberg, E. F. DeLong, S. Lory, E. Stackebrandt, & F. Thompson (Eds.), *The Prokaryotes* (pp. 635-662): Springer Berlin Heidelberg. doi:10.1007/978-3-642-30141-4_81
- Heid, C. A., Stevens, J., Livak, K. J., & Williams, P. M. (1996). Real time quantitative PCR. *Genome Research*, 6(10), 986-994.
- Henriksen, K., & Kemp, W. M. (1988). *Nitrification in estuarine and coastal marine sediments*. Retrieved from http://dgc.stanford.edu/SCOPE/SCOPE_33/SCOPE_33_2.07_Henriksen_207-250.pdf
- Herbert, R. A. (1999). Nitrogen cycling in coastal marine ecosystems. *FEMS Microbiology Reviews*, 23, 563-590.
- Higgins, R. P., & Thiel, H. (1988). *Introduction to the study of meiofauna*. Washington, D.C.: Smithsonian Institution Press.
- Hill, M. O. (1973). Diversity and evenness: A unifying notation and its consequences. *Ecology*, 54(2), 427-432.
- Hoehler, T. M., Alperin, M. J., Albert, D. B., & Martens, C. S. (2012). Field and laboratory studies of methane oxidation in an anoxic marine sediment: Evidence for a methanogen-sulfate reducer consortium. *Global Biogeochemical Cycles*, 8(4), 451-463. doi:10.1029/94GB01800

- Hofmann, G. E., Takeshita, Y., Matson, P. G., Crook, E. D., Kroeker, K. J., Gambi, M. C., . . . Peterson, B. (2011). High-frequency dynamics of ocean pH: a multi-ecosystem comparison. *PLoS One*, *6*(12), e28983. doi:10.1371/journal.pone.0028983
- Höss, M., Kohn, M., Pääbo, S., Knauer, F., & Schröder, W. (1992). Excrement analysis by PCR. *Science*, *359*, 199.
- Höss, M., & Pääbo, S. (1993). DNA extraction from Pleistocene bones by a silica-based purification method. *Nucleic Acids Research*, *21*(16), 3913-3914.
- Howe, R. L., Rees, A. P., & Widdicombe, S. (2004). The impact of two species of bioturbating shrimp (*Callianassa subterranea* and *Upogebia deltaura*) on sediment denitrification. *Journal of the Marine Biological Association of the UK*, *84*(3), 629-632. doi:10.1017/S002531540400966Xh
- Huang, X., Gao, D., Peng, S., & Tao, Y. (2014). Effects of ferrous and manganese ions on anammox process in sequencing batch biofilm reactors. *Journal of Environmental Sciences*, *26*(5), 1034-1039. doi:10.1016/S1001-0742(13)60531-8
- Huesemann, M. H., Skillman, A. D., & Crecelius, E. A. (2002). The inhibition of marine nitrification by ocean disposal of carbon dioxide. *Marine Pollution Bulletin*, *44*(2), 142-148. doi:10.1016/S0025-326X(01)00194-1
- Hughes, K. M., Kaiser, M. J., Jennings, S., McConnaughey, R. A., Pitcher, R., Hilborn, R., . . . Rijnsdorp, A. (2014). Investigating the effects of mobile bottom fishing on benthic biota: a systematic review protocol. *Environmental Evidence*, *3*(23), 1-9. doi:10.1186/2047-2382-3-23
- Hügler, M., & Sievert, S. M. (2010). Beyond the Calvin cycle: autotrophic carbon fixation in the ocean. *Annual Review of Marine Science*, *3*, 261-289. doi:10.1146/annurev-marine-120709-142712
- Hurlbert, S. H. (1984). Pseudoreplication and the design of ecological field experiments. *Ecological Monographs*, *54*(2), 187-211.
- Hutchins, D. A., Fu, F. X., Zhang, Y., Warner, M. E., Feng, Y., Portune, K., . . . Mulholland, M. R. (2007). CO₂ control of *Trichodesmium* N₂ fixation, photosynthesis, growth rates, and elemental ratios: Implications for past, present, and future ocean biogeochemistry. *Limnology and Oceanography*, *52*(4).
- Hutchins, D. A., Mulholland, M. R., & Fu, F. (2009). Nutrient cycles and marine microbes in a CO₂-enriched ocean. *Oceanography*, *22*(4), 128-145.
- IPCC. (2014). Climate Change 2014: Synthesis report. In R. K. Pachauri & L. A. Meyer (Eds.), *Contribution of Working Groups I, II and III to the Fifth Assessment Report of the Intergovernmental Panel on Climate Change* (pp. 151). Geneva, Switzerland: IPCC.
- Jensen, M. H., Lomstein, E., & Sørensen, J. (1990). Benthic NH₄⁺ and NO₃⁻ flux following sedimentation of a spring phytoplankton bloom in Aarhus Bight, Denmark. *Marine Ecology Progress Series*, *61*(1-2), 87-96.
- Jensen, K., Revsbech, N. P., & Nielsen, L. P. (1993). Microscale distribution of nitrification activity in sediment determined with a shielded microsensor for nitrate. *Applied and Environmental Microbiology*, *59*(10), 3287-3296.
- Jiménez, E., Giménez, J. B., Ruano, M. V., Ferrer, J., & Serralta, J. (2011). Effect of pH and nitrite concentration on nitrite oxidation rate. *Bioresource Technology*, *102*, 8741-8747. doi:10.1016/j.biortech.2011.07.092

- Jørgensen, B. B. (1982). Mineralization of organic matter in the sea bed—the role of sulphate reduction. *Nature*, *296*, 643-645. doi:10.1038/296643a0
- Jørgensen, B. B., & Revsbech, N. P. (1985). Diffusive boundary layers and the oxygen uptake of sediments and detritus. *Limnology and Oceanography*, *30*(1), 111-122.
- Jourabchi, P., Cappellen, P. V., & Regnier, P. (2005). Quantitative interpretation of pH distributions in aquatic sediments: A reaction–transport modeling approach. *American Journal of Science*, *305*, 919-956.
- Joye, S. B., & Hollibaugh, J. T. (1995). Influence of sulfide inhibition of nitrification on nitrogen regeneration in sediments. *Science*, *270*(5236), 623-625. doi:10.1126/science.270.5236.623
- Kampschreur, M. J., Picioreanu, C., Tan, N., Kleerebezem, R., Jetten, M. S. M., & Loosdrecht, M. C. M. v. (2007). Unraveling the source of nitric oxide emission during nitrification. *Water Environment Research*, *79*(13), 2499-2509. doi:10.2175/106143007X220815
- Katcher, H., & Schwartz, I. (1994). A distinctive property of Tth DNA polymerase: enzymatic amplification in the presence of phenol. *Biotechniques*, *16*(1), 84-92.
- Kelly, J. R., & Nixon, S. W. (1984). Experimental studies of the effect of organic deposition on the metabolism of a coastal marine bottom community. *Marine Ecology Progress Series*, *17*, 157-169.
- Kelly, D. P., & Wood, A. P. (2000). Confirmation of *Thiobacillus denitrificans* as a species of the genus *Thiobacillus*, in the beta-subclass of the Proteobacteria, with strain NCIMB 9548 as the type strain. *International Journal of Systematic and Evolutionary Microbiology*, *50*, 547-550. doi:10.1099/00207713-50-2-547
- Kerfahi, D., Hall-Spencer, J. M., Tripathi, B. M., Milazzo, M., Lee, J., & Adams, J. M. (2014). Shallow water marine sediment bacterial community shifts along a natural CO₂ gradient in the Mediterranean Sea off Vulcano, Italy. *Environmental Microbiology*, *67*(4), 819–828. doi:10.1007/s00248-014-0368-7
- Ketil, B. S., & Andreas, T. (2006). Stratified communities of active archaea in deep marine subsurface sediments. *Applied and Environmental Microbiology*, *72*(7), 4596-4603. doi:10.1128/AEM.00562-06
- Kim, D.-J., Ahn, D. H., & Lee, D.-I. (2005). Effects of free ammonia and dissolved oxygen on nitrification and nitrite accumulation in a biofilm airlift reactor. *Korean Journal of Chemical Engineering*, *22*(1), 85-90. doi:10.1007/BF02701467
- Kitidis, V., Laverock, B., McNeill, L. C., Beesley, A., Cummings, D., Tait, K., . . . Widdicombe, S. (2011). Impact of ocean acidification on benthic and water column ammonia oxidation. *Geophysical Research Letters*, *38*, L21603. doi:10.1029/2011GL049095
- Könneke, M., Bernhard, A. E., de la Torre, J. R., Walker, C. B., Waterbury, J. B., & Stahl, D. A. (2005). Isolation of an autotrophic ammonia-oxidizing marine archaeon. *Nature*, *437*, 543-546. doi:10.1038/nature03911
- Koonin, E., Makarova, K., & Aravind, L. (2001). Horizontal gene transfer in prokaryotes: quantification and classification. *Annual Review of Microbiology*, *55*, 709-742.
- Kranz, S. A., Levitan, O., Richter, K.-U., Prášil, O., Berman-Frank, I., & Rost, B. (2010). Combined effects of CO₂ and light on the N₂-fixing cyanobacterium *Trichodesmium* IMS101: Physiological responses. *Plant Physiology*, *154*(1), 334-345.

- Krekeler, D., Teske, A., & Cypionka, H. (1998). Strategies of sulfate-reducing bacteria to escape oxygen stress in a cyanobacterial mat. *FEMS Microbiology Ecology*, *25*(2), 89–96. doi:10.1016/S0168-6496(97)00085-8
- Kristensen, E. (2000). Organic matter diagenesis at the oxic/anoxic interface in coastal marine sediments, with emphasis on the role of burrowing animals. *Hydrobiologia*, *426*, 1-24.
- Kristensen, E., Penha-Lopes, G., Delefosse, M., Valdemarsen, T., Quintana, C. O., & Banta, G. T. (2012). What is bioturbation? The need for a precise definition for fauna in aquatic sciences. *Marine Ecology Progress Series*, *446*, 285–302. doi:10.3354/meps09506
- Lam, P., & Kuypers, M. M. M. (2011). Microbial nitrogen cycling processes in oxygen minimum zones. *Annual Review of Marine Science*, *3*, 317-345. doi:10.1146/annurev-marine-120709-142814
- Larsen, M., Borisov, S. M., Grunwald, B., Klimant, I., & Glud, R. N. (2011). A simple and inexpensive high resolution color ratiometric planar optode imaging approach: application to oxygen and pH sensing. *Limnology and Oceanography*, *9*, 348–360. doi:10.4319/lom.2011.9.348
- Larsen, P. E., Field, D., & Gilbert, J. A. (2012). Predicting bacterial community assemblages using an artificial neural network approach. *Nature*, *9*(6), 621-627. doi:10.1038/nmeth.1975
- Laverock, B., Kitidis, V., Tait, K., Gilbert, J. A., Osborn, A. M., & Widdicombe, S. (2013). Bioturbation determines the response of benthic ammonia-oxidizing microorganisms to ocean acidification. *Philosophical Transactions of the Royal Society of London Series B, Biological Sciences*, *368*(1627), 20120441. doi:10.1098/rstb.2012.0441
- Laverock, B., Smith, C. J., Tait, K., Osborn, A. M., Widdicombe, S., & Gilbert, J. A. (2010). Bioturbating shrimp alter the structure and diversity of bacterial communities in coastal marine sediments. *International Society for Microbial Ecology*, *4*, 1531-1544. doi:10.1038/ismej.2010.86
- Lawrence, D., Dagg, M. J., Liu, H., Cummings, S. R., Ortner, P. B., & Kelble, C. (2004). Wind events and benthic–pelagic coupling in a shallow subtropical bay in Florida. *Marine Ecology Progress Series*, *266*, 1-13.
- Leach, W. E. (1816). A tabular view of the external characters of four classes of animals, which Linné arranged under Insecta; with the distribution of the genera composing three of these classes into orders, &c. and descriptions of several new genera and species. *Transactions of the Linnean Society of London*, *11*(2), 306-400.
- Lee, J. V., Gibson, D. M., & Shewan, J. M. (1977). A numerical taxonomic study of some *Pseudomonas*-like marine bacteria. *Journal of General Microbiology*, *98*, 439-451. doi:10.1099/00221287-98-2-439
- Lejzerowicz, F., Esling, P., Pillet, L., Wilding, T. A., Black, K. D., & Pawlowski, J. (2015). High-throughput sequencing and morphology perform equally well for benthic monitoring of marine ecosystems. *Scientific Reports*, *5*, 1393210.1391038/srep1313932.
- Leloup, J., Fossing, H., Kohls, K., Holmkvist, L., Borowski, C., & Jørgensen, B. B. (2009). Sulfate-reducing bacteria in marine sediment (Aarhus Bay, Denmark): abundance and diversity related to geochemical zonation. *Environmental Microbiology*, *11*(5), 1278. doi:10.1111/j.1462-2920.2008.01855.x
- Levy-Booth, D. J., Campbell, R. G., Gulden, R. H., Hart, M. M., Powell, J. R., Klironomos, J. N., . . . Dunfield, K. E. (2007). Cycling of extracellular DNA in the soil environment. *Soil Biology and Biochemistry*, *39*, 2977–2991. doi:10.1016/j.soilbio.2007.06.020

- Logue, J. B., Findlay, S. E. G., & Comte, J. (2015). Microbial responses to environmental changes [Editorial]. *Frontiers in Microbiology*, *6*. doi:10.3389/fmicb.2015.01364
- Lohrenz, S. E., Fahnenstiel, G. L., Redalje, D. G., Lang, G. A., Chen, X., & Dagg, M. J. (1997). Variations in primary production of northern Gulf of Mexico continental shelf waters linked to nutrient inputs from the Mississippi River. *Marine Ecology Progress Series*, *155*, 45-54.
- Lomstein, B. A., Jensen, A. U., Hansen, J. W., Andreasen, J. B., Hansen, L. S., Berntsen, J., & Kunzendorf, H. (1998). Budgets of sediment nitrogen and carbon cycling in the shallow water of Knebel Vig, Denmark. *Aquatic Microbial Ecology*, *14*, 69-80.
- Lovley, D. (2013). Dissimilatory Fe (III)-and Mn (IV)-reducing prokaryotes. In E. Rosenberg, E. F. DeLong, S. Lory, E. Stackebrandt, & F. Thompson (Eds.), *The Prokaryotes* (pp. 287-308): Springer Berlin Heidelberg. doi:10.1007/978-3-642-30141-4_69
- Lücker, S., & Daims, H. (2013). The family *Nitrospinaceae*. In E. Rosenberg, E. F. DeLong, S. Lory, E. Stackebrandt, & F. Thompson (Eds.), *The Prokaryotes* (pp. 231-237): Springer Berlin Heidelberg. doi:10.1007/978-3-642-30141-4_81
- Lyle, M. (1983). The brown-green color transition in marine sediments: A marker of the Fe(III)-Fe(II) redox boundary. *Limnology and Oceanography*, *28*(5), 1026-1033.
- MacDonell, M. T., & Colwell, R. R. (1985). Phylogeny of the *Vibrionaceae*, and recommendation for two new genera, *Listonella* and *Shewanella*. *Systematic and Applied Microbiology*, *6*(2), 171-182. doi:10.1016/S0723-2020(85)80051-5
- Mackie, D., McGraw, C., & Hunter, K. (2011). *OA is not OK: An introduction to the chemistry of ocean acidification*. Retrieved from <http://skepticalscience.com/>
- Magalhães, C. M., Joye, S. B., Moreira, R. M., Wiebe, W. J., & Bordalo, A. A. (2005). Effect of salinity and inorganic nitrogen concentrations on nitrification and denitrification rates in intertidal sediments and rocky biofilms of the Douro River estuary, Portugal. *Water Research*, *39*(9), 1783-1794. doi:10.1016/j.watres.2005.03.008
- Magalhães, C. M., Machado, A., & Bordalo, A. A. (2009). Temporal variability in the abundance of ammonia oxidizing bacteria vs. archaea in sandy sediments of the Douro River estuary, Portugal. *Aquatic Microbial Ecology*, *56*, 13-23. doi:10.3354/ame01313
- Mahaffey, C., Michaels, A. F., & Capone, D. G. (2005). The conundrum of marine N₂ fixation. *American Journal of Science*, *305*(6), 546-595. doi:10.2475/ajs.305.6-8.546
- Mahmoudi, N., Robeson-II, M. S., Castro, H. F., Fortney, J. L., Techtmann, S. M., Joyner, D. C., . . . Hazen, T. C. (2015). Microbial community composition and diversity in Caspian Sea sediments. *Microbiology Ecology*, *91*, 1-11. doi:10.1093/femsec/fiu013
- Marcus, N. H., & Boero, F. (1998). Minireview: The importance of benthic-pelagic coupling and the forgotten role of life cycles in coastal aquatic systems. *American Society of Limnology and Oceanography*, *43*(5), 763-768.
- Marschall, C., Frenzel, P., & Cypionka, H. (1993). Influence of oxygen on sulfate reduction and growth of sulfate-reducing bacteria. *Archives of Microbiology*, *159*, 168-173.
- Martens-Habbena, W., Berube, P. M., Urakawa, H., Torre, J. R. d. I., & Stahl, D. A. (2009). Ammonia oxidation kinetics determine niche separation of nitrifying archaea and bacteria. *Nature*, *461*(7266), 976-979. doi:10.1038/nature08465
- Martz, T. R., Daly, K. L., Byrne, R. H., Stillman, J. H., & Turk, D. (2015). Technology for ocean acidification research: Needs and availability. *Oceanography*, *28*(2), 40-47.

- McBride, M. J. (2001). Bacterial gliding motility: Multiple mechanisms for cell movement over surfaces. *Annual Review of Microbiology*, *55*, 49–75.
- McGlynn, S. E., Chadwick, G. L., Kempes, C. P., & Orphan, V. J. (2015). Single cell activity reveals direct electron transfer in methanotrophic consortia. *Nature*, *526*, 531–535. doi:10.1038/nature15512
- McKew, B. A., Taylor, J. D., McGenity, T. J., & Underwood, G. J. (2011). Resistance and resilience of benthic biofilm communities from a temperate saltmarsh to desiccation and rewetting. *The ISME journal*, *5*, 30–41. doi:10.1038/ismej.2010.91
- Mehrbach, C., Culberson, C. H., Hawley, J. E., & Pytkowicz, R. N. (1973). Measurement of the apparent dissociation constants of carbonic acid in seawater at atmospheric pressure. *Limnology and Oceanography*, *18* (6), 897–907. doi:10.4319/lo.1973.18.6.0897
- Mehrer, H., & Stolwijk, N. A. (2009). Heroes and highlights in the history of diffusion. *Journal for the Basic Principles of Diffusion Theory, Experiment and Application*, *11*(1), 1–32.
- Meyer-Reil, L.-A., & Köster, M. (2000). Eutrophication of marine waters: effects on benthic microbial communities. *Marine Pollution Bulletin*, *41*, 255–263.
- Milligan, A. J., Varela, D. E., Brzezinski, M. A., & Morel, F. M. M. (2004). Dynamics of silicon metabolism and silicon isotopic discrimination in a marine diatom as a function of pCO₂. *Limnology and Oceanography*, *49*(2), 322–329.
- Mitchell, A., Romano, G. H., Groisman, B., Yona, A., Dekel, E., Kupiec, M., . . . Pilpel, Y. (2009). Adaptive prediction of environmental changes by microorganisms. *Nature*, *460*(7252), 220–224. doi:10.1038/nature08112
- Mohammadi, T., Reesink, H. W., Vandenbroucke-Grauls, C. M. J. E., & Savelkoul, P. H. M. (2003). Optimization of real-time PCR assay for rapid and sensitive detection of eubacterial 16S ribosomal DNA in platelet concentrates. *Journal of Clinical Microbiology*, *41*(10), 4796–4798. doi:10.1128/JCM.41.10.4796–4798.2003
- Montagu, G. (1814). Description of several marine animals found on the south coast of Devonshire. *Transactions of the Linnean Society of London*, *9*, 81–114.
- Mortazavi, B., Riggs, A. A., Caffrey, J. M., Genet, H., & Phipps, S. W. (2012). The contribution of benthic nutrient regeneration to primary production in a shallow eutrophic estuary, Weeks Bay, Alabama. *Estuaries and Coasts*, *35*(3), 862–877. doi:10.1007/s12237-012-9478-y
- Mulder, A., Graaf, A. A. v. d., Robertson, L. A., & Kuenen, J. G. (1995). Anaerobic ammonium oxidation discovered in a denitrifying fluidized bed reactor. *FEMS Microbiology Ecology*, *16*(3), 177–183. doi:10.1016/0168-6496(94)00081-7
- Mullis, K., Faloona, F., Scharf, S., Saiki, R., Horn, G., & Erlich, H. (1986). Specific enzymatic amplification of DNA *in vitro*: the polymerase chain reaction. *Cold Spring Harbor Laboratory*, *51*, 263–273.
- Nealson, K. H. (1997). Sediment bacteria: Who's there, what are they doing, and what's new? *Annual Review of Earth and Planetary Sciences*, *25*, 403–434. doi:10.1146/annurev.earth.25.1.403
- Nealson, K. H., & Saffarini, D. (1994). Iron and manganese in anaerobic respiration: environmental significance, physiology, and regulation. *Annual Review of Microbiology*, *48*, 311–343.
- Niel, C. B. V. (1954). The chemoautotrophic and photosynthetic bacteria. *Annual Review of Microbiology*, *8*, 105–132. doi:10.1146/annurev.mi.08.100154.000541

- Nielsen, T. G., & Kjørboe, T. (1991). Effects of a storm event on the structure of the pelagic food web with special emphasis on planktonic ciliates. *Journal of Plankton Research*, 13(1), 35-51.
- Nixon, S. W. (1981). Remineralization and nutrient cycling in coastal marine ecosystems. In B. Nelson & L. E. Cronin (Eds.), *Estuaries and Nutrients* (pp. 111-138). New Jersey: Humana Press.
- Nixon, S. W. (1995). Coastal marine eutrophication: A definition, social causes, and future concerns. *Ophelia*, 41(1), 199-219. doi:10.1080/00785236.1995.10422044
- Nixon, S. W., Fulweiler, R. W., Buckley, B. A., Granger, S. L., Nowicki, B. L., & Henry, K. M. (2009). The impact of changing climate on phenology, productivity, and benthic–pelagic coupling in Narragansett Bay. *Estuarine, Coastal and Shelf Science*, 82(1), 1-18. doi:10.1016/j.ecss.2008.12.016
- Nogales, B., Timmis, K. N., Nedwell, D. B., & Osborn, A. M. (2002). Detection and diversity of expressed denitrification genes in estuarine sediments after reverse transcription-PCR amplification from mRNA. *Applied and Environmental Microbiology*, 68(10), 5017-5025. doi:10.1128/AEM.68.10.5017-5025.2002
- Ogram, A., Saylor, G. S., Gustln, D., & Lewis, R. J. (1988). DNA adsorption to soils and sediments *Environmental Science and Technology*, 22, 982-984.
- Olsen, G. J., Lane, D. J., Giovannoni, S. J., & Pace, N. R. (1986). Microbial ecology and evolution: A ribosomal RNA approach. *Annual Review of Microbiology*, 40, 337-365.
- Opel, K. L., Chung, D., & McCord, B. R. (2009). A study of PCR inhibition mechanisms using real time PCR. *Journal Of Forensic Sciences*, 55(1), 25-33. doi:10.1111/j.1556-4029.2009.01245.x
- Otte, S., Kuenen, J. G., Nielsen, L. P., Paerl, H. W., Zopfi, J., Schulz, H. N., . . . Jørgensen, B. B. (1999). Nitrogen, carbon, and sulfur metabolism in natural *Thioploca* samples. *Applied and Environmental Microbiology*, 65(7), 3148–3157.
- Pambrun, V., Paul, E., & Spérandio, M. (2006). Modeling the partial nitrification in sequencing batch reactor for biomass adapted to high ammonia concentrations. *Biotechnology and Bioengineering*, 95(1), 120-131. doi:10.1002/bit.21008
- Park, S. J., Park, B. J., & Rhee, S. K. (2008). Comparative analysis of archaeal 16S rRNA and *amoA* genes to estimate the abundance and diversity of ammonia-oxidizing archaea in marine sediments. *Extremophiles*, 12(4), 605-615. doi:10.1007/s00792-008-0165-7
- Payne, W. J. (1970). Energy yields and growth of heterotrophs. *Annual Review of Microbiology*, 24, 17-52. doi:10.1146/annurev.mi.24.100170.000313
- Pennant, T. (1777). *British Zoology, vol. IV. Crustacea. Mollusca. Testacea*. London, U.K.: Plates.
- Peters, J. W., Fisher, K., & Dean, D. R. (1995). Nitrogenase structure and function: A biochemical-genetic perspective. *Annual Review of Microbiology*, 49, 335-366. doi:10.1146/annurev.mi.49.100195.002003
- Pfeiffer, T., Schuster, S., & Bonhoeffer, S. (2001). Cooperation and competition in the evolution of ATP-producing pathways. *Science*, 292, 504-507.
- Pilcher, K. E., Gaudet, P., Fey, P., Kowal, A. S., & Chisholm, R. L. (2007). A general purpose method for extracting RNA from *Dictyostelium* cells. *Nature Protocols*, 2(6), 1329-1332. doi:10.1038/nprot.2007.191

- Postma, D. (1985). Concentration of Mn and separation from Fe in sediments: Kinetics and stoichiometry of the reduction between birnessite and dissolved Fe(II) at 10°C. *Geochimica et Cosmochimica Acta*, 49(4), 1023-1033.
- Preisler, A., Beer, D. d., Lichtschlag, A., Lavik, G., Boetius, A., & Jørgensen, B. B. (2007). Biological and chemical sulfide oxidation in a *Beggiatoa* inhabited marine sediment. *The ISME journal*, 1, 341–353. doi:10.1038/ismej.2007.50
- Prosser, J. I. (2010). Replicate or lie. *Environmental Microbiology*, 12(7), 1806–1810. doi:10.1111/j.1462-2920.2010.02201.x
- Purkhold, U., Pommerening-Röser, A., Juretschko, S., Schmid, M. C., Koops, H.-P., & Wagner, M. (2000). Phylogeny of all recognized species of ammonia oxidizers based on comparative 16S rRNA and *amoA* sequence analysis: Implications for molecular diversity surveys. *Applied and Environmental Microbiology*, 66(12), 5368-5382. doi:10.1128/AEM.66.12.5368-5382.2000
- Rabus, R., Hansen, T. A., & Widdel, F. (2013). Dissimilatory sulfate- and sulfur-reducing prokaryotes. In E. Rosenberg, E. F. DeLong, S. Lory, E. Stackebrandt, & F. Thompson (Eds.), *The Prokaryotes* (pp. 309-404): Springer Berlin Heidelberg. doi:10.1007/978-3-642-30141-4_70
- Raffaelli, D., Bell, E., Weithoff, G., Matsumoto, A., Cruz-Motta, J. J., Kershaw, P., . . . Jones, M. (2003). The ups and downs of benthic ecology: considerations of scale, heterogeneity and surveillance for benthic–pelagic coupling. *Journal of Experimental Marine Biology and Ecology*, 285, 191-203. doi:10.1016/S0022-0981(02)00527-0
- Raulf, F. F., Fabricius, K., Uthicke, S., Beer, D. d., Abed, R. M. M., & Ramette, A. (2015). Changes in microbial communities in coastal sediments along natural CO₂ gradients at a volcanic vent in Papua New Guinea. *Environmental Microbiology*, 17(10), 3678–3691. doi:10.1111/1462-2920.12729
- Raupach, M. R., Marland, G., Ciais, P., Quéré, C. L., Canadell, J. G., Klepper, G., & Field, C. B. (2007). Global and regional drivers of accelerating CO₂ emissions. *PNAS*, 104(24), 10288 –10293. doi:10.1073_pnas.0700609104
- Redfield, A. C. (1934). On the proportions of organic derivatives in sea water and their relation to the composition of plankton. In R. J. Daniel (Ed.), *James Johnstone memorial volume* (pp. 177–192): University Press of Liverpool.
- Rensing, C., Newby, D. T., & Pepper, I. L. (2002). The role of selective pressure and selfish DNA in horizontal gene transfer and soil microbial community adaptation. *Soil Biology and Biochemistry*, 34(3), 285–296. doi:10.1016/S0038-0717(01)00183-3
- Revsbech, N. P., Jørgensen, B. B., Blackburn, T. H., & Cohen, Y. (1983). Microelectrode studies of photosynthesis and O₂, H₂S, and pH profiles of a microbial mat. *Limnology and Oceanography*, 28(6), 1062-1074. doi:10.4319/lo.1983.28.6.1062
- Revsbech, N. P., Madsen, B., & Jørgensen, B. B. (1986). Oxygen production and consumption in sediments determined at high spatial resolution by computer simulation of oxygen microelectrode data. *Limnology and Oceanography*, 31(2), 293-304. doi:10.4319/lo.1986.31.2.0293
- Revsbech, N. P., Sorensen, J., & Blackburn, T. H. (1980). Distribution of oxygen in marine sediments measured with microelectrodes. *Limnology and Oceanography*, 25(3), 403-411.

- Riebesell, U., Fabry, V. J., Hansson, L., & Gattuso, J.-P. (2010). *Guide to best practices for ocean acidification research and data reporting*. Luxembourg, Luxembourg: Publications Office of the European Union.
- Ririe, K. M., Rasmussen, R. P., & Wittwer, C. T. (1997). Product differentiation by analysis of DNA melting curves during the polymerase chain reaction. *Analytical Biochemistry*, *245*(2), 154-160.
- Risgaard-Petersen, N., Nicolaisen, M. H., Revsbech, N. P., & Lomstein, B. A. (2004). Competition between ammonia-oxidizing bacteria and benthic microalgae. *Applied and Environmental Microbiology*, *70*(9), 5528-5537. doi:10.1128/AEM.70.9.5528-5537.2004
- Rivkin, R. B., & Putt, M. (2007). Heterotrophy and photoheterotrophy by Antarctic microalgae: light-dependent incorporation of amino acids and glucose. *Journal of Phycology*, *23*(3), 442-452. doi:10.1111/j.1529-8817.1987.tb02530.x
- Robbins, L. L., Hansen, M. E., Kleypas, J. A., & Meylan, S. C. (2010). *CO₂calc—A user-friendly seawater carbon calculator for Windows, Max OS X, and iOS (iPhone)*. U.S.: Geological Survey Open-File Report 2010_1280, 17 p.
- Rojas-Herrera, R., Narvaez-Zapata, J., Zamudio-Maya, M., & Mena-Martinez, M. E. (2008). A simple silica-based method for metagenomic DNA extraction from soil and sediments. *Molecular Biotechnology*, *40*, 13-17. doi:10.1007/s12033-008-9061-8
- Romanowski, G., Lorenz, M. G., & Wackernagel, W. (1993). Use of polymerase chain reaction and electroporation of *Escherichia coli* to monitor the persistence of extracellular plasmid DNA introduced into natural soils. *Applied and Environmental Microbiology*, *59*(10), 3438-3446.
- Rothberg, J. M., Hinz, W., Rearick, T. M., Schultz, J., Mileski, W., Davey, M., . . . Bustillo, J. (2011). An integrated semiconductor device enabling non-optical genome sequencing. *Nature*, *475*, 348-352. doi:10.1038/nature10242
- RStudio Team. (2015). *RStudio: Integrated Development for R*. RStudio, Inc. Boston, MA. Retrieved from <http://www.rstudio.com/>
- Rueckert, A., & Morgan, H. W. (2007). Removal of contaminating DNA from polymerase chain reaction using ethidium monoazide. *Journal of Microbiological Methods*, *68*(3), 596-600. doi:10.1016/j.mimet.2006.11.006
- Saiki, R., Gelfand, D., Stoffel, S., Scharf, S., Higuchi, R., Horn, G., . . . Erlich, H. (1988). Primer-directed enzymatic amplification of DNA with a thermostable DNA polymerase. *Science*, *239*(4839), 487-491.
- Salisbury, J., Vandemark, D., Hunt, C., Campbell, J., Jonsson, B., Mahadevan, A., . . . Xue, H. (2009). Episodic riverine influence on surface DIC in the coastal Gulf of Maine. *Estuarine, Coastal and Shelf Science*, *82*(1), 108-118. doi:10.1016/j.ecss.2008.12.021
- Sanger, F., Air, G. M., Barrell, B. G., Brown, N. L., Coulson, A. R., Fiddes, J. C., . . . Smith, M. (1977). Nucleotide sequence of bacteriophage phiX174 DNA. *Nature*, *265*, 687-695. doi:10.1038/265687a0
- Santos, I. R., Eyre, B. D., & Huettel, M. (2012). The driving forces of porewater and groundwater flow in permeable coastal sediments: A review. *Estuarine, Coastal and Shelf Science*, *98*, 1-15. doi:10.1016/j.ecss.2011.10.024
- Sarkar, G., & Sommer, S. (1991). Parameters affecting susceptibility of PCR contamination to UV inactivation. *Biotechniques*, *10*(5), 590-594.

- Saviozzi, S., Cordero, F., Iacono, M. L., Novello, S., Scagliotti, G. V., & Calogero, R. A. (2006). Selection of suitable reference genes for accurate normalization of gene expression profile studies in non-small cell lung cancer. *BMC Cancer*, *6*(200), 1-10. doi:10.1186/1471-2407-6-200
- Schippers, A., & Neretin, L. N. (2006). Quantification of microbial communities in near-surface and deeply buried marine sediments on the Peru continental margin using real-time PCR. *Environmental Microbiology*, *8*(7), 1251-1260. doi:10.1111/j.1462-2920.2006.01019.x
- Schleper, C., Jurgens, G., & Jonuscheit, M. (2005). Genomic studies of uncultivated archaea. *Nature Reviews Microbiology*, *3*(6), 479-488. doi:10.1038/nrmicro1159
- Schloss, P. D., Westcott, S. L., Ryabin, T., Hall, J. R., Hartmann, M., Hollister, E. B., . . . Weber, C. F. (2009). Introducing mothur: Open-source, platform-independent, community-supported software for describing and comparing microbial communities. *Applied and Environmental Microbiology*, *75*(3), 7537-7541. doi:10.1128/AEM.01541-09
- Schneegurt, M. A., Dore, S. Y., & Kulpa, C. F. J. (2003). Direct extraction of DNA from soils for studies in microbial ecology. *Current Issues in Molecular Biology*, *5*, 1-8.
- Schrader, C., Schielke, A., Ellerbroek, L., & Johne, R. (2012). PCR inhibitors – occurrence, properties and removal. *Journal of Applied Microbiology*, *113*, 1014--1026. doi:10.1111/j.1365-2672.2012.05384.x
- Schulz, H. N., & Beer, D. D. (2002). Uptake rates of oxygen and sulfide measured with individual *Thiomargarita namibiensis* cells by using microelectrodes. *Applied and Environmental Microbiology*, *68*(11), 5746–5749. doi:10.1128/AEM.68.11.5746-5749.2002
- Shetye, S., Sudhakar, M., Jena, B., & Mohan, R. (2013). Occurrence of nitrogen fixing cyanobacterium *Trichodesmium* under elevated pCO₂ conditions in the western bay of Bengal. *International Journal of Oceanography*, *2013*, 1-8. doi:10.1155/2013/350465
- Sidstedt, M., Jansson, L., Nilsson, E., Noppa, L., Forsman, M., Rådström, P., & Hedman, J. (2015). Humic substances cause fluorescence inhibition in real-time polymerase chain reaction. *Analytical Biochemistry*, *487*, 30-37. doi:10.1016/j.ab.2015.07.002
- Sikes, E. L., Uhle, M. E., Nodder, S. D., & Howard, M. E. (2009). Sources of organic matter in a coastal marine environment: Evidence from *n*-alkanes and their δ¹³C distributions in the Hauraki Gulf, New Zealand. *Marine Chemistry*, *113*, 149–163. doi:10.1016/j.marchem.2008.12.003
- Smith, C. R., Austen, M. C., Boucher, G., Heip, C., Hutchings, P. A., King, G. M., . . . Snelgrove, P. (2000). Global change and biodiversity linkages across the sediment–water interface. *BioScience*, *50*(12), 1108-1120.
- Soetaert, K., Hofmann, A. F., Middelburg, J. J., Meysman, F. J. R., & Greenwood, J. (2007). The effect of biogeochemical processes on pH. *Marine Chemistry*, *105*(1-2), 30–51. doi:10.1016/j.marchem.2006.12.012
- Sørensen, J. (1978). Capacity for denitrification and reduction of nitrate to ammonia in a coastal marine sediment. *Applied and Environmental Microbiology*, *35*(2), 301–305.
- Sørensen, J. (1982). Reduction of ferric iron in anaerobic, marine sediment and interaction with reduction of nitrate and sulfate. *Applied and Environmental Microbiology*, *43*(2), 319-324.
- Stamen. (2015, August 24). *Tauranga harbour*, [map], S 37° 29' 29", E 175° 56' 51". Retrieved from <http://maps.stamen.com>

- Stamen. (2015, August 24). *Man O'War Bay, [map], S 36° 47' 38", E 175° 10' 14"*. Retrieved from <http://maps.stamen.com>
- Stark, J. M., & Firestone, M. K. (1996). Kinetic characteristics of ammonium-oxidizer communities in a California oak woodland-annual grassland. *Soil Biology and Biochemistry*, *28*(10), 1307-1317. doi:10.1016/S0038-0717(96)00133-2
- Stein, L. Y., & Arp, D. J. (1998). Loss of ammonia monooxygenase activity in *Nitrosomonas europaea* upon exposure to nitrite. *Applied and Environmental Microbiology*, *64*(10), 4098-4102.
- Stein, L. Y., Arp, D. J., & Hyman, M. R. (1997). Regulation of the synthesis and activity of ammonia monooxygenase in *Nitrosomonas europaea* by altering pH to affect NH₃ availability. *Applied and Environmental Microbiology*, *63*(11), 4588-4592.
- Sunda, W. G., & Cai, W.-J. (2012). Eutrophication induced CO₂-acidification of subsurface coastal waters: interactive effects of temperature, salinity, and atmospheric pCO₂. *Environmental Science and Technology*, *46*(19), 10651-10659. doi:10.1021/es300626f
- Sutlovic, D., Gojanovic, M. D., Andelinovic, S., Gugic, D., & Primorac, D. (2005). Taq polymerase reverses inhibition of quantitative real time polymerase chain reaction by humic acid. *Croatian Medical Journal*, *46*(4), 556-562.
- Suzuki, I., Dular, U., & Kwok, S. C. (1974). Ammonia or ammonium ion as substrate for oxidation by *Nitrosomonas europaea* cells and extract. *Journal of Bacteriology*, *120*(1), 556-558.
- Tait, K., Laverock, B., Shaw, J., Somerfield, P. J., & Widdicombe, S. (2013). Minor impact of ocean acidification to the composition of the active microbial community in an Arctic sediment. *Environmental Microbiology Reports*, *5*(6), 851-860. doi:10.1111/1758-2229.12087
- Tait, K., Laverock, B., & Widdicombe, S. (2014). Response of an arctic sediment nitrogen cycling community to increased CO₂. *Estuaries and Coasts*, *37*(3), 724-735. doi:10.1007/s12237-013-9709-x
- Tait, K., Stahl, H., Taylor, P., & Widdicombe, S. (2015). Rapid response of the active microbial community to CO₂ exposure from a controlled sub-seabed CO₂ leak in Ardmucknish Bay (Oban, Scotland). *International Journal of Greenhouse Gas Control*, *38*, 171-181. doi:10.1016/j.ijggc.2014.11.021
- Tanaka, T., Zöllner, E., Riebesell, U., Thingstad, T. F., Løvdal, T., Grossart, H. P., . . . Wohlers, J. (2008). Availability of phosphate for phytoplankton and bacteria and of glucose for bacteria at different pCO₂ levels in a mesocosm study. *Biogeosciences*, *5*(3), 669-678. doi:10.5194/bg-5-669-2008
- Temin, H., & Mizutani, S. (1970). RNA-dependent DNA polymerase in virions of Rous sarcoma virus. *Nature*, *226*, 1211-1213.
- Thamdrup, B., & Dalsgaard, T. (2000). The fate of ammonium in anoxic manganese oxide-rich marine sediment. *Geochimica et Cosmochimica Acta*, *64*(24), 4157-4164. doi:10.1016/S0016-7037(00)00496-8
- Therkildsen, M. S., King, G. M., & Lomstein, B. A. (1996). Urea production and turnover following the addition of AMP, CMP, RNA and a protein mixture to a marine sediment. *Aquatic Microbial Ecology*, *10*, 173-179.
- Treusch, A., Leininger, S., Kletzin, A., Schuster, S., Klenk, H., & Schleper, C. (2005). Novel genes for nitrite reductase and Amo-related proteins indicate a role of uncultivated

- mesophilic crenarchaeota in nitrogen cycling. *Environmental Microbiology*, 7(12), 1985-1995.
- Tsai, Y.-L., & Olson, B. H. (1992). Rapid method for separation of bacterial DNA from humic substances in sediments for polymerase chain reaction. *Applied and Environmental Microbiology*, 58(7), 2292-2295.
- Turk, D., Zappa, C. J., Meinen, C. S., Christian, J. R., Ho, D. T., Dickson, A. G., & McGillis, W. R. (2010). Rain impacts on CO₂ exchange in the western equatorial Pacific Ocean. *Geophysical Research Letters*, 37(23), L23610. doi:10.1029/2010GL045520
- van de Graaf, A. A., Mulder, A., de Bruijn, P., Jetten, M. S., Robertson, L. A., & Kuenen, J. G. (1995). Anaerobic oxidation of ammonium is a biologically mediated process. *Applied and Environmental Microbiology*, 61(4), 1246-1251.
- Wacker, M. J., & Godard, M. P. (2005). Analysis of one-step and two-step real-time RT-PCR using SuperScript III. *Journal of Biomolecular Techniques*, 16(3), 266-271.
- Waldbusser, G. G., & Salisbury, J. E. (2014). Ocean acidification in the coastal zone from an organism's perspective: multiple system parameters, frequency domains, and habitats. *Annual Review of Marine Science*, 6, 221-247. doi:10.1146/annurev-marine-121211-172238
- Wallenstein, M. D., & Hall, E. K. (2012). A trait-based framework for predicting when and where microbial adaptation to climate change will affect ecosystem functioning. *Biogeochemistry*, 109, 35-47. doi:10.1007/s10533-011-9641-8
- Ward, B. B. (2008). Nitrification in marine systems. In *Nitrogen in the Marine Environment* (2 ed., pp. 199-262). Retrieved from <http://ac.els-cdn.com/>
- Watanabe, Y., Tait, K., Gregory, S., Hayashi, M., Shimamoto, A., Taylor, P., . . . Kita, J. (2015). Response of the ammonia oxidation activity of microorganisms in surface sediment to a controlled sub-seabed release of CO₂. *International Journal of Greenhouse Gas Control*, 38, 162-170. doi:10.1016/j.ijggc.2014.11.013
- Wegener, G., Krukenberg, V., Riedel, D., Tegetmeyer, H. E., & Boetius, A. (2015). Intercellular wiring enables electron transfer between methanotrophic archaea and bacteria. *Nature*, 526, 587-590. doi:10.1038/nature15733
- Weston, D. P. (1990). Quantitative examination of macrobenthic community changes along an organic enrichment gradient. *Marine Ecology Progress Series*, 61, 233-244.
- Whitman, W. B., Bowen, T. L., & Boone, D. R. (2014). The methanogenic bacteria. In E. Rosenberg, E. F. DeLong, S. Lory, E. Stackebrandt, & F. Thompson (Eds.), *The Prokaryotes* (pp. 123-163): Springer Berlin Heidelberg. doi:10.1007/978-3-642-38954-2_407
- Widdicombe, S., Beesley, A., Berge, J. A., Dashfield, S. L., McNeill, C. L., Needham, H. R., & Øxnevad, S. (2013). Impact of elevated levels of CO₂ on animal mediated ecosystem function: The modification of sediment nutrient fluxes by burrowing urchins. *Marine pollution bulletin*, 73, 416-427. doi:10.1016/j.marpolbul.2012.11.008
- Widdicombe, S., Dashfield, S. L., McNeill, C. L., Needham, H. R., Beesley, A., McEvoy, A., . . . Berge, J. A. (2009). Effects of CO₂ induced seawater acidification on infaunal diversity and sediment nutrient fluxes. *Marine Ecology Progress Series*, 379, 59-75.
- Widdicombe, S., Dupont, S., & Thorndyke, M. (2010). Laboratory experiments and benthic mesocosm studies. In U. Riebesell, V. J. Fabry, L. Hansson, & J.-P. Gattuso (Eds.), *Guide*

to *Best Practices for Ocean Acidification Research and Data Reporting* (pp. 113-122). Luxembourg: Publications Office of the European Union.

- Widdicombe, S., & Needham, H. R. (2007). Impact of CO₂-induced seawater acidification on the burrowing activity of *Nereis virens* and sediment nutrient flux. *Marine Ecology Progress Series*, 341, 111-122. doi:10.3354/meps341111
- Winogradsky, S. (1891). Recherches sur les organismes de la nitrification. *Annales de l'Institut Pasteur*, 5(577–616).
- Wolf-Gladrow, D. A., Zeebe, R. E., Klaas, C., Körtzinger, A., & Dickson, A. G. (2007). Total alkalinity: The explicit conservative expression and its application to biogeochemical processes. *Marine Chemistry*, 106, 287-300. doi:10.1016/j.marchem.2007.01.006
- Wong, M. L., & Medrano, J. F. (2005). Real-time PCR for mRNA quantitation. *Biotechniques*, 39(1), 1-11.
- Wuchter, C., Middelburg, J. J., Schouten, S., Sinninghe Damsté, J. S., Abbas, B., Coolen, M. J. L., . . . Herndl, G. J. (2006). Archaeal nitrification in the ocean. *Proceedings of the National Academy of Sciences of the United States of America*, 103(33), 12317-12322. doi:10.1073/pnas.0600756103
- Zapperi, G., Pratolongo, P., Piovan, M. J., & Marcovecchio, J. E. (2015). Benthic-pelagic coupling in an intertidal mudflat in the Bahía Blanca Estuary (SW Atlantic). *Journal of Coastal Research*. doi:10.2112/JCOASTRES-D-14-00064.1
- Zeebe, R. E. (2012). History of seawater carbonate chemistry, atmospheric CO₂, and ocean acidification. *Annual Review of Earth and Planetary Sciences*, 40, 141-165. doi:10.1146/annurev-earth-042711-105521
- Zehr, J. P., Carpenter, E. J., & Villareal, T. A. (2000). New perspectives on nitrogen-fixing microorganisms in tropical and subtropical oceans. *Trends in Microbiology*, 8(2), 68–73. doi:10.1016/S0966-842X(99)01670-4
- Zehr, J. P., & Kudela, R. M. (2011). Nitrogen cycle of the open ocean: from genes to ecosystems. *Annual Review of Marine Science*, 3, 197–225. doi:10.1146/annurev-marine-120709-142819
- Zhu, Q., Aller, R. C., & Fan, Y. (2006). Two-dimensional pH distributions and dynamics in bioturbated marine sediments. *Geochimica et Cosmochimica Acta*, 19(1), 4933–4949. doi:10.1016/j.gca.2006.07.033